ISTANBUL TECHNICAL UNIVERSITY ★ GRADUATE SCHOOL OF SCIENCE ENGINEERING AND TECHNOLOGY

SELF-TUNING STRUCTURES OF INTERVAL TYPE-2 FUZZY PID CONTROLLERS

M.Sc. THESIS

Ahmet SAKALLI

Department of Control and Automation Engineering

Control and Automation Engineering Programme

MAY 2014

ISTANBUL TECHNICAL UNIVERSITY ★ GRADUATE SCHOOL OF SCIENCE ENGINEERING AND TECHNOLOGY

SELF-TUNING STRUCTURES OF INTERVAL TYPE-2 FUZZY PID CONTROLLERS

M.Sc. THESIS

Ahmet SAKALLI
(504121102)

Department of Control and Automation Engineering

Control and Automation Engineering Programme

Thesis Advisor: Asst. Prof. Dr. Engin YEŞİL

MAY 2014

İSTANBUL TEKNİK ÜNİVERSİTESİ ★ FEN BİLİMLERİ ENSTİTÜSÜ

ARALIK DEĞERLİ TİP-2 BULANIK PID KONTROLÖRLER İÇİN ÖZ-AYARLAMA YAPILARI

YÜKSEK LİSANS TEZİ

Ahmet SAKALLI
(504121102)

Kontrol ve Otomasyon Mühendisliği Anabilim Dalı

Kontrol ve Otomasyon Mühendisliği Programı

Tez Danışmanı: Yrd. Doç. Dr. Engin YEŞİL

MAYIS 2014

Ahmet Sakallı, a **M.Sc.** student of ITU **Graduate School of Science Engineering And Technology** student ID **504121102**, successfully defended the **thesis/dissertation** entitled **"SELF-TUNING STRUCTURES OF INTERVAL TYPE-2 FUZZY PID CONTROLLERS",** which he/she prepared after fulfilling the requirements specified in the associated legislations, before the jury whose signatures are below.

Thesis Advisor : **Asst. Prof. Dr. Engin YEŞİL**
Istanbul Technical University

Jury Members : **Asst. Prof. Dr. Tufan KUMBASAR**
Istanbul Technical University

Asst. Prof. Dr. İlker ÜSTOĞLU
Yıldız Technical University

Date of Submission : 05 May 2014
Date of Defense : 30 May 2014

To my family,

FOREWORD

I would like to thank the following people without their help and support this thesis would not have been possible. I would like to show my gratitude to my thesis advisor Asst. Prof. Dr. Engin Yeşil for his encouragements, sincerity and guidance during the period of my university education. I would like to thank Asst. Prof. Dr. Tufan Kumbasar for his help, suggestions and vision during the period of my thesis and laboratory studies. I would also like to thank Başak Pınar for her presence and consistent support. Finally, I would like to thank my parents and my friends for their assistance and confidence.

I would like to thank the Scientific and Technological Research Council of Turkey (TUBITAK) for their support and graduate student scholarship under the research project 113E206 (1001, the Support Program for Scientific and Technological Research Project). I would also like to thank project members M. Furkan Dodurka and Cihan Öztürk for their cooperation.

I would like to thank Istanbul Technical University Scientific Research Projects Unit for their support to my master thesis under the Support Program for Graduate Thesis Research Project.

May 2014 Ahmet SAKALLI

TABLE OF CONTENTS

Page

ABBREVIATIONS

ACO : Ant Colony Optimization
BBBC : Big Bang – Big Crunch
BF : Boundary Function
BF-KM : Boundary Function based Karnik-Mendel
ERWIT2-FPID : Error based Rule Weighting of Interval Type-2 Fuzzy PID
FLS : Fuzzy Logic System
FLC : Fuzzy Logic Controller
FOU : Footprint of Uncertainty
FPID : Fuzzy PID
FTT1-FPID : Function Tuner based Type-1 Fuzzy PID
GA : Genetic Algorithm
IT2-FLS : Interval Type-2 Fuzzy Logic System
IT2-FS : Interval Type-2 Fuzzy Set
IT2-FPID : Interval Type-2 Fuzzy PID
KM : Karnik-Mendel
LMF : Lower Membership Function
MAGLEV : Magnetic Levitation
MF : Membership Function
OIT2-FPID : Optimized Interval Type-2 Fuzzy PID
OPID : Optimized PID
ORWIT2-FPID : Optimization based Rule Weighting of IT2-FPID
OT1-FPID : Optimized Type-1 Fuzzy PID
OIT2-FPID : Optimized Interval Type-2 Fuzzy PID
PD : Proportional-Derivative
PI : Proportional-Integral
PID : Proportional-Integral-Derivative
RROT1-FPID : Relative Rate Observer based Type-1 Fuzzy PID
S-MAP : Surface of Switching Point Map
SC : SubController
SF : Scaling Factor
SP : Switching Point
STIT2-FPID : Self-tuning Interval Type-2 Fuzzy PID
STT1-FPID : Self-tuning Type-1 Fuzzy PID
T1-FLS : Type-1 Fuzzy Logic System
T2-FLS : Type-2 Fuzzy Logic System
T1-FPID : Type-1 Fuzzy PID
T1-FS : Type-1 Fuzzy Set
T2-FS : Type-2 Fuzzy Set
UMF : Upper Membership Function

LIST OF TABLES

Page

LIST OF FIGURES

SELF-TUNING STRUCTURES OF
INTERVAL TYPE-2 FUZZY PID CONTROLLERS

SUMMARY

The fuzzy logic systems have been successfully implemented in various engineering areas including control, robotics, image processing, decision making, estimation and modelling. Nowadays, the fuzzy logic systems have been attracting massive research interest especially in control theory due to their superiority against nonlinearities and uncertainties of system dynamics. In literature there are various study on fuzzy logic controllers and also, in most of control studies, the fuzzy PID controllers is preferred because analogous structures to conventional PID controller from the input-output relationship point of view.

Lately, it is demonstrated that there might be some obstacles for the ordinary (type-1) fuzzy logic systems in the ability of expressing the uncertainties and nonlinearities. It is also showed that this limitation might partly occurred due to the crisp membership grades of the employed type-1 fuzzy sets. Therefore, type-1 fuzzy logic system are generalized to type-2 fuzzy logic systems, however, dealing with type-2 fuzzy sets (instead of type-1 fuzzy sets) requires an additional procedure in fuzzy inference mechanism called type reduction. The type reduction procedure is used to reduce type-2 fuzzy sets in antecedent part of the fuzzy rules into type-1 fuzzy sets before the defuzzification process. The type reduction is generally be performed by iterative algorithms. The type-2 fuzzy logic systems is still not well developed research topic due to its complex internal structures and computational burden caused by type-2 fuzzy sets. Therefore, in order to overthrow the bottlenecks of the type-2 fuzzy logic systems, the interval type-2 fuzzy systems is proposes as a special case of type-2 fuzzy logic systems. Recently, interval type-2 fuzzy logic systems obviously dominate the research areas on the fuzzy logic theory and relating research topics.

Recently, interval type-2 fuzzy logic systems have been successfully implemented in various control applications such as liquid level control, autonomous mobile robots, nonlinear plant control, pH control, bioreactor control and fuzzy modelling. It is demonstrated the interval type-2 fuzzy logic systems provide better control performances when comparing to its type-1 or conventional counterparts due its additional degree of freedom provided by the footprint of uncertainty in their antecedent membership functions. It is also shown that the interval type-2 fuzzy logic systems provide more smooth control actions comparing to type-1 counterparts and this feature provides better control performances in case of uncertainty. Moreover, interval type-2 fuzzy logic systems use a well-known iterative type reduction algorithm, namely Karnik-Mendel type reduction method. The various alternative methods to original Karnik-Mendel algorithm and extended versions of original Karnik-Mendel algorithm is proposed in order to reduce computational burden. Yet, the problem still exists since the alternative methods do not have superior features of Karnik-Mendel algorithm, adaptiveness and novelty, while extended algorithms cannot be explicitly represented like original Karnik-Mendel algorithm. Furthermore, the internal structures and the stability analysis of the interval type-2 fuzzy logic controllers have been investigating. The stability analysis for a Takagi-Sugeno-Kang fuzzy system is performed for particular circumstances. The analytical derivation of interval type-2 fuzzy PI and PD controllers are examined by dividing input space into several number of subregions. Although some studies for the design of interval type-

2 fuzzy logic controllers is performed, the topic is still not well-develop. Therefore, the research interest on this topic still continues in order to better understand of the nature of the interval type-2 fuzzy logic controller and develop more complex controller structures such as self-tuning mechanisms.

In this thesis, first two alternative approaches to the Karnik-Mendel type reduction method is proposed in order to better understand the switching point selection of the iterative Karnik-Mendel algorithm and represent it in a closed form. The first proposed approach is called as Surface of Switching Points Map; it is a novel visualizing method that shows the switching points of Karnik-Mendel algorithms clearly. The Surface of Switching Points Map points outs the switching point sets and their valid region on the input space. The second proposed approach is called as Boundary Function based Karnik-Mendel type reduction method and it determines the optimal switching points of the Karnik-Mendel algorithm without performing an iterative algorithm by the advantage of the decomposition property. Decomposition property provide to dividing input space into subcontroller and the proposed Boundary Function based Karnik-Mendel type reduction method determines the optimal switching points for corresponding subcontroller for an input set. The proposed alternative approaches is complementary studies because the Boundary Function based Karnik-Mendel type reduction method determines the optimal switching points exactly and the Surface of Switching Points Map visualize them clearly.

Secondly, the analytical derivations of interval type-2 fuzzy PID controller performed. Here, the mathematical expressions of the 4-rule interval type-2 fuzzy PID controller is analytically derived with the aids of the proposed alternative approaches. The output formulations of the employed interval type-2 fuzzy PID controllers are explicitly expressed. The main goal of these derivations is that the control laws of the interval type-2 fuzzy PID controllers is represented mathematically in closed form in terms of input variables and design parameters. It is also discovered that the control laws switches to other in time with respect to the values of the switching points. Even though the obtained control laws is nonlinear functions, these observations the might be useful for the stability analysis of the controller or the controller design for the further research studies.

Thirdly, two novel self-tuning structures based a heuristic function and optimization for interval type-2 fuzzy PID controllers is proposed. A simple heuristic self-tuning function is proposed for the simplest interval type-2 fuzzy PID controllers with respect to the derived mathematical expressions. The function is constructed according to the obtained controller gain curve of the simplest interval type-2 fuzzy PID controller around the origin. The self-tuning structure adjust the size of the FOU via changing the heights of the lower membership functions in online manner. Another self-tuning structure adjust the rule weights of the 9-rule interval type-2 fuzzy PID controller in an online manner via optimization regarding to a control cost function. The optimization procedure determines the optimal rule weights that force the system to attain to the reference as fast as possible with an applicable control effort.

Finally, in order to show effectiveness of proposed self-tuning structures and the main differences between interval type-2 fuzzy PID controller and its counterparts, two simulation studies and a comprehensive comparative real-time experimental study are performed. The real-time comprehensive comparative study is performed on an open loop unstable, time varying and nonlinear magnetic levitation plant and the interval type-2 fuzzy PID controller is compared with four fuzzy PID controller including self-tuning type-1 structures. The real-time results demonstrated that the interval type-2 fuzzy PID controller has better control performances in most cases comparing to the other controllers. In addition, the superiority of it lies in the way to handle against uncertainties rather than only having extra degree of freedom. In addition, the proposed self-tuning structures is simulated on challenging benchmark models. First, the self-tuning simplest interval type-2 fuzzy PID controller is tested on a perturbed first order plus dead time process in order to verify the controller performance in cases of uncertainty. Then, the optimization based rule-weighting method for interval type-2 fuzzy PID controllers is tested on a two cascaded tank process with a second order nonlinear model in order to verify the controller performance in case of nonlinearity. Therefore, the simulation results show that the proposed self-tuning interval type-2 fuzzy PID controllers improve the overall performances of the closed loop control system and they are more robust against uncertainties and nonlinearities when comparing to their interval type-2 bases and type-1 counterparts.

In this thesis, two novel methods are proposed as alternative approaches to the Karnik-Mendel type reduction algorithm, the mathematical expressions of two kinds of interval type-2 fuzzy PID controller is analytically derived in a closed form formulation, two self-tuning structures for interval type-2 fuzzy PID controller is proposed, it is shown to be an effective method in controlling processes which inherit nonlinear dynamics and uncertainties and the interval type-2 fuzzy PID controller is compared with various controllers as a part of a comprehensive comparative real-time study.

ARALIK DEĞERLİ TİP-2 BULANIK PID KONTROLÖRLER İÇİN ÖZ-AYARLAMA YAPILARI

ÖZET

Bulanık mantık tabanlı sistemler kontrol, robotik, görüntü işleme, karar verme, tahmin, modelleme gibi birçok farklı mühendislik uygulanasında başarıyla uygulanmıştır. Günümüzde ise bulanık mantık tabanlı sistemler özellikle kontrol teorisi üzerinde önemli bir araştırma konusunu bulmaktadır. Literatürde bulanık mantık sistemlerin özel bir hali olan bulanık PID kontrolörler üzerine birçok çalışma bulunmaktadır çünkü giriş çıkış ilişkileri gereğince bu kontrolörler, klasik PID kontrolörlere eşdeğer olabilmektedirler.

Ancak sıradan yani tip-1 bulanık mantık sistemlerinin belirsizlikleri ve doğrusal olmayan özellikleri ifade etme konusunda yetersiz kalabileceği yapılan çalışmalarla gösterilmiştir. Ayrıca bu sınırlamanın temelde tip-1 bulanık kümelerin keskin üyelik değerlerinden kaynaklandığı gösterilmiştir. Bu yüzden tip-1 bulanık sistemler tip-2 bulanık sistemlere genişletilmiştir ancak karmaşık iç yapıları ve tip-2 bulanık kümelerin hesaplama yükü sebebiyle tip-2 bulanık sistemler günümüzde hala yeterince geliştirilememiştir. Çünkü tip-1 bulanık kümeler yerine tip-2 bulanık kümeler ile uğraşmak bulanık çıkarım mekanizmasına tip-indirgeme adında yeni bir operasyon eklemiştir. Tip indirgeme işlemi, bulanık kuralların öncül kısmındaki tip-2 bulanık kümelerini durulama işlemi öncesinde tip-1 bulanık kümelere indirgemek için kullanılır. Ancak tip-indirgeme genelde iteratif algoritması ile gerçeklenmesi tip-2 bulanık sistemlerin hesaplama yükünü arttırmış ve iç yapısının incelenmesini engellemiştir. Bu sebeple tip-2 bulanık sistemlerin zorluklarını yok etmek için, tip-2 bulanık sistemlerin özel bir hali olan aralık değerli tip-2 bulanık sistemler önerilmiş ve günümüzde de aralık değerli tip-2 bulanık sistem açık bir şekilde bulanık mantık alanında yapılan çalışmalara yön vermektedir.

Aralık değerli tip-2 bulanık mantık sistemler, sıvı seviye kontrolü, otonom mobil robot kontrolü, süreç kontrolü, pH kontrolü, biyoreaktör kontrolü ve modelleme gibi birçok farklı kontrol alanındaki uygulamalarda gerçeklenmiştir. Yapılan çalışmalarla gösterilmiştir ki aralık değerli tip-2 bulanık mantık sistemleri öncül üyelik fonksiyonlarındaki belirsizlik izdüşümü tarafından sağlanan fazladan serbestlik derecesi sayesinde tip-1 eşdeğerlerine kıyasla daha iyi kontrol performansı sağlamaktadır. Ayrıca aralık değerli tip-2 bulanık mantık tabanlı sistemler, tip-1 eşdeğerlerine kıyasla daha yumuşak kontrol eylemine sahiptir ve bu durum belirsizlikler karşısında daha iyi kontrol performanları sağlamaktadır. Yapılan bazı çalışmalarda değinilmiş olmasına rağmen, aralık değerli tip-2 bulanık mantık sistemlerinin tasarımı hala geliştirmeye açık bir konudur. Bunlara ilaveten, hesaplama yükünü azaltmak için orijinal Karnik-Mendel algoritmasına bir çok alternatif algoritmalar önerilmiştir. Ancak temel problemler hala devam etmektedir çünkü alternatif yöntemler Karnik-Mendel algoritmasının yenilikçi ve uyarlamalı olmak üzere iki temel özelliğini taşımamaktadır, gelişmiş algoritmalar ise orijinal Karnik-Mendel algoritması gibi açık bir biçimde ifade edilememektedir. Bunlara ilaveten günümüzde aralık değerli tip-2 bulanık mantık sistemlerinin iç yapıları ve kararlılıkları farklı yönlerden incelenmektedir. Bu bağlamda alternatif tip indirgeme yöntemi kullanılarak Takagi-Sugeno-Kang bulanık sistemlerin özel durumlar için kararlılıkları gösterilmiş, aralık değerli tip-2 bulanık PI ve PD kontrolörlerin analitik

ifadeleri giriş uzayı çok sayıda alt parçaya bölünerek elde edilmiş olsa da bu konudaki çalışmalar hala devam etmektedir. Günümüzde araştırmacıların ilgisi aralık değerli tip-2 bulanık kontrolörleri daha iyi anlamak, kararlılık analizlerini gerçekleştirmek, tasarım yöntemleri önermek ve öz-ayarlama gibi daha karmaşık kontrol yapıları geliştirebilmek için devam etmektedir.

Bu tez çalışmasında, Karnik-Mendel tip-indirgeme algoritmasına alternatif iki yöntem önerilmiştir. Bu iki yöntem ile kesme noktası seçiminin daha iyi anlaşılması ve kapalı biçimde ifade edilmesi hedeflenmektedir. Önerilen ilk yöntem Kesme Noktaları Haritasının Yüzeyi olarak adlandırılmakta ve bu yeni görsel yöntem Karnik-Mendel algoritmasının kesme noktalarını açık bir biçimde göstermektedir. Kesme Noktaları Haritasının Yüzeyi, kesme noktalarını ve bu noktaların geçerli olduğu bölgeleri giriş uzayı üzerinde temsil etmektedir. İkinci önerilen yöntem Sınır Fonksiyonları tabanlı Karnik-Mendel tip-indirgeme yöntemi olarak adlandırılmakta ve bu yöntem Karnik-Mendel algoritmasının optimal kesme noktalarını ayrıştırma özelliğinden yararlanarak bulmaktadır. Ayrıştırma özelliği giriş uzayının birçok alt uzaya bölünmesini sağlamakta ve önerilen Sınır Fonksiyonları tabanlı Karnik-Mendel tip-indirgeme yöntemi bu alt uzaylara bağlı olarak optimal kesme noktaları hesaplamaktadır. Aslında önerilen bu alternatif yöntemler birbirini tamamlayıcı yöntemlerdir çünkü Sınır Fonksiyonları tabanlı Karnik-Mendel tip-indirgeme yöntemi optimal kesme noktalarını hesaplarken, Kesme Noktaları Haritasının Yüzeyi ise bu noktaları açıkça görsel hale getirir.

Tez çalışmasının ikinci aşamasında 4 kurallı aralık değerli tip-2 bulanık PID kontrolörin analitik çıkarımları yapılmıştır. Bu amaçla 4 kurallı aralık değerli tip-2 bulanık PID kontrolör yapılarının matematiksel ifadeleri önerilen Karnik-Mendel tip-indirgeme yöntemine alternatif yöntemler kullanılarak elde edilmiştir. Böylece kullanılan aralık değerli tip-2 bulanık PID kontrolörlerin çıkış ifadeleri açıkça ifade edilmiştir. Bu çalışmanın en önemli getirilerinden biri olarak aralık değerli tip-2 bulanık PID kontrolörlerinin kontrol kurallarının giriş değişkenleri ve tasarım parametreleri cinsinden matematiksel olarak ifade edilmesi gösterilebilir. Ayrıca bu çalışmalar esnasında kontrol kurallarının giriş değerlerine bağlı olarak zamanla birbirini arasında değiştiği de gözlenmiştir. Elde edilen kontrol kuralları doğrusal olmayan karmaşık ifadeler olsa bile bu ifadeler kontrolör tasarımı ve kararlılık analizlerinde rahatlıkla kullanılabilir olduğu görülmüştür.

Ayrıca bu tezde biri sezgisel fonksiyon diğeri optimizasyon tabanlı olmak üzere aralık değerli tip-2 bulanık PID kontrolörler için iki farklı öz-ayarlamalı yöntem önerilmiştir. Sezgisel öz-ayarlamalı fonksiyon en basit aralık değerli tip-2 bulanık PID kontrolör için elde edilen matematiksel ifadelere bağlı olarak önerilmiştir. Ele alınan fonksiyon en basit aralık değerli tip-2 bulanık PID kontrolörün sürekli hal noktası etrafındaki kazanç eğrisine bağlı olarak oluşturulmuştur. Bu öz ayarlamalı yöntem, alt üyelik fonksiyonlarının yüksekliklerini sürekli bir şekilde değiştirerek belirsizlik izdüşümünün büyüklüğünü ayarlamaktadır. Diğer öz-ayarlama yöntemi 9 kurallı aralık değerli tip-2 bulanık PID kontrolörlerin kural ağırlıklarını optimizasyon tabanlı ve sürekli bir şekilde ayarlamaktadır. Optimizasyon işlemi sistemi en hızlı şekilde ve uygun bir kontrol işareti ile referansa ulaşmasını sağlayacak olan bulanık kural ağırlıklarını belirlemektedir.

Son olarak, önerilen öz-ayarlamalı yöntemlerin başarımlarını ve aralık değerli tip-2 bulanık PID kontrolörler ile eşdeğerleri arasındaki temel farkları göstermek amacıyla, iki benzetim çalışması ve kapsamlı bir gerçek zamanlı karşılaştırmalı deney çalışması gerçekleştirilmiştir. Gerçek zamanlı deneyler açık çevrim kararsız doğrusal olmayan ve zamanla değişken bir manyetik askı sisteminde gerçeklenmiş ve aralık değerli tip-2 bulanık PID kontrolörler dört farklı yöntem ile karşılaştırılmıştır. Deney sonuçları göstermiştir ki aralık değerli tip-2 bulanık PID kontrolörler daha iyi kontrol performansları sergilemiştir. Ayrıca aralık değerli tip-2 bulanık PID kontrolörlerinin üstünlüğün fazladan serbestlik derecesine sahip olmasından ziyade belirsizlikler ile başa çıkma şeklinden kaynaklandığı görülmüştür. Buna ilaveten, önerilen öz-ayarlamalı kontrol yapılarının zorlu örnek test modelleri üzerinden benzetimleri yapılmıştır. İlk olarak öz ayarlamalı en basit aralık değerli tip-2 bulanık PID kontrolör yapısı bozulmuş birinci mertebeden ölü zamanlı sistemler üzerinde, kontrolör performansını belirsizlik altında incelemek adına benzetimler yapılmıştır. Daha sonra, aralık değerli tip-2 bulanık PID kontrolör için önerilen optimizasyon tabanlı kural ağırlıklandırma yöntemi ikinci mertebeden doğrusal olmayan bir modeli olan kaskat çift tank sistemi üzerinde, kontrolör performansını doğrusal olmayan dinamikler altında incelemek adına benzetimler yapılmıştır. Elde edilen benzetim sonuçları göstermiştir ki önerilen yapılar kontrol sistem performansını arttırmakta ve genel anlamda belirsizliklere ve doğrusal olmayan dinamiklere karşı daha dayanıklı gözükmektedirler.

Bu çalışmada özetle, Karnik-Mendel tip indirgeme yöntemine eşdeğer olan iki adet alternatif yöntem önerilmiş, iki farklı aralık değerli tip-2 bulanık PID kontrolör için kapalı formda analitik ifadeler elde edilmiş, iki farklı öz-ayarlamalı yöntem önerilmiştir, önerilen yöntemlerin performansları doğrusal olmayan dinamikler ve belirsizler içeren sistemler üzerinde denemiş ve aralık değerli tip-2 bulanık PID kontrolörler diğer kontrolörler ile gerçek zamanlı bir çalışmanın parçası olarak karşılaştırılmıştır.

1. INTRODUCTION

Nowadays, Fuzzy Logic Systems (FLSs) have been successfully implemented in various engineering areas and their applications including control, robotics, image processing, decision making, estimation and modelling. The fuzzy logic concept was firstly introduced by Zadeh in 1965 (Zadeh, 1965). The first industrial application example of the fuzzy logic was accomplished by Mamdani in 1974 in the area of control theory by constructing to the linguistic control rules of a skilled human operator (Mamdani, 1974). The FLSs become more and more popular and take part in many studies from that date. One of the most well known structure fuzzy logic systems is Takagi-Sugeno-Kang fuzzy logic system which was first proposed in 1985. That system is widely used in control applications (Takagi and Sugeno, 1985). Also it is presented that Takagi-Sugeno-Kang type (instead of the Mamdani-type) FLSs made it possible to design and analyze fuzzy control systems more obvious (Sugeno and Kang, 1988). In this context, the various studies on the fuzzy logic control and fuzzy logic theory adopt the Takagi-Sugeno-Kang FLS structure (Eksin et al., 2001; Guzelkaya et al., 2003; Yeşil et al., 2004; Kumbasar et al., 2008; Karasakal et al., 2011). Moreover, since most of the systems and processes are characterized by uncertainties and nonlinearities, various fuzzy modeling and fuzzy control strategies have been successfully implemented in many engineering problems (Babuska et al., 2002; Guzelkaya et al., 2003; Precup et. al, 2004; Duan et al., 2008; Ahn et al., 2009; Karasakal et. al, 2013).

In literature, various study have been performed on Fuzzy PID (FPID) controllers. In general, the FPID controllers classified into two major categories with respect to the way they are constructed (Xu et al., 2000). The first category is that the gains of the conventional PID controller is tuned online by a fuzzy logic system with a knowledge base and inference mechanism (Zhao et al., 1993) in other words, the conventional PID controller generates actual control signal while its gains are tuned by a FLS. The second category is that a FLS is directly used for generating actual control signal regarding to its knowledge base, inference mechanism and fuzzy rules

(Mizumoto, 1992; Li et al., 1996). Nowadays, FPID controllers referred as second category because from the input-output relationship point of view, the structure of FPID controller is analogous to a conventional PID controller (Galichet et al., 1995; Li et al., 1996; Quio and Muzimoto, 1998; Huang et al. 1999). There are various recent studies which are performed for FPID controllers with various self-tuning structures such as heuristic or non-heuristic functions, rule weighting and optimization (Ahn et. al, 2009; Bouallegue et al., 2011; Karasakal et al., 2013; Yeşil et al., 2013).

However, researchers demonstrated that there might be limitations in the ability of ordinary fuzzy logic systems or type-1 fuzzy logic systems (T1-FLSs) in the ability of expressing the uncertainties and nonlinearities (Hagras 2004, Wu, 2006). This limitation is partly occurred because of the fact that, the membership grade for each input value is a crisp value (Mendel, 2007). It has been shown that Type-2 Fuzzy Sets (T2-FSs) are more suitable in some circumstances where it is difficult to determine the accurate membership function for a fuzzy set (Karnik et al., 1999). The concept of T2-FSs is a generalization of ordinary fuzzy sets (type-1 fuzzy sets, T1-FSs) and was firstly introduced by Zadeh (Zadeh, 1975). Mendel, (2000) stated that FLSs that are described with at least one T2-FSs are named as Type-2 Fuzzy Logic Systems (T2-FLSs). The major importance of T2-FLSs is the Footprint of Uncertainty (FOU) that models the uncertainties and nonlinearities in a secondary membership function. It has been illustrated that T2-FSs are much more powerful to handle uncertainties and nonlinearities compared to type-1 fuzzy logic systems (Liang et al., 2000 and Coupland et al., 2007). On the other hand, the major problem with T2-FLSs is the computational burden in the type reduction operation which is used for reducing T2-FSs to T1-FSs in the rule base (Liang and Mendel, 2000; Wu and Mendel, 2002; Mendel et al. 2006). Therefore, to overcome this problem, Liang et al. (2000) and Mendel (2000) proposed a special type of T2-FSs called Interval Type-2 Fuzzy Sets (IT2-FSs), in details, the secondary grades of an IT2-FS is always one while it is variable for T2-FSs. In IT2-FLSs, the type-reduction mechanism is used to map the IT2-FSs into a T1-FSs and afterwards routine defuzzification procedure is accomplished to obtain a crisp quantity (Liang and Mendel, 2000; Mendel, 2000; Wu and Mendel, 2011). However, researchers still concern the computational cost of calculating the output of IT2-FLSs. Here, the type reduction mechanism is the main cause of the complexity issue. The most commonly used algorithm for type reduction is called Karnik-Mendel type-reduction method and it is presented in detail in (Wu and Mendel, 2007). In this method, the type reduced set is formed after determination of the optimal switching points. However, since these important switching points cannot be predetermined as explicit functions of the inputs the (Karnik-Mendel) KM algorithm has to calculate the type reduced set of the IT2-FLS iteratively (Liang and Mendel, 2000; Wu and Mendel, 2007). Therefore, the computation of the type reduced set becomes a bottleneck for IT2-FLSs due to iterative nature of KM algorithm. Therefore, several approximations of the KM algorithm have been proposed (Begian et al., 2008; Du and Ying, 2010; Nie and Tan, 2008; Wu and Tan, 2005; Wu and Mendel, 2002). Nevertheless, it has been shown that the alternative type reduction methods cannot capture the features of the KM algorithm (Wu, 2011).

IT2-FLSs have been successfully used in various study for controller design and controller analysis. In order to show the feasibility of type-2 fuzzy logic systems, real-time control applications such as liquid-level process control (Wu and Tan, 2006b), autonomous mobile robots (Martinez et al., 2009), nonlinear plant control (Castillo et al., 2005), bioreactor control (Galluzzo et al., 2008), pH control (Kumbasar et al., 2011, Kumbasar et al.,2012) have been handled and implemented successfully. Moreover recently, researchers began investigating the internal structure and stability analysis of the IT2-FLSs. It is demonstrated that significant control performance improvements can be achieved by IT2-FLSs in comparison to its type-1 counterpart (Hagras, 2004; Wu ad Tan, 2010; Wu 2012; Castillo and Melin, 2008). It has been shown in various works that IT2-FLSs achieve better control performances because of the additional degree of freedom provided by the FOU in their antecedent membership functions (Wu, 2012; Kumbasar et al., 2012). In literature, the design of the IT2-FLS is also solved by extending membership functions of an existing T1-FLS or by employing optimization algorithms (Wu and Tan, 2006; Kumbasar and Hagras, 2013a; Yeşil, 2014).The stability analysis of the interval type-2 fuzzy model based control systems is examined (Lam and Seneviratne, 2008) and the stability of the IT2-FLCs is presented in (Biglarbegion et al., 2010) by using an alternative type-reduction method which enables to write the output of the IT2-FLC in a closed form (Wu and Mendel, 2002). Moreover, analytical derivations of the Interval Type-2 Fuzzy PI and PD (IT2-FPI and IT2-FPD) controllers are obtained in (Du and Ying, 2010; Nie and Tan, 2012) by dividing the input space to several number of sub-regions. It is derived that the closed-from formulation of the single input Interval Type-2 Fuzzy PID (IT2-FPID) controller (Kumbasar, 2013c). The research interest on this topic still continues to understand and analyze the internal structure of the IT2-FLCs better and design more systematic controllers.

In this thesis, the analytical structural analysis of a special kind of IT2-FPID controller which is composed of four rules are presented with respect to the switching points of KM type reduction method. For this purpose, first a novel graphical method called Surface of Switching Points Map (S-MAP) to visualize and understand better the variation of the switching point selection of the KM algorithm is explained (Sakalli et al., 2014a). The switching points which are determined by KM algorithm define the formulation of the control law which is the output of the IT2-FLS for IT2-FPID controller structure. The S-MAP is a novel plot that illustrates the switching point selection of the KM algorithm which is based on the Boundary Function based Karnik-Mendel (BF-KM) type reduction method (Dodurka et al., 2014). In order to derive the BF-KM, first a novel representation of the switching points of the IT2-FPID controller is first decomposed into subcontrollers and then the Boundary Functions (BFs) are derived to determine the optimal switching points of each subcontrollers. The analytical formulation of determining optimal switching points is derived from by solving determined inequality type equations in order to obtain the crisp output of the IT2-FPID controller. The BF-KM type reduction method can be assumed as an enhancement to the original KM type reduction algorithm because it eliminates the iterative nature of the KM algorithm and it reduces the computational complexity of the KM type reduction algorithm. Then with the aids of the proposed alternative approaches, S-MAP and BF-KM, the closed-form formulation of the 4-rule IT2-FPID controllers are derived. Here, the mathematical expressions of the 4-rule IT2-FPID controllers is obtained by using decomposition property of the employed controller structure in terms of the different control laws of each decomposed subcontroller of the IT2-FPID controller.

Moreover, the closed-form formulation of the simplest IT2-FPID controller around the steady state is derived and it is showed that the IT2-FPID controller is analogous to a PID controller. The output of the simplest IT2-FPID controller is expressed in terms of the parameters of the antecedent IT2-FSs of the rules. In the light of the observations, a simple self-tuning mechanism that adjust the controller gain via the size of the FOU is proposed and the effectiveness of the proposed self-tuning structure for 4-rule IT2-FPID controller is discussed with the simulation studies. Furthermore, a comparative real-time experimental results between ordinary FPID (Type-1 Fuzzy PID, T1-FPID) IT2-FPID controller structures on the QUANSER Magnetic Levitation Plant (MAGLEV) is presented (Sakalli et al., 2014b). The real-time experimental results of IT2-FPID controller is also compared with two STT1-FPID controller structures which are based on the Function Tuner (FTT1-FPID) and based on the Relative Rate Observer (RROT1-FPID). The employed self-tuning mechanisms allow the T1-FPID structures to have more degrees of freedom. In this context, if the power of the IT2-FPID lies in its ability to handle the high level of uncertainties rather than only having an extra degree of freedom is investigated on a open loop unstable and nonlinear plant.

The thesis organized in 7 sections including conclusion. In section 2, the general and internal structures of IT2-FPID controllers is explained in terms of structure of FPID controllers, definitions and advantages of IT2-FSs and IT2-FLSs. In Section 3, proposed a novel visualizing method S-MAP and a type-reduction method BF-KM is explained in detail. In section 4, the mathematical expressions of IT2-FPID controllers for 4-rule structure are derived explicitly with respect to the S-MAP and BF-KM. In section 5, a self-tuning structure for the simplest IT2-FPID controller is presented with respect to the control law around the steady state, after that an optimization based rule weighting method for IT2-FPID controllers is presented. In Section 6, simulation and real-time experimental studies are presented. First, a comparison study between IT2-FPID controller and T1-FPID controllers on MAGLEV is presented and then a self-tuning structures are examined on benchmark plants with uncertainties and nonlinearities. Consequently, the results are concluded and discussed in the conclusion section.

2. INTERVAL TYPE-2 FUZZY PID CONTROLLERS

2.1 General Structure of Fuzzy PID Controllers

Interval Type-2 Fuzzy PID (IT2-FPID) controllers are generalized forms of those Type-1 Fuzzy PID (T1-FPID) controllers and also T1-FPID controllers are often mentioned as an alternative to conventional PID (Proportional-Integral-Derivative) controllers since they are analogous to the PID controllers from input-output relationship point of view (Galichet and Foulloy, 1995; Qiao and Muzimoto, 1996). Recently, PID controllers are widely used in many control areas such as process control, adaptive control, robust control, nonlinear control, automation and robotics and they are still the most used controller type in the industry (Astrom and Hagglund, 2005). The design strategies of conventional PID controllers depends on the mathematical model of the system, however conventional PID controllers may not provide satisfactory results in case of unperfect model. In this context fuzzy logic controllers especially approximately analogous to conventional controllers are widely used in case of high-order system model, nonlinear system behavior or uncertainty in the system. Conventional PID controllers provide a linear transformation or mapping between their inputs and outputs while Fuzzy PID (FPID) controllers provide a nonlinear transformation or mapping between their inputs and outputs. It can be also said that a FPID controller is a conventional PID controller with variable controller gain (Huang et al., 1999).

In literature, various fuzzy controller structures are proposed including PD-type (Proportional-Derivative), PI-type (Proportional-Integral) and PID-type (Li and Gatland 1996, Yeşil et al. 2003). These fuzzy controller structures consists of input and output Scaling Factors (SFs) and a Fuzzy Logic System (FLS). Here notice that, all of these fuzzy controllers could use the same FLS but the number and usage of SFs determines the fuzzy controller structure. In this context, fuzzy controllers are constructed by choosing the inputs to the error (e) and derivative of the error ($\dot{e}$) and the output as the control signal (u). Also in some studies (Mudi and Pal, 1999; Güzelkaya et al., 2003; Karasakal et al., 2011) inputs are defined in discrete time expression instead of continuous time expression by using error ($e(k)$) and change of the error ($\Delta e(k)$) but these expressions do not change the general structure of fuzzy controllers. In this thesis, we prefer the continuous time expression in definitions and explanations of employed structures and methods for the sake of consistency. Then, definitions of inputs of a fuzzy controller (regardless to the type of the controller) can be given as follows:

$$e = r - y \tag{2.1}$$

$$\dot{e} = \frac{de}{dt} = \frac{d(r-y)}{dt} \tag{2.2}$$

where r is the reference signal or set point and y is the system output. In fuzzy controller structures (regardless to the type of the controller), input SFs normalize the inputs to the universe of discourse, particularly, K_e normalize the error input and K_d normalize the derivative of error input as follows:

$$E = K_e e, \qquad E \in [-1,1] \tag{2.3}$$

$$D = K_d \dot{e}, \qquad D \in [-1,1] \tag{2.4}$$

where E is the normalized error input of the FLS and D is the normalized derivative of error input of the FLS. Here, the universe of discourse is defined in the interval, which is defined as $[-1, 1]$, so inputs E and D are also defined in the same interval. Also notice that, e is the input of a fuzzy controller regardless to the type of controller structure; PD, PI or PID while E is the input of FLS that is used in the fuzzy controller. Similarly, $\dot{e}$ is another input of a fuzzy controller regardless to the type of controller structure; PD, PI or PID while D is another input of the FLS that is used in the fuzzy controller. Moreover, the output of the fuzzy controller (u), which is also control signal, is generated by the output of the FLS that is used in the fuzzy controller (U) and output SFs, in other words, the output of the FLS is converted into the control signal by the output SFs. In details, K_a is a constant gain of the output of the FLS and K_b is the integral gain of the output of the FLS. Here also notice that, output SFs make the control signal applicable for a particular problem or a real life problem because the output of the FLS could only take values in the interval $[-1,1]$

due to universe of discourse. Therefore, the generalized formulation of the output of a fuzzy controller that used in this thesis is defined as follows:

$$u = K_a U + K_b \int U\, dt, \qquad U \in [-1,1] \tag{2.5}$$

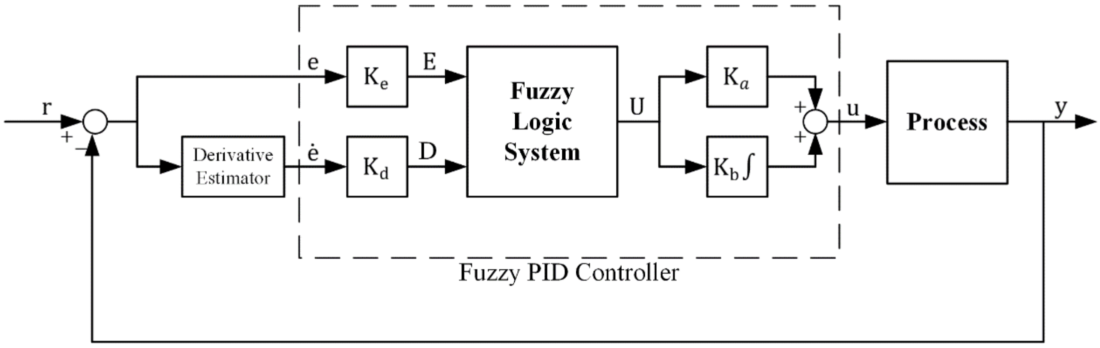

Figure 2.1 : Closed loop control structure of fuzzy logic systems.

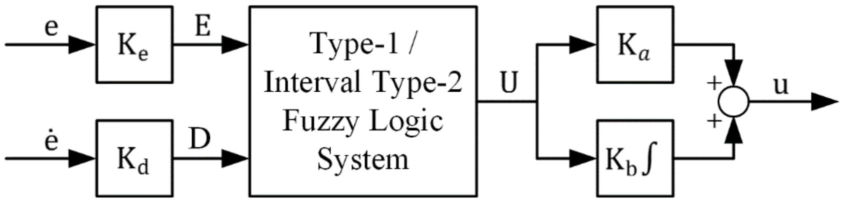

Figure 2.2 : Fuzzy PID controller structure.

The FPID controller structure including input and SFs and the FLS (regardless to the type) and a model closed-loop control block diagram are illustrated as in Figure 2.1 and Figure 2.2. Here obviously, one can generate various fuzzy controller structures (PI, PD or PID) with respect to the SFs. For example, a FPID controller is obtained in case of all SFs are assigned, a Fuzzy PD (FPD) controller is obtained in case of $K_b = 0$ while other SFs are assigned, and a Fuzzy PI (FPI) controller is obtained in case of $K_a = 0$ while other SFs are assigned. In fact, a FPID controller reduces into FPI controller or FPD controller if a SF is not assigned. Then, potential combinations of fuzzy controllers are summurized in Table 2.1.

Table 2.1 : Potential combinations of fuzzy PI- PD-PID controllers.

Controller Type	K_e	K_d	K_a	K_b
FPD	✓	✓	✓	-
FPD	✓	-	✓	✓
FPI	✓	✓	-	✓
FPI	✓	-	✓	✓
FPID	✓	✓	✓	✓

As shown in Figure 2.1 and Figure 2.2, the actual control signal of the closed loop system is a function of scaling factors and the output of the FLS as $u = f(U, K_a, K_b)$ or $u = f(U, \int U, K_a, K_b)$. The FLS performs a nonlinear mapping between its inputs and output, so the output of the FLS can also be expressed as a function of its inputs namely, error and derivative of the error as $U = f(E, D)$ or $U = f(e, \dot{e}, K_e, K_d)$. Therefore, the actual control signal can be represented by combining meta functions in terms of input and output scaling factors, the error, the derivative of the error and integral of the error as $u = f(e, \dot{e}, \int e, K_e, K_d, K_a, K_b)$. Note that $f(.)$ represents a function and it is used for the sake of simplicity. Consequently, the general FPID controller structure becomes analogous to conventional PID structure. This analysis was examined in detail by considering the input space into several subplanes and mathematical expression of membership functions (Qiao and Muzimoto 1996) and the actual control signal can be written as

$$\begin{aligned} u = K_a K_0 + K_b K_0 t + (K_a K_e K_1 + K_b K_d K_2) e \\ + (K_b K_e K_1) \int e \, dt + (K_a K_d K_2) \dot{e} \end{aligned} \quad \textbf{(2.6)}$$

where K_0, K_1 and K_2 are the constants which are calculated with respect to antecedent and consequent membership functions. They are calculated with respect to values of consequent sets and apexes of the antecedent membership functions for corresponding inputs and subplanes. Here, K_0 is a nonlinear term, which converges to zero in time. So one can say that a FPID controller is similar to a conventional PID controller with variable gain. Then after eliminating the nonlinear term considering steady state behavior, the equivalent formulation of FPID and PID controllers can be achieved as follows:

$$u_{PID} = K_P e + K_I \int e \, dt + K_D \dot{e} \quad \textbf{(2.7)}$$

$$K_p = K_a K_e K_1 + K_b K_d K_2 \quad \textbf{(2.8)}$$

$$K_I = K_b K_e K_1 \quad \textbf{(2.9)}$$

$$K_D = K_a K_d K_2 \quad \textbf{(2.10)}$$

2.2 Internal Structure of Interval Type-2 Fuzzy PID Controllers

2.2.1 Interval type-2 fuzzy sets

Type-2 fuzzy sets (T2-FSs) are assumed as generalized form of those Type-1 Fuzzy Sets (T1-FSs). T1-FSs are also called as ordinary fuzzy sets since the first proposed fuzzy sets point out this type of fuzzy sets. Although T2-FSs are generalized form of T1-FSs and the base of it is a T1-FS, unfortunately T2-FSs cannot be easily described mathematically like T1-FSs due to their additional dimension (Mendel, 2007). The membership degree of a type-1 membership function (which means that a T1-FS is used as a membership function) is a crisp number, while the membership degree of a type-2 membership function is a T1-FS (Wagner and Hagras, 2010). Moreover, the membership degree of an interval type-2 membership function which is special case of type-2 membership functions, is also a type-1 fuzzy set but whole non-zero membership degrees always equals to one, in other words, the secondary grades of it always equals to one with respect to the input variable and corresponding primary membership. That is the why Interval Type-2 Fuzzy Sets (IT2-FSs) are called as interval. Moreover, one can notice that IT2-FSs are particular form of those T2-FSs and generalized form of those T1-FSs.

The input variable (x) definition in T1-FSs is also called as primary variable (x) for T2-FSs and IT2-FSs. The membership function corresponding to the primary variable can be called as primary membership function $(\mu(x))$ for both T1-FSs and T2-FSs. The grade of a primary membership function with respect to input value is called membership degree or membership grade for T1-FSs while it is called primary membership of x (J_x) for T2-FSs. Then one can observe that a T1-FS (A) consists of only a primary variable, a primary membership function and a membership grade while a T2-FS $(\tilde{A})$ includes uncountable number of primary membership function and membership degree and primary membership is in fact the union of the all membership degrees. The secondary variable (u) is an element of a primary membership. Here notice that a T2-FS include uncountable element of primary membership and these primary memberships generate the input of the secondary membership function $(\mu_{\tilde{A}}(x,u))$ which is special for T2-FSs when comparing to T1-FSs. The secondary membership function is a T1-FS and it might be triangular, trapezoid, gaussian, interval etc. The secondary grade is the weight of each secondary variable. Here, when the interval secondary membership function is used, an IT2-FS is obtained (Liang and Mendel, 2000). Therefore, a type-2 fuzzy set denoted by $\tilde{A}$, is characterized by a type-2 membership function as

$$\tilde{A} = \{((x,u), \mu_{\tilde{A}}(x,u)) \mid \; \forall x \in X, \; \forall u \in J_x \subseteq [0,1]\} \qquad \textbf{(2.11)}$$

where X is the domain of the input variable, x is the value of the input variable, u is the primary grade of a type-2 fuzzy set and J_x is the primary membership of a type-2 fuzzy set, $\mu_{\tilde{A}}(x,u)$ is the secondary membership function which is also T1-FS and defined as $0 \leq \mu_{\tilde{A}}(x,u) \leq 1$. Moreover, for a continuous universe of discourse a T2-FS can be expressed as follows:

$$\tilde{A} = \int_{x\in X} \int_{u\in J_x} \frac{\mu_A(x,u)}{(x,u)}, \subseteq [0,1] \qquad \textbf{(2.12)}$$

where $\iint$ denotes the union over all admissible x and u pair. The union of all primary memberships is called as Footprint of Uncertainty (FOU), the FOU represent in fact uncertainties in antecedent membership functions. In addition, the FOU is the superiority of a T2-FS. It is expressed by projecting it into the base plane (primary variable versus secondary variable plane), and after shading the closed area because, visualizing a T2-FS or IT2-FS in 2D instead of 3D is easier and more thoughtful. If all secondary grades of a T2-FS equal to one ($\mu_{\tilde{A}}(x,u) \leq 1 \text{for} \forall u \in J_x \subseteq [0,1]$), then an IT2-FS is obtained. An IT2-FS or T2-FS can be described in terms of Lower Membership Function (LMF) and Upper Membership function (UMF). Here lower and upper bound of footprint of the uncertainty (or shading area in 2D representation) are called LMF ($\underline{\mu}_{\tilde{A}}$) of type-2 fuzzy set and UMF ($\overline{\mu}_{\tilde{A}}$) of type-2 fuzzy set respectively. Obviously, an IT2-FS can be represented by the collection of a LMF and UMF and by the shading area between them.

The main differences between T1-FS, T2-FSs and IT2-FS are illustrated in following examples. First, consider a triangular membership function defined in the interval $x \in [1,9]$. The core of the membership function is at $c = 3$ and supports of the membership function are at $l = 3$ and $r = 7$. Here, some uncertainty about supports of the membership function is considered ($l = 3 \pm 1$ and $r = 7 \pm 1$) for T2-FS and IT2-FS. The input value is $x = 4.2$ for all following membership functions.

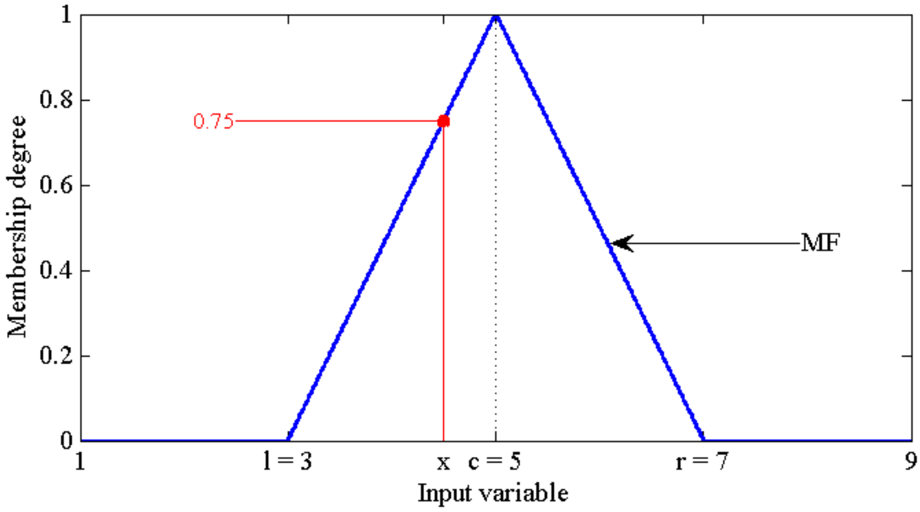

Figure 2.3 : Triangular type-1 fuzzy set.

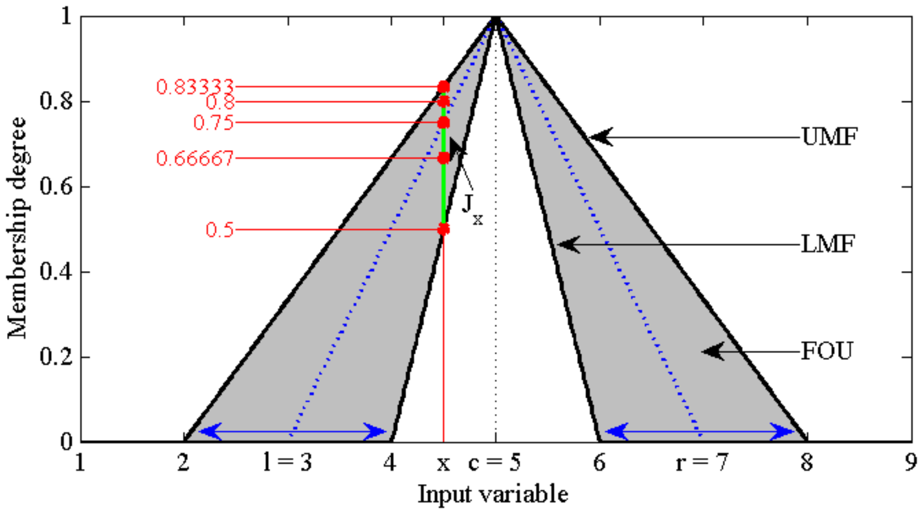

Figure 2.4 : Triangular type-2 fuzzy set.

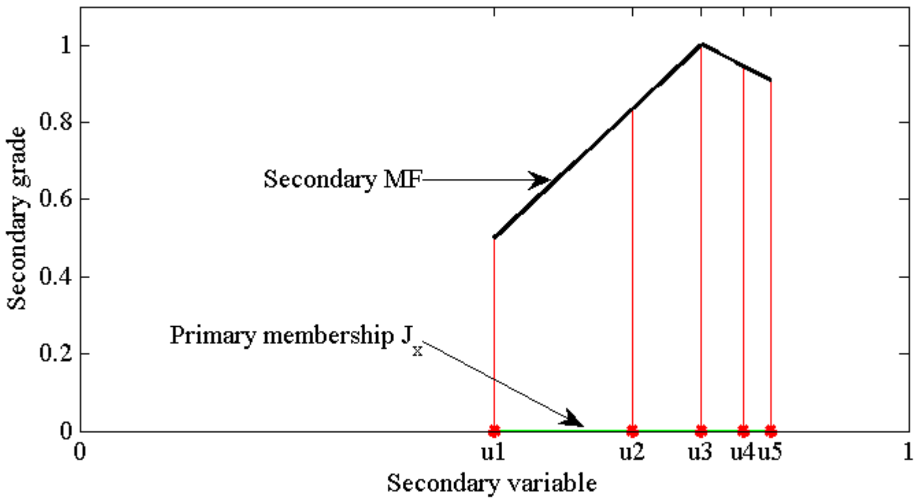

Figure 2.5 : Secondary membership function of type-2 fuzzy set.

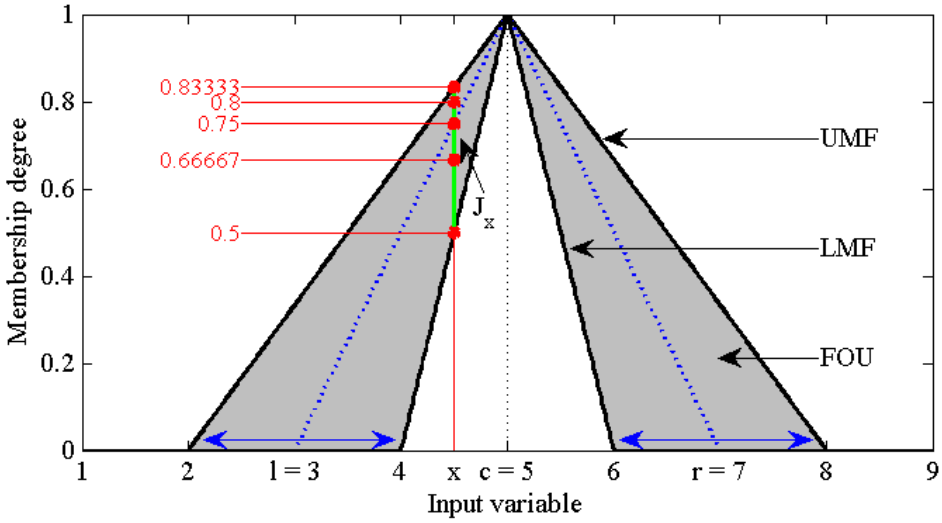

Figure 2.6 : Triangular interval type-2 fuzzy set.

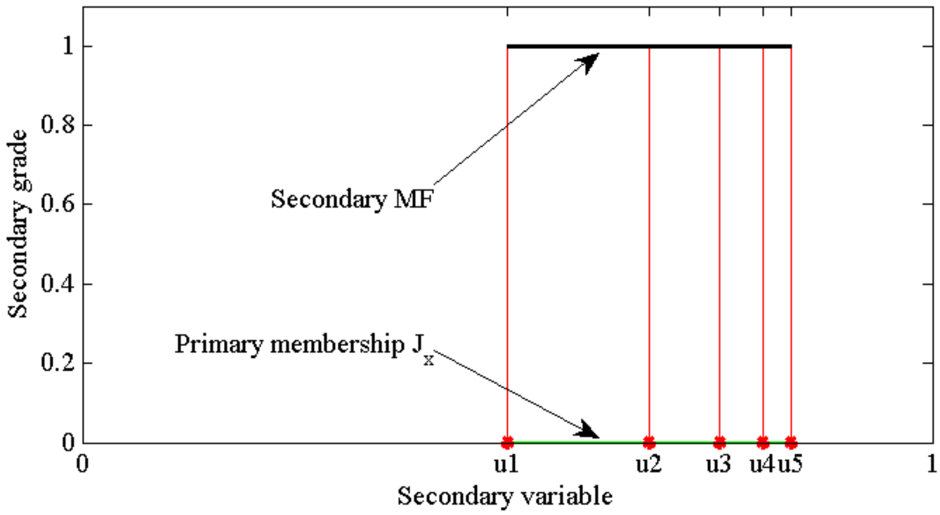

Figure 2.7 : Secondary membership function of interval type-2 fuzzy set.

As shown in Figure 2.3 the T1-FS has a crisp membership degree for a given input while T2-FS and IT2-FS have uncountable number of membership degree in an interval as shown in Figure 2.5 and Figure 2.7. Here only five points (red dots) are considered in order to better explanation of T2-FSs but remember that the number of element of primary membership is uncountable. Also T2-FS and IT2-FS have different membership degrees in the bounded interval for a given input value and this bounded interval is called primary membership and a T2-FS have uncountable number of primary membership in input domain with different values. Moreover, IT2-FSs can be explicitly described by only LMF and UMF because the secondary grades of IT2-FSs are constant and always equal to one as shown in Figure 2.10.

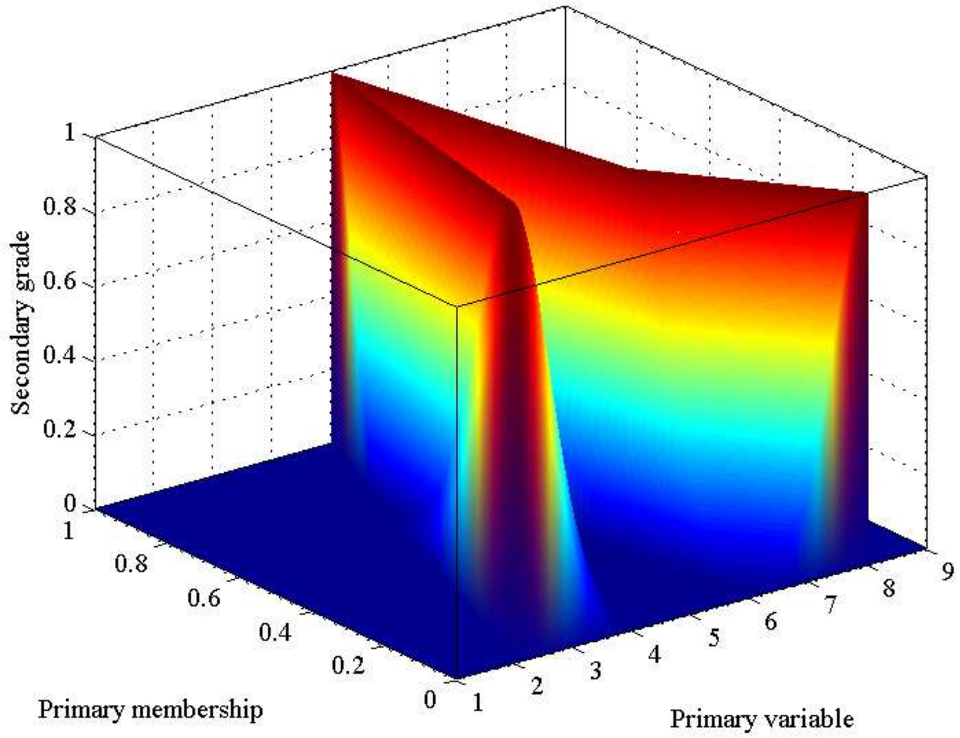

Figure 2.8 : 3D representation of type-2 fuzzy sets.

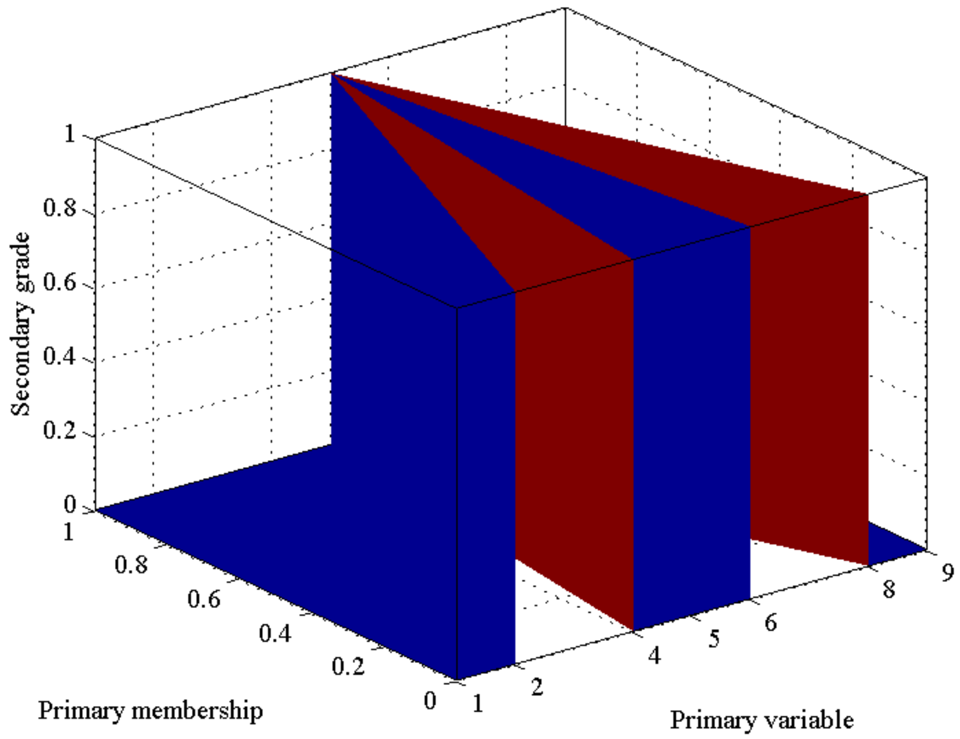

Figure 2.9 : 3D representation of interval type-2 fuzzy sets.

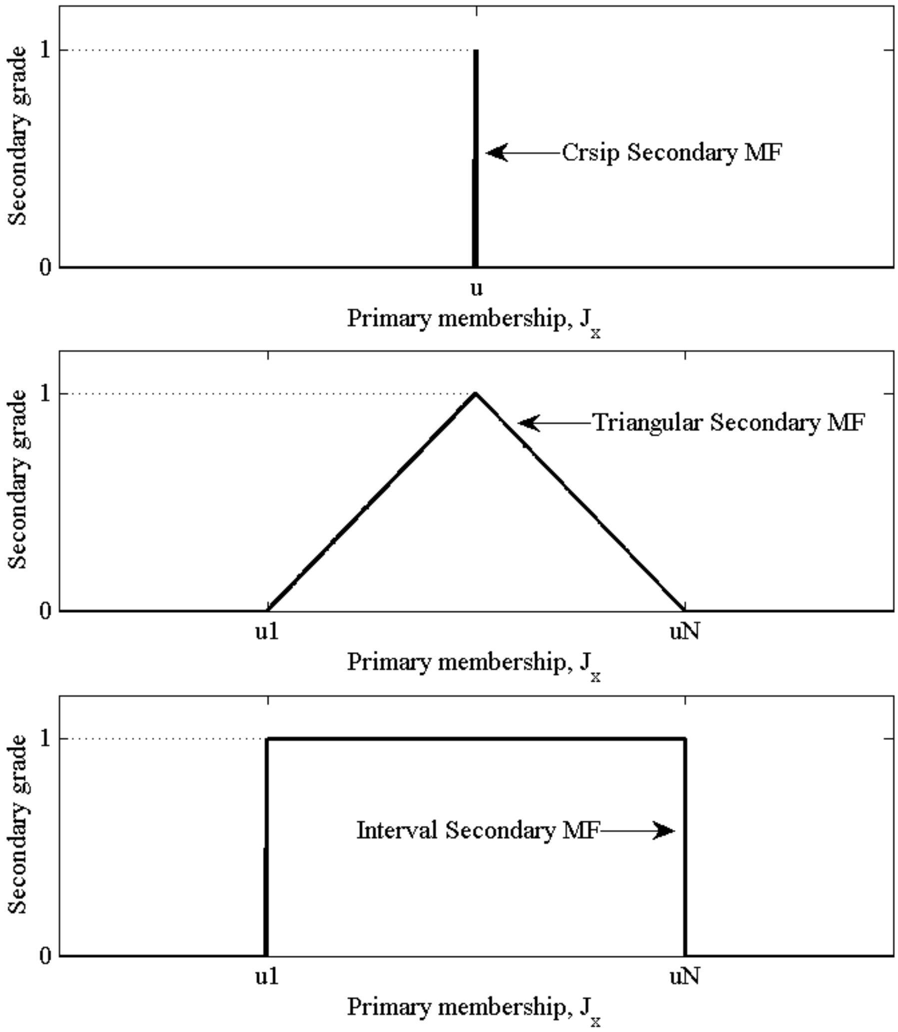

Figure 2.10 : Secondary grades of different type-2 fuzzy sets.

The main difference between T2-FS and IT2-FS is also illustrated in Figure 2.10, here the secondary grade of an IT2-FS is always 1 while T2-FS depends on the secondary membership function and secondary grade of an T1-FS is singleton. Here notice that a IT2-FS and its FOU can be explicitly described by LMF and UMF in 2D while a T2-FS can not. As stated in (Mendel, 2007), T1-FS is 2D (primary variable vs membership degree) while T2-FS is 3D (primary variable, secondary variable/primary membership vs secondary grade) as shown in Figure 2.8 and Figure 2.9. The further observation might be that the FOU provides extra dimension to T2-FSs and extra degrees of freedom to T2-FLSs comparing to type-1 counterparts.

Secondly, consider a Gaussian membership function, which is defined in the interval $x \in [1,9]$. The center point of the Gaussian membership function is at $c = 5$ and the standard deviation is $\sigma = 1$. Here, some uncertainty about center point is considered $(c = 5 \pm a, a = 0.5)$ for IT2-FS while standard deviation is constant. Therefore, LMF and UMF become in different fashion (unlike previous example). In addition, the input value is $x = 4$ for all following membership functions.

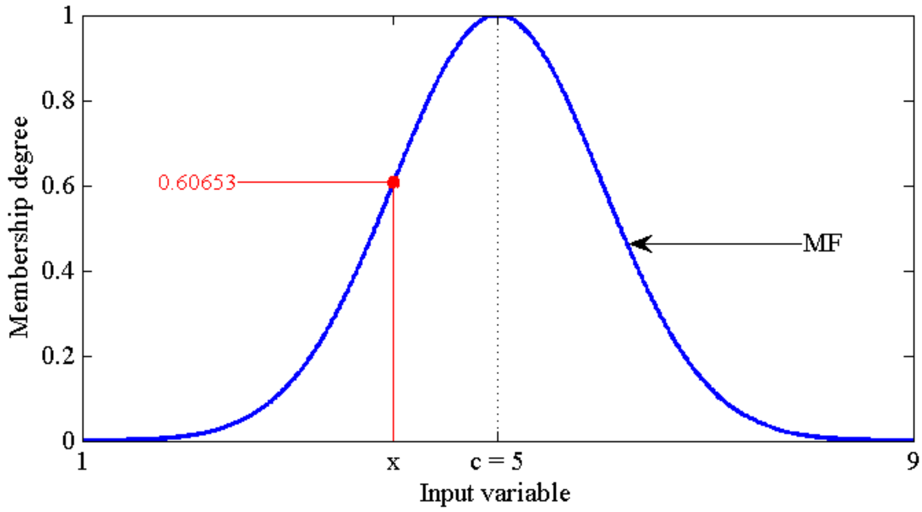

Figure 2.11 : Gaussian type-1 fuzzy set.

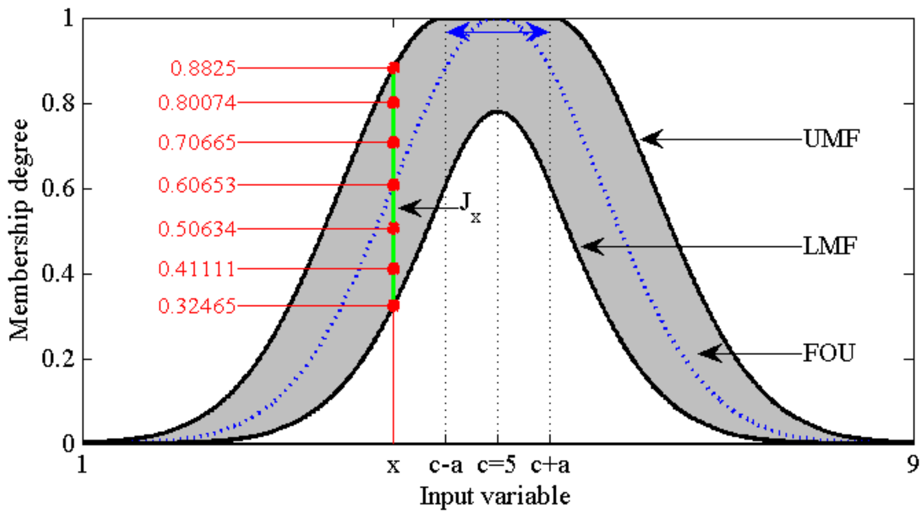

Figure 2.12 : Gaussian interval type-2 fuzzy set constucted via uncertainty.

Note that, the FOU can be generated in various methods, i.e. blurring (Wu, 2012), uncertainty (Mendel 2007) and scaling of the height of the LMFs (Kumbasar 2011). The blurring means that T2-FS is obtained by moving the base T1-FS on the horizontal axis as shown in Figure 2.13. The uncertainty points out the uncertainty about parameters of membership functions as shown in previous examples, Figure 2.7 and Figure 2.12. The scaling of the height of the LMFs means that T2-FS is obtained by changing the height of the base T1-FS as shown in Figure 2.14. In this thesis, the scaling method is preferred for IT2-FLS because LMF and UMF can be constructed in same fashion and the mathematical expression of the IT2-FS can be written as a function of its input variable and additional parameter which represents the height of the LMF. The additional parameter is defined in the interval [0,1]. Moreover, the size of the FOU changes with respect to the value of the additional parameter. While the parameter increases, the size of the FOU vanishes, while the parameter decreases, the size of the FOU expanded.

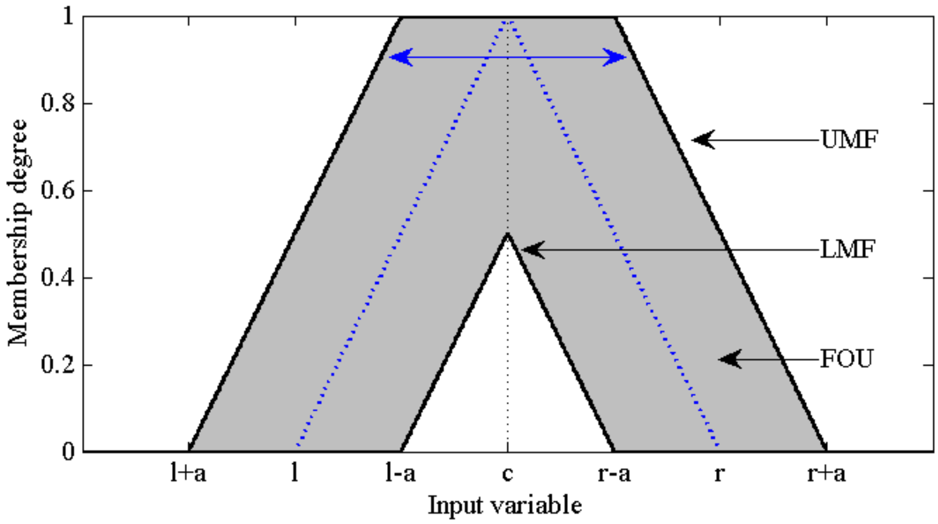

Figure 2.13 : Triangular interval type-2 fuzzy set constructed via blurring.

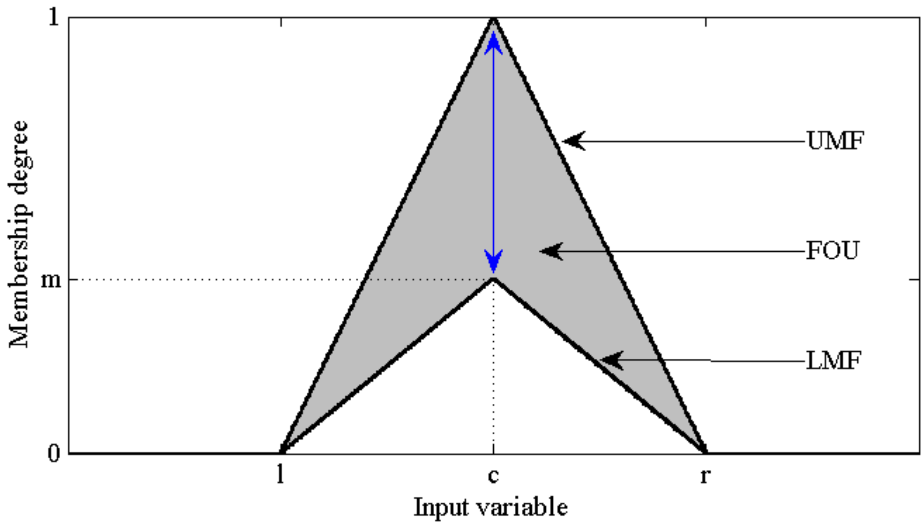

Figure 2.14 : Triangular interval type-2 fuzzy set constructed via scaling.

As shown in Figure 2.14, the LMF can be explicitly expressed in terms of UMF and the height value (m). That situation reduces the mathematical complexity of IT2-FSs while it still includes the FOU. Therefore, that is the why it is preferred in this thesis for constructing a IT2-FPD controllers.

2.2.2 Interval type-2 fuzzy logic systems

A fuzzy logic system that is described with at least one T2-FS is called as an Interval Type-2 Fuzzy Logic System (IT2-FLS). Similar to a Type-1 Fuzzy Logic Systems (T1-FLS), T2-FLS (or IT2-FLS) consist of four main parts: fuzzifier, fuzzy rule base, inference engine, defuzzifier as shown in Figure 2.15. However an additional part which is named type-reducer is used in T2-FLSs because T2-FLSs evaluate and calculate T2-FSs instead of T1-FSs. In this context, type-reducer, converts type-2 information to type-1 information which is only usable for defuzzifier, in details, the type-reducer combines the type-2 output fuzzy sets and leads to type-1 fuzzy sets which are also called as type-reduced sets, then the defuzzifier uses the type-reduced sets for defuzzification process. A simple block diagram of an IT2-FLS, which is also a particular case of a general Type-2 Fuzzy Logic System (T2-FLS) is given in Figure 2.16.

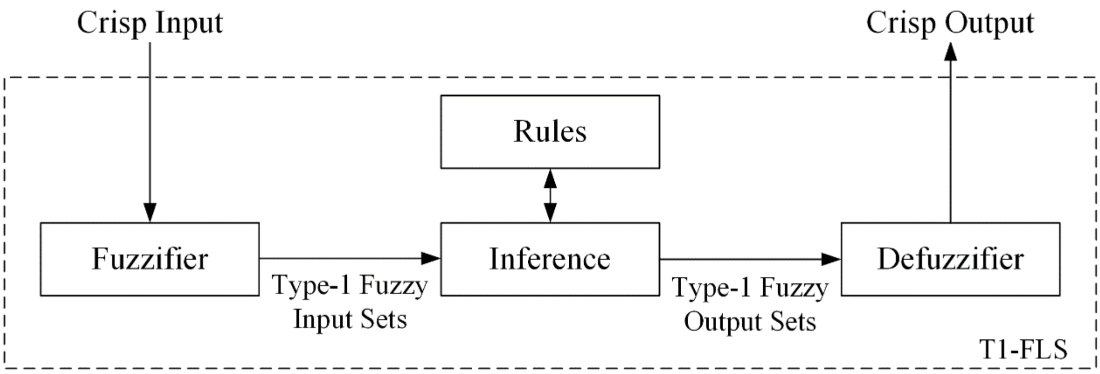

Figure 2.15 : Block diagram of type-1 fuzzy logic system.

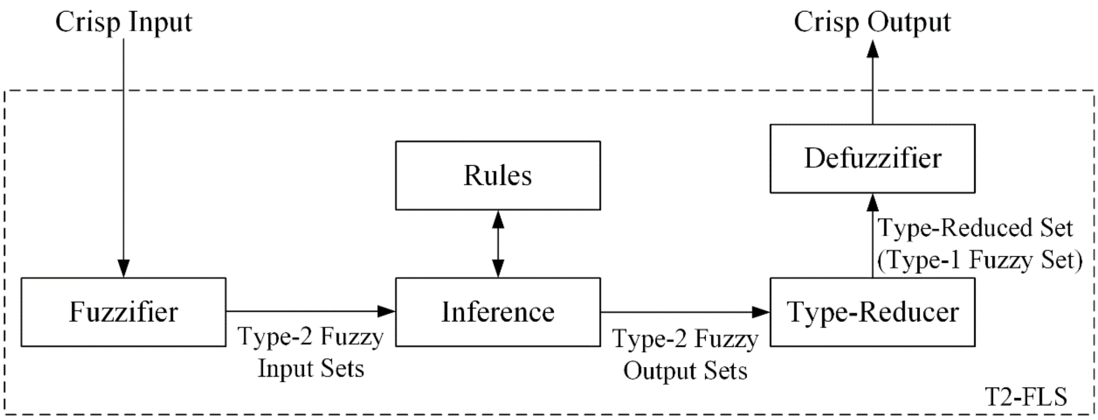

Figure 2.16 : Block diagram of interval type-2 fuzzy logic system.

In this thesis, a Takagi-Sugeno-type FLS is considered for IT2-FPID controller, which means that, the consequent part of the FLS is a crisp function of inputs or crisp constant values (singleton). Then by considering the fuzzy controller structure, antecedent membership functions of the IT2-FLS is defined by IT2-FSs while consequent membership functions of the IT2-FLS is defined by type-0 fuzzy sets (crisp or singleton). In addition, this type of FLS structure is also called as A2C0 system, pointing that antecedent part is type-2 and consequent part is singleton. Then a fuzzy rule of IT2-FLS of IT2-FPID controller can be expressed as follows:

$$R_q: \quad \text{IF} \quad E \text{ is } \tilde{A}_i \quad \text{and} \quad D \text{ is } \tilde{B}_j \quad \text{THEN} \quad U \text{ is } C_q \text{with } w_q \tag{2.13}$$

where E and D are inputs of the IT2-FLS, $\tilde{A}_i$ and $\tilde{B}_j$ are IT2-FLSs which are the antecedent membership functions of E and D inputs respectively, U is the output of the IT2-FLS, C_q is the consequent crisp set. Here, R_q is the rule number, q is the rule index and w_q is the weight of corresponding a fuzzy rule. The total firing interval of a rule is defined as

$$f_q = \left[\underline{f_q} \quad \overline{f}_q\right] \tag{2.14}$$

where

$$\underline{f_q} = \underline{\mu}_{\tilde{A}_i}(E) \cap \underline{\mu}_{\tilde{B}_j}(D) \tag{2.15}$$

$$\overline{f}_q = \overline{\mu}_{\tilde{A}_i}(E) \cap \overline{\mu}_{\tilde{B}_j}(D) \tag{2.16}$$

where $\underline{\mu}_{\tilde{A}_i}(E)$ is the member degree of a LMF of the error input E, $\overline{\mu}_{\tilde{A}_i}(E)$ is the member degree of an UMF of the error input E, $\underline{\mu}_{\tilde{B}_j}(D)$ is the member degree of a LMF of the derivative of the error input D, $\overline{\mu}_{\tilde{B}_j}(D)$ is the member degree of an UMF of the derivative of the error input D. Here, ∩ also denotes the t-norm operator, which is the algebraic product in this thesis. Obviously, the firing strength (or firing interval) of a rule in IT2-FLS has two values, the lower firing interval and the upper firing interval. However, firing intervals cannot be directly computed in defuzzification process so the type-reducer uses these firing intervals and converts them into the type-reduced set as shown in Figure 2.16. The crisp output of the IT2-FLS can be described with the type-reduced sets as shown (Liang and Mendel, 2000) thus; the output of the IT2-FLS can be formulized as follows:

$$U = \frac{U_l + U_r}{2} \quad \textbf{(2.17)}$$

where U_l and U_r are the left and right end points of the type-reduced set. It is shown that the end points of the type-reduced set can be defined for IT2-FLS as following (Mendel 2006):

$$U_{cos} = \bigcup \frac{\sum_{q=1}^{Q} f_q C_q}{\sum_{q=1}^{Q} f_q} = [U_l, U_r] \quad \textbf{(2.18)}$$

$$U_l = \min \frac{\sum_{q=1}^{k} \overline{f}_q \underline{C}_q + \sum_{q=k+1}^{Q} \underline{f}_q \underline{C}_q}{\sum_{q=1}^{k} \overline{f}_q + \sum_{q=k+1}^{Q} \underline{f}_q} \quad \textbf{(2.19)}$$

$$U_r = \max \frac{\sum_{q=1}^{k} \underline{f}_q \overline{C}_q + \sum_{q=k+1}^{Q} \overline{f}_q \overline{C}_q}{\sum_{q=1}^{k} \underline{f}_q + \sum_{q=k+1}^{Q} \overline{f}_q} \quad \textbf{(2.20)}$$

In IT2-FLS structure of IT2-FPID controller, uniformly distributed piecewise %50 overlapped triangular antecedent membership functions and crisp consequent sets are considered. For the reason when uniformly distributed piecewise %50 overlapped triangular antecedent membership functions are used, the output formulation of the fuzzy controller is derived easily after simplifications and it becomes analogous to conventional PID controller (Quio and Muzimoto, 1996). Moreover, the rule base structure is constructed as a symmetric as preferred in many control applications (Li and Gatland, 1996; Kumbasar et al. 2011). In this context and without losing generality, the antecedent membership functions of the employed IT2-FLS structure of IT2-FPID controller is constructed as follows:

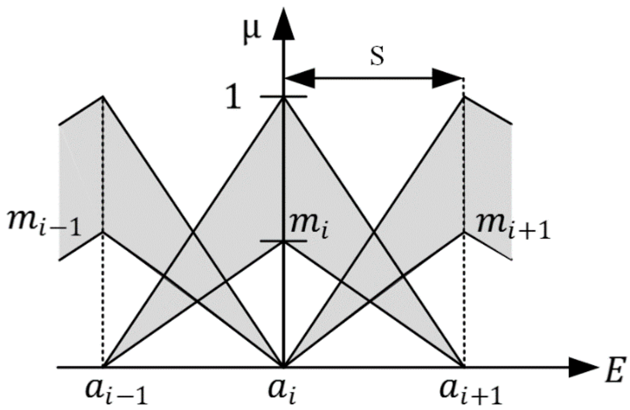

Figure 2.17 : Antecedent membership functions for the error input.

$$\underline{\mu}_{\tilde{A}_i}(E) = \begin{cases} \dfrac{a_{i+1} - E}{a_{i+1} - a_i} m_i & E > a_i \\ \dfrac{E - a_{i-i}}{a_i - a_{i-1}} m_i & E \leq a_i \end{cases} \tag{2.21}$$

$$\overline{\mu}_{\tilde{A}_i}(E) = \begin{cases} \dfrac{a_{i+1} - E}{a_{i+1} - a_i} & E > a_i \\ \dfrac{E - a_{i-i}}{a_i - a_{i-1}} & E \leq a_i \end{cases} \tag{2.22}$$

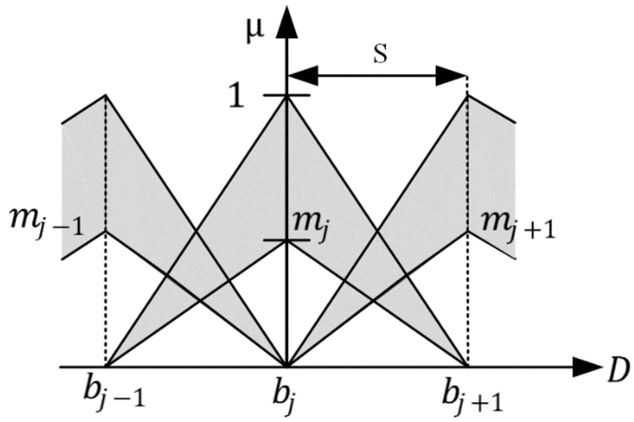

Figure 2.18 : Antecedent membership functions for the derivative of error input.

$$\underline{\mu}_{\tilde{B}_j}(D) = \begin{cases} \dfrac{b_{j+1} - D}{b_{j+1} - b_j} m_j & D > b_i \\ \dfrac{D - b_{j-i}}{b_j - b_{j-1}} m_j & D \leq b_i \end{cases} \tag{2.23}$$

$$\overline{\mu}_{\tilde{B}_j}(D) = \begin{cases} \dfrac{b_{j+1} - D}{b_{j+1} - b_j} & D > b_j \\ \dfrac{D - b_{j-i}}{b_j - b_{j-1}} & D \leq b_i \end{cases} \tag{2.24}$$

Here, S represents the distance between the apexes of membership functions as illustrated in Figure 2.15 and Figure 2.16,. It is also constant for all membership functions in the universe of discourse with respect to the total number of the membership functions of corresponding input. Clearly, depending on the S, the parameters of the antecedent membership functions is determined. For example, when total numbers of the membership functions is 5, then S becomes 0.5 and the cores of membership functions are chosen as {-1, -0.5, 0, 0.5, 1}.

2.2.3 Karnik-Mendel algorithm

The most commonly used type-reduction method is the iterative Karnik-Mendel type-reduction method. Wu pointed out two important features of Karnik-Mendel type-reduction methods, namely, inconsistency and addictiveness (Wu, 2012). The inconsistency means that LMFs and UMFs of the same IT2-FLS may or may not be used simultaneously in computing the type reduced set. The addictiveness means that the bounds of the type-reduced interval set change if the inputs change. Moreover, the globality and the exponentially convergence of the KM algorithm is clearly investigated. On the other hand, KM algorithm has high computational cost because of its iterative nature therefore some approximations are proposed in order to fasten the type-reduction process. Although five alternative approximations for type-reduction method are already used in many studies (Begian et al., 2008; Du and Ying, 2010; Nie and Tan, 2008; Wu and Tan, 2005; Wu and Mendel, 2002), KM type reduction method still provides more satisfactory results because of its two unique features. In this context, the Karnik-Mendel type reduction method is preferred in this thesis.

The KM algorithm determines the left end point (U_l) and the right end point (U_r) of the type reduced set ($U_{TR} = [U_l \quad U_r]$) and left and right switching points (L and R) separately. The steps of KM algorithm for computing left and right end points are summarized in (Wu and Mendel, 2007). Here notice that the bottleneck of the IT2-FLSs is to determine the end points of the type reduced sets of the IT2-FLS. In brief, the left and right end points of the type-reduced set and SPs are determined separately by two iterative algorithms as explained below.

Consequently following steps should be performed for computing U_l:

Step 1 : Sort lower values of consequents ($\underline{C}_q$ where $q = 1,2,\dots,Q$ and Q is the total number of rules) in increasing order and then match the firing intervals with respect to new index of consequents.

$$\underline{C}_1 \leq \underline{C}_2 \leq \cdots \leq \underline{C}_Q \quad \textbf{(2.25)}$$

$$\underline{f}_1 \leq \underline{f}_2 \leq \cdots \leq \underline{f}_Q \quad \textbf{(2.26)}$$

$$\overline{f}_1 \leq \overline{f}_2 \leq \cdots \leq \overline{f}_Q \quad \textbf{(2.27)}$$

Step 2 : Initialize the algorithm by setting initial total firing intervals as follows:

$$f_q = \frac{\underline{f}_q + \overline{f}_q}{2}, \qquad q = 1,2,\dots,Q \tag{2.28}$$

and compute the initial output value for the left end point of type reduced set (U_0) with respect to calculated initial total firing interval as

$$U_0 = \frac{\sum_{q=1}^{Q} f_q \underline{C}_q}{\sum_{q=1}^{Q} f_q} \tag{2.29}$$

Step 3 : Find a candidate left switching point (L) such that

$$\underline{C}_L \le U_0 \le \underline{C}_{L+1}, \qquad 1 \le L \le Q-1 \tag{2.30}$$

Step 4 : Update the total firing intervals with respect to the obtained candidate switching point as follows:

$$f_q = \begin{Bmatrix} \overline{f}_q & q \le L \\ \underline{f}_q & q > L \end{Bmatrix}, \qquad q = 1,2,\dots,Q \tag{2.31}$$

and compute the new output (candidate left end point of the type-reduced set, U') with respect to updated common firing strength as follows:

$$U' = \frac{\sum_{q=1}^{Q} f_q \underline{C}_q}{\sum_{q=1}^{Q} f_q} \tag{2.32}$$

Step 5: If the initial output do not equal to new output, go to Step 3 for next iteration after setting new output to the initial output in order to use in next iteration as

$$U_0 = U' \tag{2.33}$$

otherwise, stop the algorithm, set the left end point of the type reduced set (U_l) and optimal left SP (L^*) as follows:

$$U_l = U_0 = U' \tag{2.34}$$

$$L^* = L \tag{2.35}$$

Consequently, following steps should be performed for computing U_r:

Step 1: Sort upper values of consequents ($\overline{C}_q$ where $q = 1,2, \dots, Q$ and Q is the total number of rules) in increasing order and then match the firing intervals with respect to new index of consequents.

$$\overline{C}_1 \leq \overline{C}_2 \leq \cdots \leq \overline{C}_Q \tag{2.36}$$

$$\overline{f}_1 \leq \overline{f}_2 \leq \cdots \leq \overline{f}_Q \tag{2.37}$$

$$\underline{f}_1 \leq \underline{f}_2 \leq \cdots \leq \underline{f}_Q \tag{2.38}$$

Step 2 : Initialize the algorithm by setting initial total firing intervals as follows:

$$f_q = \frac{\underline{f}_q + \overline{f}_q}{2}, \qquad q = 1,2, \dots, Q \tag{2.39}$$

and compute the initial output value for the right end point of type reduced set (U_0) with respect tocalculated initial total firing interval as as

$$U_0 = \frac{\sum_{q=1}^{Q} f_q \overline{C}_q}{\sum_{q=1}^{Q} f_q} \tag{2.40}$$

Step 3 : Find a candidate right switching point (R) such that

$$\overline{C}_R \leq U_0 \leq \overline{C}_{R+1}, \qquad 1 \leq R \leq Q - 1 \tag{2.41}$$

Step 4: Update the total firing intervals with respect to the obtained candidate switching point as follows:

$$f_q = \begin{Bmatrix} \underline{f}_q & q \leq R \\ \overline{f}_q & q > R \end{Bmatrix}, \qquad q = 1,2, \dots, Q \tag{2.42}$$

and compute the new output (candidate right end point of the type-reduced set, U') with respect to updated common firing strength as follows:

$$U' = \frac{\sum_{q=1}^{Q} f_q \overline{C}_q}{\sum_{q=1}^{Q} f_q} \tag{2.43}$$

Step 5: If the initial output do not equal to new output, go to Step 3 for next iteration after setting new output to the initial output in order to use in next iteration as

$$U_0 = U' \quad \textbf{(2.44)}$$

otherwise, stop the algorithm, set the right end point of the type reduced set (U_r) and the optimal right SP (R^*) as follows:

$$U_r = U_0 = U' \quad \textbf{(2.45)}$$

$$R^* = R \quad \textbf{(2.46)}$$

3. ALTERNATIVE APPROACHES TO KM TYPE-REDUCTION

In this section, a visual method, which is called the Surface of Switching Points Map (S-MAP), is proposed in order to better analyze the determination of SPs of the KM algorithms (Sakalli et al., 2014a). In brief, the S-MAP helps us to understand and analyze the selection of SPs of the KM algorithm without using its iterative procedure. Then a novel type-reduction method which is called Boundary Function based Karnik-Mendel (BF-KM) type-reduction method is proposed (Dodurka et al., 2014) in order to reduce computational burden of KM algorithm. In brief, The BF-KM is used for determining the SPs of the IT2-FPID controllers for a given input set. Then, a comparison study between BF-KM and other KM based type reduction methods is given. Finally, an illustrative numerical example is presented for the sake of clear demonstration of the proposed alternative methods.

3.1 Surface of Switching Points Map (S-MAP)

The KM algorithm determines iteratively the left and right end points of the type-reduced set with respect to the values of SPs for a given input set as explained in previous section. However, the iterative nature of the KM algorithm inhibits the estimation of SPs for any given input set. In this context, the S-MAP is a useful method for visualizing and understanding the selection of the SPs of the KM algorithm. Note that S-MAP is an auxiliary method in order to investigate the bases of KM algorithm. In S-MAP each SP set is represented by a certain region, thus, the values of SPs can be visualized corresponding to the values of inputs. Each region on the S-MAP also points out different SP set of KM algorithm and different control laws of IT2-FPID controller. Moreover, the S-MAP is a helpful method especially for IT2-FPID controller structure, since the effect of the size of the FOU can easily interpreted via the S-MAP. For example, when uniformly distributed piecewise %50 overlapped triangular IT2-FS is used for antecedent membership functions of 4-rule IT2-FPID controller, the size of FOU directly depends on the heights of the LMFs (m_i) of IT2-FLS. Therefore, we can clearly say that the areas of the different regions on the S-MAP is changed with respect to the values of the heights of the LMFs (m_i) of IT2-FLS.

In this visual method, values of the SPs are project to a three dimensional space with respect to the input variables. In the three-dimensional space, a point is expressed with three terms, the values of inputs E and D (for x-axis and y-axis) and the translated SPs values (for z-axis). For this purpose, first of all input space ($E \in [-1,1]$ and $D \in [-1,1]$) quantized into several pieces, notice that if the density increases (or number of grids increases or the value of quantization interval decreases), the accuracy of the S-MAP increases. Then, the SPs are calculated separately for all point on the input space grid and the obtained SPs (L^* and R^*). They are combined in an additional parameter which is also called as Translated SP value (T_{SP}) and defined as follows:

$$T_{SP} = L^* \times 10^{d(N-1)} + R^* \tag{3.1}$$

where R^* is the right SP of the KM algorithm, L^* is the left SP of the KM algorithm, N is the total number of rules, $d(.)$ is a function that indicates the number of digits on its input. In order to be more precise consider following illustrative cases, when $L^* = 3$, $R^* = 15$ and $N = 25$ then $T_{SP} = 0315$, when $L^* = 12$, $R^* = 15$ and $N = 25$ then $T_{SP} = 1215$, when $R^* = 8$, $L^* = 6$ and $N = 9$ then $T_{SP} = 68$. Here, T_{SP} has totally 2n digits and its first n digit represent the left SP (L^*) while the last n digit represents right SP (R^*). Then, the obtained T_{SP} values for grid points on the input space can be drawn in 3D sketch corresponding to the input values. However, in this case, the 3D figure becomes challenging to understand because of scaling problems since the different values of T_{SP} may become quite different ($L^* = 1$, $R^* = 2$ and $N = 25$ then $T_{SP_1} = 0102$ while $L^* = 22$, $R^* = 24$ and $N = 25$ then $T_{SP_2} = 2224$, thus, $T_{SP_1} = 0102 \ll 2224 = T_{SP_2}$). In this context to overcome this problem, the different values of T_{SP} is indexed in ascending order as $\{0,1,\dots,n\}$ here n represent the total number of different-valued T_{SP} and the number of the regions on the S-MAP. Then, the values of T_{SP} are projected into input space ($E \in [-1,1]$ and $D \in [-1,1]$) via a pseudocolor plot method which is alike a checkerboard. Finally, the S-MAP can be drawn in 2D, and each different region on the S-MAP indicates different values of SPs of the KM algorithm.

In order to better understand the concept of the S-MAP, let consider the following example; S-MAPs for 4-rule IT2-FLSs with different sizes of the FOU. Note that, for this example, the heights of all LMFs is considered as equal for the sake of simplicity ($m_1 = m_2 = m_3 = m_4$).

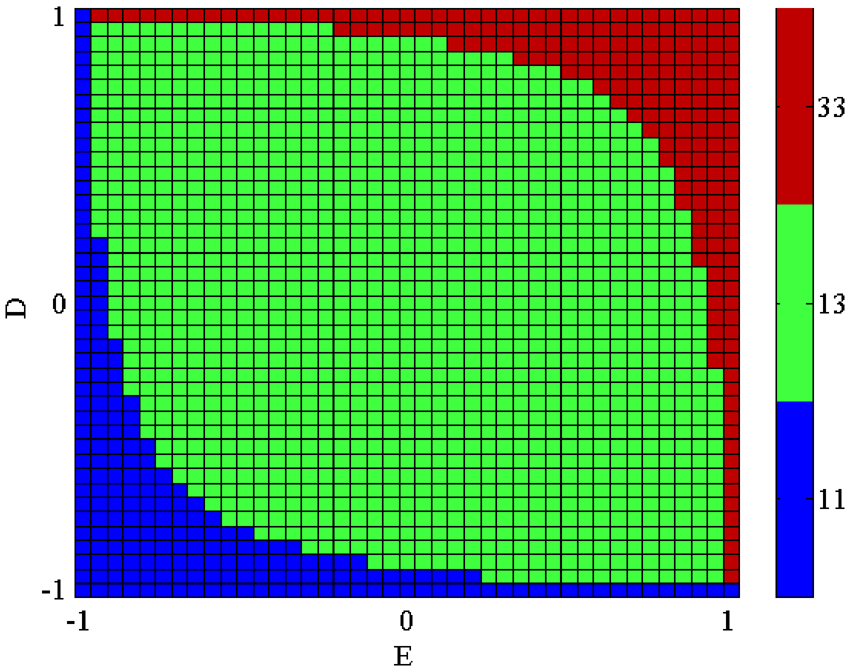

Figure 3.1 : S-MAP for 4-rule IT2-FLS ($m = 0.2$).

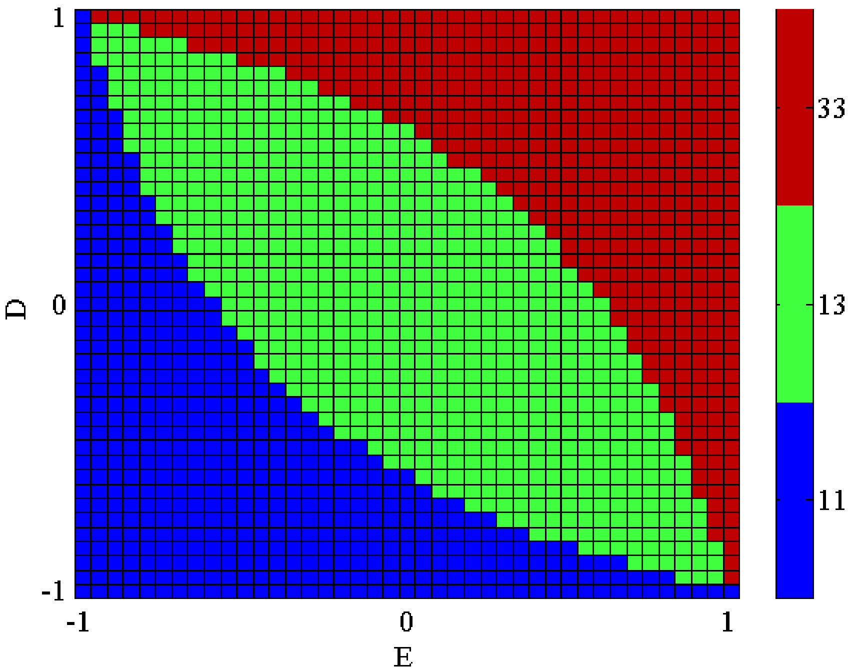

Figure 3.2 : S-MAP for 4-rule IT2-FLS ($m = 0.5$).

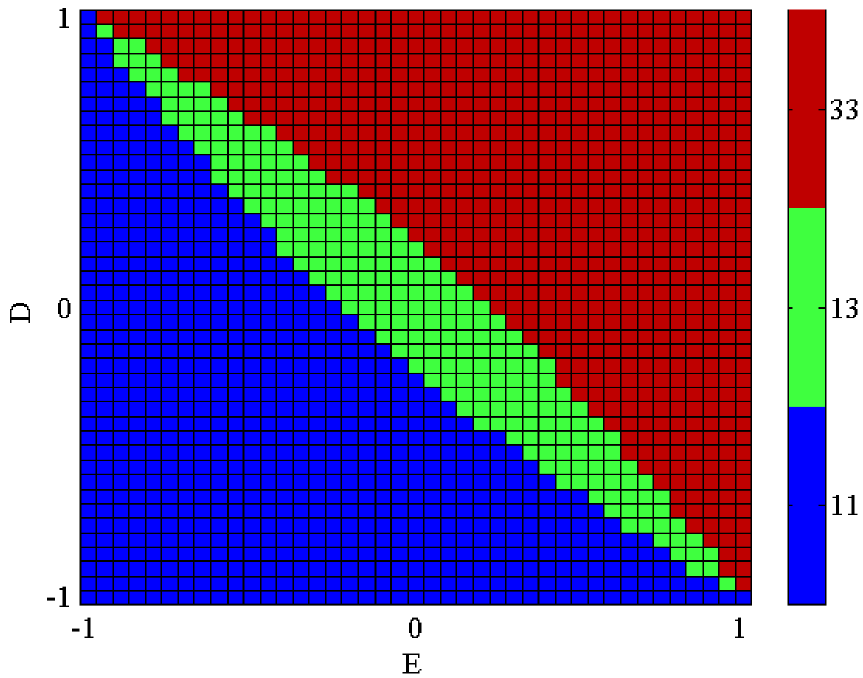

Figure 3.3 : S-MAP for 4-rule IT2-FLS ($m = 0.8$).

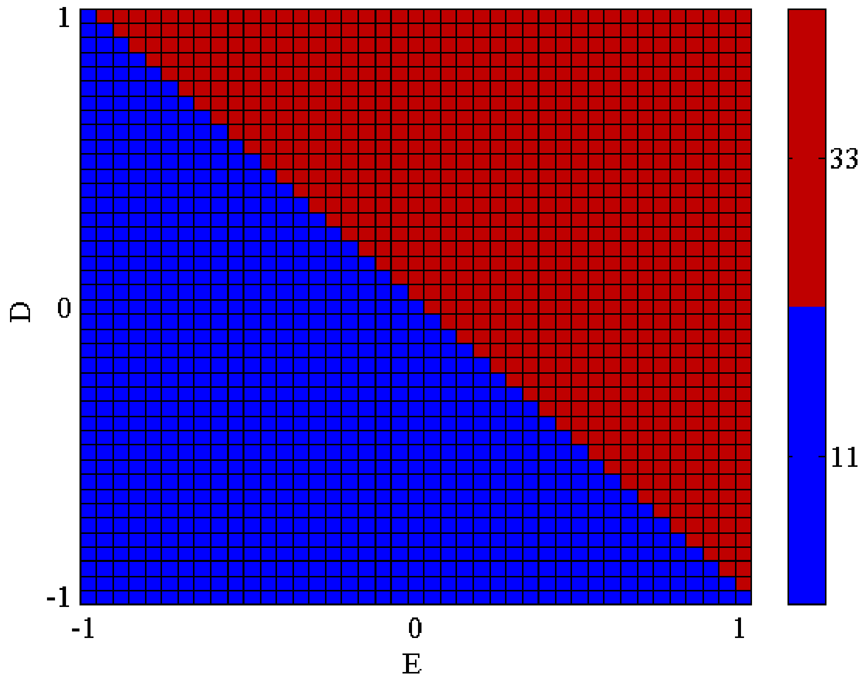

Figure 3.4 : S-MAP for 4-rule IT2-FLS ($m = 1$).

As shown in Figure 3.1, Figure 3.2 and Figure 3.3, there are only three different colored regions for 4-rule IT2-FLS with respect to the three SPs; the blue region for $\{L^* = 1, R^* = 1\}$, the green region for $\{L^* = 1, R^* = 3\}$ and the red region for $\{L^* = 3, R^* = 3\}$. In addition, while the height of the LMFs decreases (or the size of the FOU increases), the green region expands and other regions shrink for 4-rule IT2-FLS. Interestingly, the green region for 4-rule IT2-FLS is vanished in case of $M = 1$ as shown in Figure 3.4. Because the FOU vanishes for 4-rule IT2-FLS structure and some boundaries disappear and also IT2-FLS reduces into T1-FS.

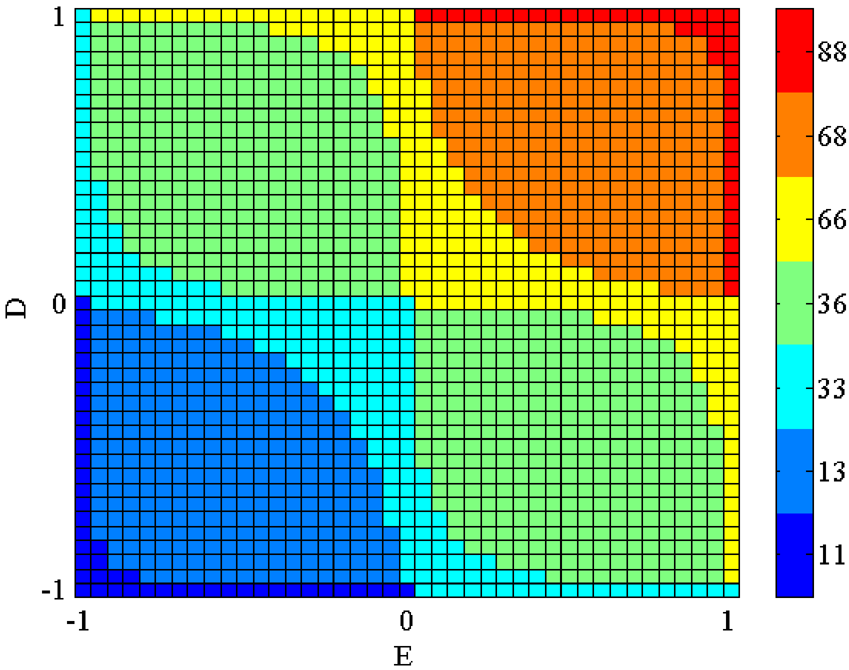

Figure 3.5 : S-MAP for 9-rule IT2-FLS ($m = 0.2$).

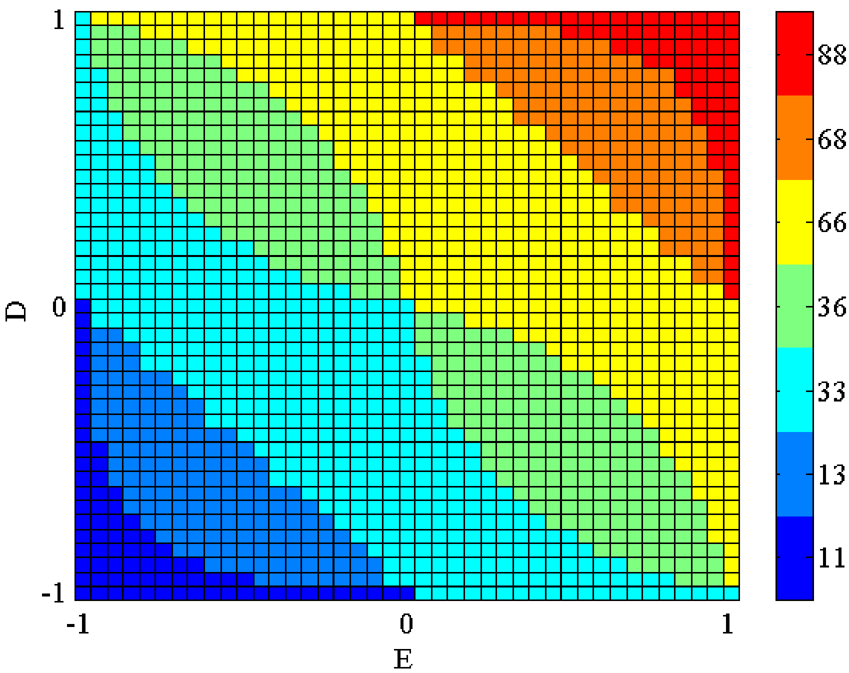

Figure 3.6 : S-MAP for 9-rule IT2-FLS ($m = 0.5$).

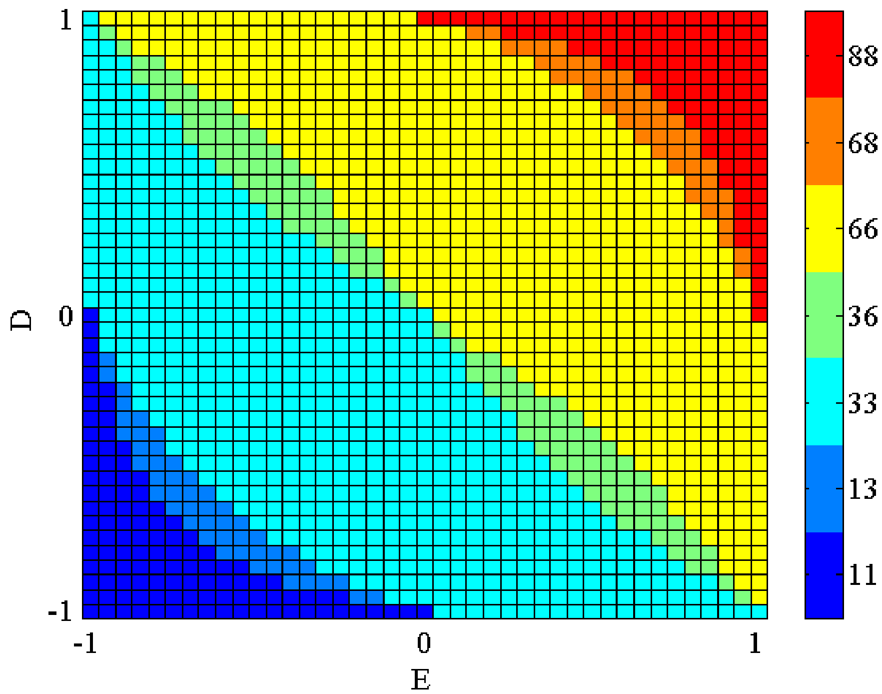

Figure 3.7 : S-MAP for 9-rule IT2-FLS (m = 0.8).

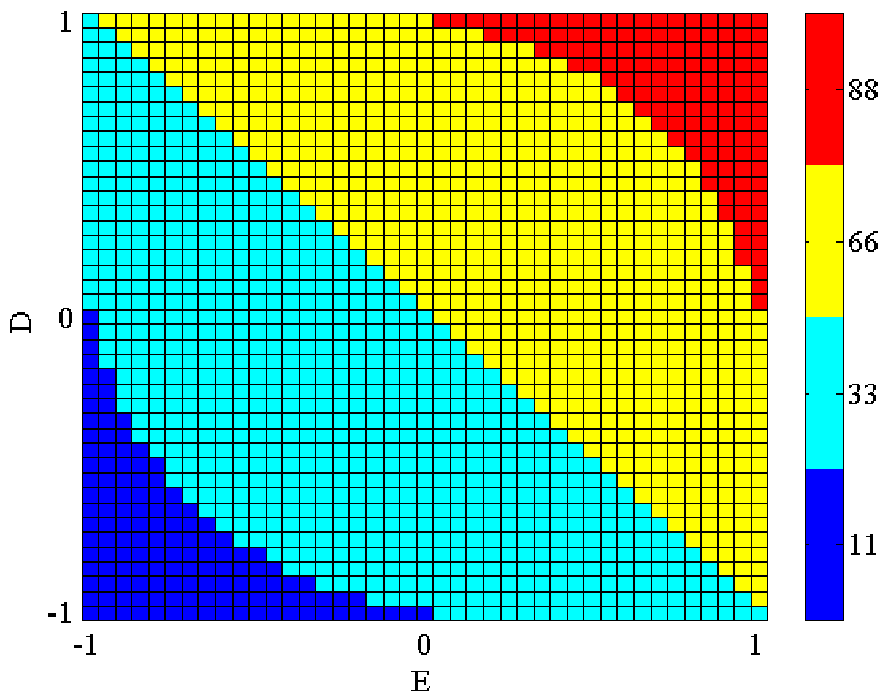

Figure 3.8 : S-MAP for 9-rule IT2-FLS (m = 1).

Let consider a 9-rule IT2-FLS as a second example as illustrated in Figure 3.5 to Figure 3.8. Here again, the heights of all membership functions are assumed as equal ($m_1 = m_2 = m_3 = m_4 = m_5 = m_6$). Here, there are totally seven colored regions for 9-rule IT2-FLS and the area of the regions vary depends on the size of the FOU as shown in Figure 3.5 to Figure 3.7. Also some regions vanish when IT2-FLS reduces to T1-FLS as shown in Figure 3.8. Obviously, while the number of rules increases, the regions on the S-MAP increases. Furthermore, there are always three different colored region at the plane which is defined by between the apexes of membership functions. For example, there are only one cell between apexes of membership functions of 4-rule IT2-FLS, while there are four cells between apexes of membership functions of 9-rule IT2-FLS.

Consequently, outcomes of the S-MAP analysis can be interpreted for simplest IT2-FPID controller as; the left and the right SPs of the KM algorithms can be clearly displayed corresponding to the values of the inputs on the S-MAP. Moreover each region on the S-MAP points out different SPs of the KM algorithm (for instance $\{L^* = 1, R^* = 3\}$). Also, the size of the FOU (in terms of M_i) changes the area around the origins of planes on the S- MAP. In addition the three regions on the S-MAP may be determined by two conditions in particular circumstances as mentioned in Section 3.2.

3.2 Boundary Function based Karnik Mendel (BF-KM) Algorithm

In this section, we will propose BF-KM for determining the switching points of the IT2-FPID controller (Dodurka et al., 2014). The derivation of the BF-KM is derived for general structure of the IT2-FLS. For this purpose, the decomposition property is used for analytical derivations to determine the optimal SPs of the KM for IT2-FPID controllers. The decomposition property is a simple constructive procedure which has been used for T1-FLSs (Li et al., 1997) and generalized for IT2-FLSs (Kumbasar et al., 2013d) and it will facilitate the determination of the SPs of KM algorithm significantly because the proposed methodology will eliminate the iterative nature of the KM algorithm. The proposed methodology consists of two main steps, decomposing the IT2-FPID controller model into several interval type-2 fuzzy SubControllers (SCs) with respect to the membership functions. Then determining the optimal SPs of the SCs to obtain the output of the IT2-FPID controller using the presented derived equations of original KM algorithm.

It has been shown that the fuzzy system can be decomposed into SCs so that the rule base can be portioned into square blocks in which all the fuzzy inference operations can be performed (Kumbasar et al. 2013). According to the decomposition property, the rule base is partitioned in the 2^{2*g} SCs as shown in Figure 3.9. Moreover the partitioned SCs can be indexed as $SC_{q,w}$ as follows:

$$SC_{(q,w)}(q, w \in \{-g, \dots, -2, -1, 0, 1, 2, \dots, g-1\}) \quad \textbf{(3.2)}$$

where index q depends on the smallest index of the fired MFSs of $\tilde{A}_i$ in a SC and similarly w depends on the smallest index of the fired MFs of $\tilde{B}_j$ in a SC. Here q and w represent the rule indexes of antecedent membership functions in fuzzy rule base with respect to the given input values.

In this thesis, we will examine the generic $SC_{q,w}$ for an easier analysis as shown in Figure 3.9 as the grey area. For the generic $SC_{q,w}$, the corresponding antecedent membership functions of error input are $\tilde{A}_i$, $\tilde{A}_{i+1}$and antecedent membership functions for derivative of error are $\tilde{B}_i$, $\tilde{B}_{i+1}$ and consequents are C_h, C_{h+1}, C_{h+2} as illustrated asgrey area in Figure 3.9. Thus, in total the number of possible activated rules is four because piecewise %50 overlapped triangular membership function is used in antecedent part of IT2-FIS. Moreover the Activated rules Index set (AI) for the $SC_{q,w}$which represent the active rule indexes is as follows:

$$AI_{SC(q,w)} = [n, n+1, n+T, n+T+1] \quad \textbf{(3.3)}$$

Thus, Equations (11) and (12) can be redefined as follows:

$$U_l = \min_{L \in [n, n+1, n+T]} (U_l^L) = U_l^{L^*} \quad \textbf{(3.4)}$$

$$U_r = \max_{R \in [n, n+1, n+T]} (U_r^R) = U_r^{R^*} \quad \textbf{(3.5)}$$

It can be clearly seen that there only three candidates for determining L^* and R^* since $L, R \in [n, n+1, n+T]$ due to only four active rule index. Taking in account of that, the candidate values of L^* and R^* can be defined under the following KM conditions with respect to Equation 2.19 and Equation 2.20.

$$L^* = \begin{cases} n, & \text{if } U_l^n \leq U_l^{n+1} \text{and} U_l^n \leq U_l^{n+T} \\ n+1, & \text{if } U_l^{n+1} \leq U_l^n \text{and} U_l^{n+1} \leq U_l^{n+T} \\ n+T, & \text{if } U_l^{n+T} \leq U_l^n \text{and} U_l^{n+T} \leq U_l^{n+1} \end{cases} \quad \textbf{(3.6)}$$

$$R^* = \begin{cases} n, & \text{if } U_r^n \geq U_r^{n+1} \text{and} U_r^n \geq U_r^{n+T} \\ n+1, & \text{if } U_r^{n+1} \geq U_r^n \text{and} U_r^{n+1} \geq U_r^{n+T} \\ n+T, & \text{if } U_r^{n+T} \geq U_r^n \text{and} U_r^{n+T} \geq U_r^{n+1} \end{cases} \tag{3.7}$$

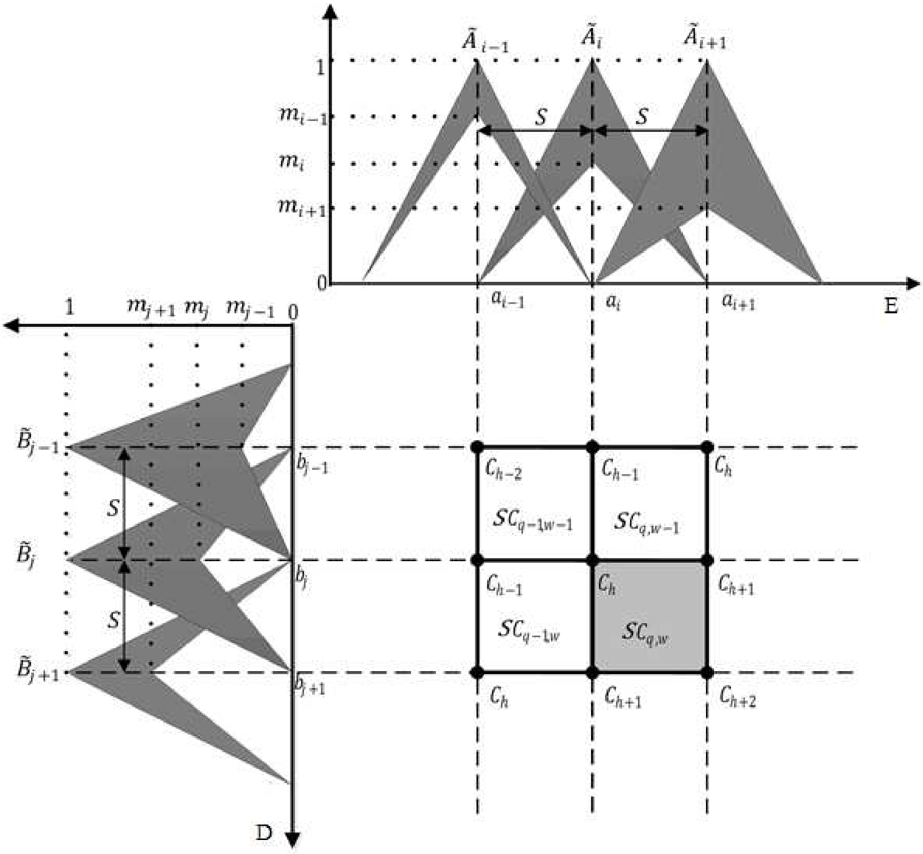

Figure 3.9 : Illustration of the decomposition property of the IT2-FPID controller.

The presented KM conditions can be stated explicitly if and only if the inequalities on the right hand side in Equation 3.6 and Equation 3.7 can be determined. In order to solve these inequalities, firstly the open form of functions in inequalities of U_l^L and U_r^R $(\forall\, L, R \in [n, n+1, n+T])$ must be determined. Thus, the total firing interval sets (F^n) are calculated for $\forall\, n \in AI_{SC(q,w)}$, i.e. for each activated SC with respect to the input variables. The corresponding firing interval sets can be calculated with respect to Equation 2. 14 to Equation 2. 16 as follows:

$$F^n = \left[\underline{\mu}_{\tilde{A}_i}(E) \cap \underline{\mu}_{\tilde{B}_j}(D), \quad \overline{\mu}_{\tilde{A}_i}(E) \cap \overline{\mu}_{\tilde{B}_j}(D)\right] \tag{3.8}$$

$$F^{n+1} = \left[\underline{\mu}_{\tilde{A}_i}(E) \cap \underline{\mu}_{\tilde{B}_{j+1}}(D), \quad \overline{\mu}_{\tilde{A}_i}(E) \cap \overline{\mu}_{\tilde{B}_{j+1}}(D)\right] \tag{3.9}$$

$$F^{n+T} = \left[\underline{\mu}_{\tilde{A}_{i+1}}(E) \cap \underline{\mu}_{\tilde{B}_j}(D), \quad \overline{\mu}_{\tilde{A}_{i+1}}(E) \cap \overline{\mu}_{\tilde{B}_j}(D)\right] \tag{3.10}$$

$$F^{n+T+1} = \left[\underline{\mu}_{\tilde{A}_{i+1}}(E) \cap \underline{\mu}_{\tilde{B}_{j+1}}(D),\quad \overline{\mu}_{\tilde{A}_{i+1}}(E) \cap \overline{\mu}_{\tilde{B}_{j+1}}(D)\right] \qquad \textbf{(3.11)}$$

where the membership grades of the $\underline{\mu}_{\tilde{A}_i}(E)$, $\underline{\mu}_{\tilde{A}_{i+1}}(E)$, $\overline{\mu}_{\tilde{A}_i}(E)$ and $\overline{\mu}_{\tilde{A}_{i+1}}(E)$ for error input in activated SC ($E \in [a_i, a_{i+1,}]$) can be calculated as

$$\underline{\mu}_{\tilde{A}_i}(E) = \frac{a_{i+1} - E}{a_{i+1} - a_i} m_i \qquad \textbf{(3.12)}$$

$$\underline{\mu}_{\tilde{A}_{i+1}}(E) = \frac{E - a_i}{a_{i+1} - a_i} m_{i+1} \qquad \textbf{(3.13)}$$

$$\overline{\mu}_{\tilde{A}_i}(E) = \frac{a_{i+1} - E}{a_{i+1} - a_i} \qquad \textbf{(3.14)}$$

$$\overline{\mu}_{\tilde{A}_{i+1}}(E) = \frac{E - a_i}{a_{i+1} - a_i} \qquad \textbf{(3.15)}$$

Similarly, the membership grades of the $\underline{\mu}_{\tilde{B}_j}(D)$, $\underline{\mu}_{\tilde{B}_{j+1}}(D)$, $\overline{\mu}_{\tilde{B}_j}(D)$ and $\overline{\mu}_{\tilde{B}_{j+1}}(D)$ for the derivative of the error input in activated SC ($D \in [b_j, b_{j+1}]$) can be calculated as

$$\underline{\mu}_{\tilde{B}_j}(D) = \frac{b_{j+1} - D}{b_{j+1} - b_j} m_j \qquad \textbf{(3.16)}$$

$$\underline{\mu}_{\tilde{B}_{j+1}}(D) = \frac{D - b_j}{b_{j+1} - b_j} m_{j+1} \qquad \textbf{(3.17)}$$

$$\overline{\mu}_{\tilde{B}_j}(D) = \frac{b_{j+1} - D}{b_{j+1} - b_j} \qquad \textbf{(3.18)}$$

$$\overline{\mu}_{\tilde{B}_{j+1}}(D) = \frac{D - b_j}{b_{j+1} - b_j} \qquad \textbf{(3.19)}$$

Replacing the membership grades given in from Equation 3.12 to Equation 3.19 into the corresponding firing interval sets given in from Equation 3.8 to Equation 3.11, the total firing interval sets for an activated SC(F^n for $\forall\, n \in AI_{SC(q,w)}$) can be obtained as follows. Here notice that the $\cap$ operator is product and operator.

$$F^n = \left[\frac{a_{i+1} - E}{a_{i+1} - a_i} m_i \frac{b_{j+1} - D}{b_{j+1} - b_j} m_j,\quad \frac{a_{i+1} - E}{a_{i+1} - a_i} \frac{b_{j+1} - D}{b_{j+1} - b_j}\right] \qquad \textbf{(3.20)}$$

$$F^{n+1} = \left[\frac{a_{i+1} - E}{a_{i+1} - a_i} m_i \times \frac{D - b_j}{b_{j+1} - b_j} m_{j+1}, \quad \frac{a_{i+1} - E}{a_{i+1} - a_i} \times \frac{D - b_j}{b_{j+1} - b_j}\right] \quad \textbf{(3.21)}$$

$$F^{n+T} = \left[\frac{E - a_i}{a_{i+1} - a_i} m_{i+1} \times \frac{b_{j+1} - D}{b_{j+1} - b_j} m_j, \quad \frac{E - a_i}{a_{i+1} - a_i} \times \frac{b_{j+1} - D}{b_{j+1} - b_j}\right] \quad \textbf{(3.22)}$$

$$F^{n+T+1} = \left[\frac{E - a_i}{a_{i+1} - a_i} m_{i+1} \times \frac{D - b_j}{b_{j+1} - b_j} m_{j+1}, \quad \frac{E - a_i}{a_{i+1} - a_i} \times \frac{D - b_j}{b_{j+1} - b_j}\right] \quad \textbf{(3.23)}$$

Replacing Equation 3.20 to Equation 3.23 into the KM conditions for L^* and R^* given in Equation 2.19 and Equation 2.20 respectively, before solving the KM conditions Then, the obtained explicit solution of optimal switching points L^* and R^* are obtained as follows:

$$L^* = \begin{Bmatrix} n, & E \le BF_2(D) \\ n + T, & E > BF_2(D) \end{Bmatrix} \quad \textbf{(3.24)}$$

$$R^* = \begin{Bmatrix} n, & E \le BF_1(D) \\ n + T, & E > BF_1(D) \end{Bmatrix} \quad \textbf{(3.25)}$$

where $BF_1(D)$and $BF_2(D)$ are the Boundary Functions (BFs) which are used for determining optimal switching points for a given input value and corresponding activated SC as mentioned in (Dodurka et al., 2014). Moreover, it can be obviously mention that the potential boundary functions in above equations are just functions of the derivative of error input (D) since the other parameters of IT2-FLS are constant since they are known structural parameters of the IT2-FPID controllers. Therefore, without losing generality, the boundary functions corresponding an activated SC of IT2-FPID controller are can be obtained as follows:

$$BF_1(D) = \frac{\begin{gathered}(C_{h+1} - C_{h+2})(b_j - D)\left(b_j + a_i - a_{i+1}\right) + \\ m_i m_j a_i (C_h - C_{h+1})\left(D - b_{j+1}\right)\end{gathered}}{\begin{gathered}(C_{h+1} - C_{h+2})\left(b_{j+1} - D\right) + \\ m_i m_j a_i (C_h - C_{h+1})\left(D - b_{j+1}\right)\end{gathered}} \quad \textbf{(3.26)}$$

$$BF_2(D) = \frac{\begin{gathered}(C_{h+1} - C_{h+2})(b_j - D)(b_j + a_i - a_{i+1}) m_{i+1} m_{j+1} + \\ a_{i+1}(C_h - C_{h+1})\left(D - b_{j+1}\right)\end{gathered}}{\begin{gathered}m_{i+1} m_{j+1} b_j (C_{h+1} - C_{h+2}) + \\ (C_{h+1} - C_h) b_{j+1} + D(C_h - C_{h+1})\end{gathered}} \quad \textbf{(3.27)}$$

Now, at any time (when an input signal activates the IT2-FPID) the inputs (E, D) are measured and known. Besides their corresponding membership degrees are known since the antecedent and consequent membership functions are known since design of the IT2-FPIS controller. Consequently the optimal switching points (L^* and R^*) can be determined via Equation 3.26 and Equation 3.27 by using Equation 3.24 and Equation 3.25 without performing iteration as original KM algorithm. After the switching points are determined, then the output of an IT2-FLC can be calculated directly with respect to switching points and Equation 2.19 and Equation 2.20. In fact the whole step by step procedure which is explained above is called as BF-KM algorithm and the algorithm step is summarized in detail in (Dodurka et al., 2014).

3.3 A Computational Comparison Study

In this section, the computational times of proposed BF-KM type-reduction method will be compared with the original KM type reduction method (Wu and Mendel, 2007), and Decomposition based KM (D-KM) type-reduction method (Kumbasar et al., 2013d) strategies to show the efficiency of the proposed method. The comparison study has been performed on a personal computer with CPU i7-3960X 3.3 GHz and 10GB as given in (Dodurka et al., 2014). To compare the computational time performances of the employed type-reduction algorithms, total computation time needed to calculated. Therefore, the output of IT2-FLC is measured for all type-reduction methods. For all simulation experiments, the universe of discourses of the normalized inputs (E, D) is quantized into 21 points. The execution times of the type-reduction methods on three different TxTrule bases where $T = 3, 5,7$ is compared. Moreover, in order to perform a fair comparison and in order to provide statistical information about the measured computation times, each experiment is performed for 250 times for each TxT rule base structure. Consequently, 250x3 randomly IT2-FLC has been generated totally. In the generation of an IT2-FLC with a TxT rule base, the parameters of antecedent membership functions and consequent sets are generated randomly with respect to the uniform distribution. For comparing the computation time performance of the type-reduction algorithms, minimum, maximum, mean and standard deviation times are measured. The measured times for the 3x3, 5x5 and 7x7 rule base are tabulated in Table 3.1 to Table 3.3 and the total computational times of the type-reduction methods are illustrated in Figure 3.10.

Table 3.1 : Time comparison of type-reduction methods for 3x3 rule bases.

Type-Reduction Method	Min. time	Max. time	Mean and Standard deviation
BF-KM	13.4	15.2	13.7 ± 0.184
D-KM	37.4	46.4	40 ± 1.011
KM	37.3	43.4	40.5 ± 1.091

Table 3.2 : Time comparison of type-reduction methods for 5x5 rule bases.

Type-Reduction Method	Min. time	Max. time	Mean and Standard deviation
BF-KM	13.9	15.8	14.2 ± 0.236
D-KM	37.9	47.3	39.8 ± 0.920
KM	47	53.9	51 ± 1.002

Table 3.3 : Time comparison of type-reduction methods for 7x7 rule bases.

Type-Reduction Method	Minimum time	Maximum time	Mean and Standard deviation
BF-KM	14.6	17	15.2 ± 0.408
D-KM	37.7	45.8	39.2 ± 1.097
KM	62	75.1	66.0 ± 1.501

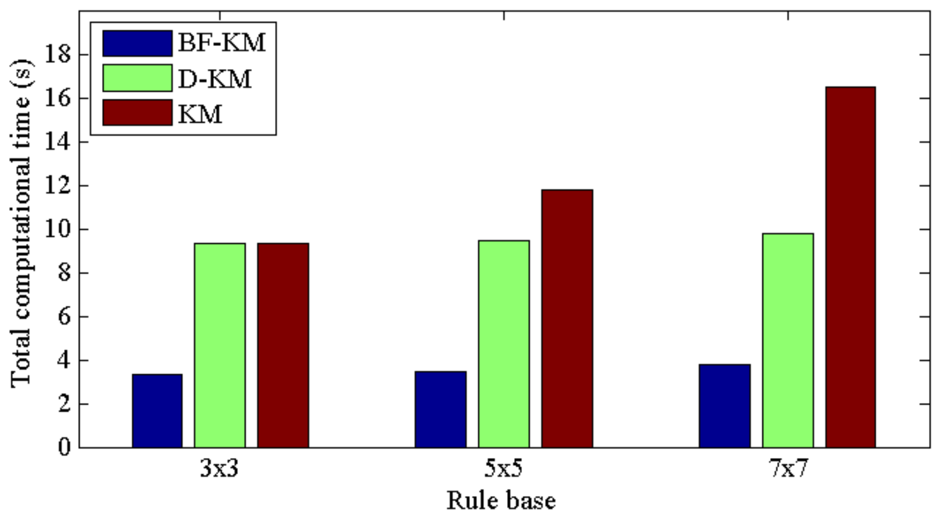

Figure 3.10 : Computational ime results of different type-reduction methods.

It can be clearly said from above tables and figure, the BF-KM type-reduction method outperforms the other methods with respect to the minimum, maximum, mean and standard deviation times. In addition when the size of rule base increases, the computation times of BF-KM and D-KM methods stay stable whereas the computation times of KM method increases dramatically. This is mainly caused because of the decomposition property since the number of possible activated rules in a decomposed rule base is always fixed to four. Therefore, computation times do not increase for both the BF-KM and D-KM methods. Moreover, the superiority of the BF-KM method can be seen clearly especially for the $7x7$ rule base structure. As tabulated in Table 3.3, it can be seen that BF-KM method is approximately 3 times faster than KM and 1.5 times faster than the D-KM. Finally, it can be concluded that the superiority of BF-KM type-reduction method comes from that it's computational time does not increases as the size of the rule base increases due to the employed decomposition theory and no iterative structure like the original KM method.

3.4 An Illustrative Example of S-MAP and BF-KM Methods

In this subsection, an illustrative example about proposed S-MAP visualizing method and BF-KM type-reduction method is considered for a simple IT2-FPID controller. In this context, widely used IT2-PID controller structure with 3x3-rule base is handled. Then, the rule base index becomes as $T = 3$ and the limit index of corresponding membership functions becomes as $g = 1$.

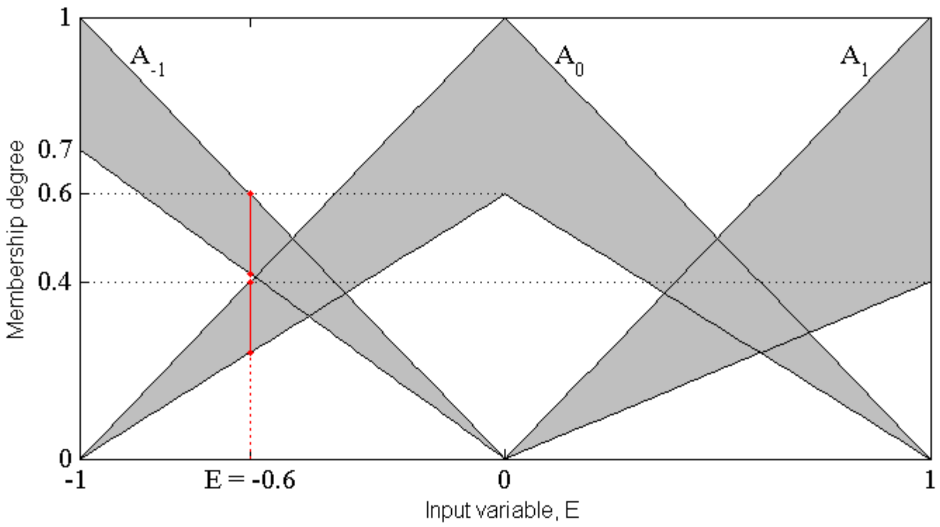

Figure 3.11 : Employed antecedent membership functions for the input E.

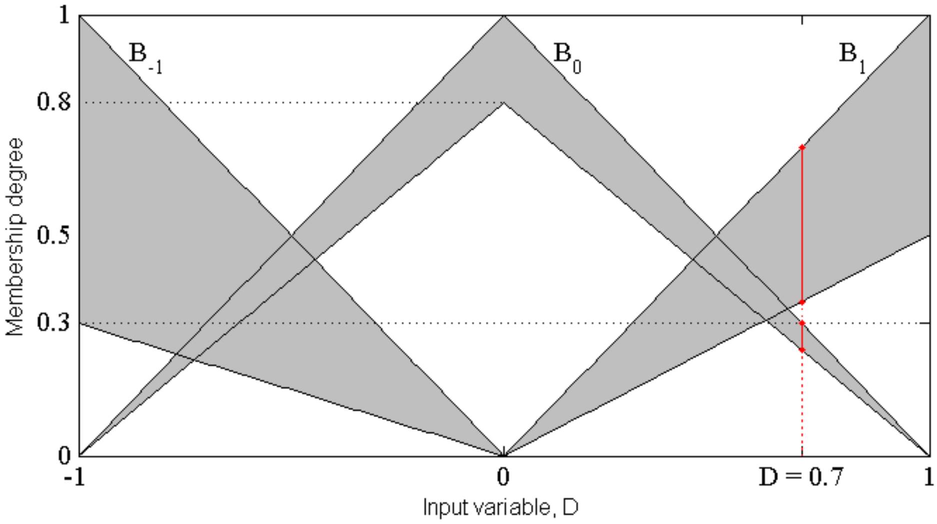

Figure 3.12 : Employed antecedent membership functions for the input D.

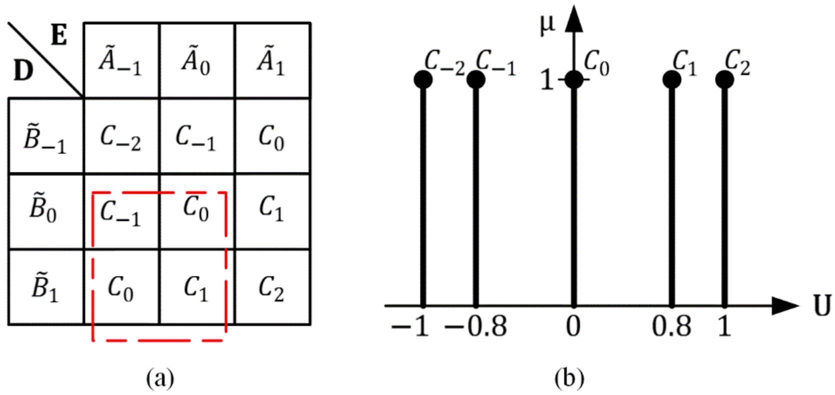

Figure 3.13 : Employed (a) rule base and (b) consequent membership functions.

The antecedent membership functions of error input and derivative of the error are illustrated in Figure 3.11 and Figure 3.12 respectively. The consequent sets and the rule table are given in Figure 3.13. According to the decomposition property, the rule base can be divided into the four SCs as generalized in Figure 3.9. Here notice that, there are only four non-zero membership degree with respect to the input values as shown in Figure 3.11 and Figure 3.12. Moreover, here red rectangular, which is illustrated in Figure13.a, represent the corresponding SC.

Then structural parameters of the employed IT2-FPID controller structure is clearly known from the antecedent membership functions and the consequent singleton sets since they are fixed in the design procedure phase of the controller. Therefore, the known parameters which are directly used for evaluating the BFs can be summarized as $a_i = -1$, $m_i = 0.7$, $a_{i+1} = 0$, $m_{i+1} = 0.6$, $b_i = 0$, $m_j = 0.8$, $b_{i+1} = 1$, $m_{j+1} = 0.5$, $C_h = -0.8$, $C_{h+1} = 0$, $C_{h+2} = 0.8$. Consequently, the BFs for the activated SC arecalculated with respect to Equation 3.26 and Equation 3.27 as a simple function the derivative of the error input as follows:

$$BF_1(D) = \frac{0.8D}{-0.448 - 0.352D} \tag{3.28}$$

$$BF_2(D) = \frac{0.24D}{-0.8 + 0.56D} \tag{3.29}$$

Replacing the value of D into Equation 3.28 and Equation 3.29, the final value of BFs can be calculated easily as $BF_1(0.7) = -0.806$ and $BF_2(0.7) = -0.412$. Then by checking conditions given in Equation 3.24 and Equation 3.25, the optimal switching points can be determined as follows:

$$L^* = \{n = 3, \qquad E = -0.6 \leq -0.412 = BF_2(D)\} \tag{3.30}$$

$$R^* = \{n + T = 6, \qquad E = -0.6 > -0.806 = BF_1(D)\} \tag{3.31}$$

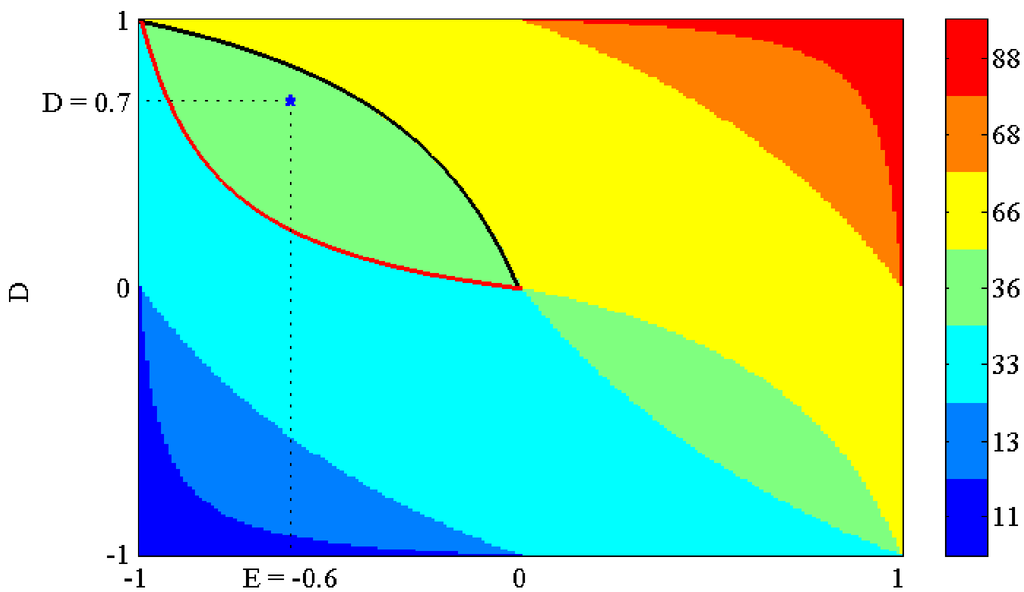

Figure 3.14 : Illustration of inputs and BFs on the S-MAP.

The BFs on the S-MAP is illustrated in Figure 3.14. Here the red curve represents $BF_1(D)$ and the black curve represents $BF_2(D)$ and the blue star represent the input set ($\{E, D\} = \{-0.6, 0.7\}$). Consequently, the end points of the type-reduced set can be found via Equation 2.19 and Equation 2.20 as $U_l = -0.1639$ and $U_r = 0.2449$ and the crisp output of the IT2-FLS as $U = 0.0405$. Here also notice that the given equations and results is only valid for the green region where $L^* = 3$ and $R^* = 6$

with respect to the values of input set. However, this circumstance does not affect the general remarks of the proposed method and the similar calculations can be performed for any values of the input set. Therefore, it can be concluded that the S-MAP and BF-KM are reliable alternative approaches to other KM based type-reduction methods because their computational cost is lower, they are represented with explicit mathematical expressions and visual features, which are not possible for the KM algorithms due to its iterative nature. In addition, the implementation of the proposed methods is quite easy as performed in previous examples.

4. ANALYTICAL DERIVATION OF IT2-FPID CONTROLLERS

In this section, the analytical derivation of 4-rule IT2-FPID controller structure are derived in a closed-form formulation by using BF-KM type-reduction method. Here, it is worth to mention that BF-KM type reduction method makes it possible to write output formulation of the IT2-FLS of IT2-FPID controller. Because, the optimal switching points might be estimated or calculated without performing an iterative algorithm by using BF-KM type reduction method instead of original KM type method. The analytical derivation of an IT2-FLS consists of several control laws depending to total number of fuzzy rules. Without losing generality, one can derive three different control laws for each SC in the input space. When considering 4-rule IT2-FPID controller structure, there is only a SC and there are totally three control laws. Moreover, the output control laws of the IT2-FLS continuously switch between the them in time with respect to corresponding BFs and inputs. Here, the two control laws that lies on a BF is equal to the others because the output surface of the IT2-FLS is continuous and there is no discontinuous or jumping on the control surface. The main objective of the analytical derivation of the IT2-FPID controller is to understand and analyze the internal structure and further abilities of the employed IT2-FLS. The analytical structure of IT2-FPID controllers might further guide the systematic controller design, development of self-tuning structures and stability analysis of IT2-FPID controllers since no pioneer study is performed on this subjectin literature yet. In this context, for the analytical derivations of the employed IT2-FLS structures, the modest structures of the 4-rule IT2-FPID controllers are considered in this thesis. Therefore, the heights of the LMFs is assumed as equal and they depend on a parameter denoted by M. Reminding that the IT2-FPID controller is constructed with an IT2-FLS and four scaling factors. Therefore in this section, the output of the employed IT2-FLSs are obtained and they are directly used for explicit formulas of IT2-FPID controllers by using general FPID controller output formulation which is given in Equation 2.5. In other words, once the input output relation of the employed IT2-FLS is obtained, the output formulation of the IT2-FPID controller can be written in a closed form.

Here, we consider 4-rule IT2-FPID controller, therefore the employed antecedent membership functions, the rule table and singleton consequent sets of the IT2-FLS of the employed 4-rule IT2-FPID controller is illustrated in Figure 3.15, Figure 3.16, Figure 3.17.a and Figure 3.17.b respectively. Here the employed IT2-FPID controller structure is also called as simplest IT2-FPID controller (Sakalli et al., 2014a). Since, the minimum configuration and design parameters is considered for the IT2-FPID controller structure by choosing the heights of the LMFs as equal. Therefore, the 4-rule IT2-FPID controller have totally five design parameters (K_e, K_d, K_a, K_b, M). In this context, the mathematical expressions of the simplest IT2-FPID controller is constructed as function of input variables (E, D), scaling factors $(K_e, K_d, K_a, K_b,)$ and the height of the LMFs (M).

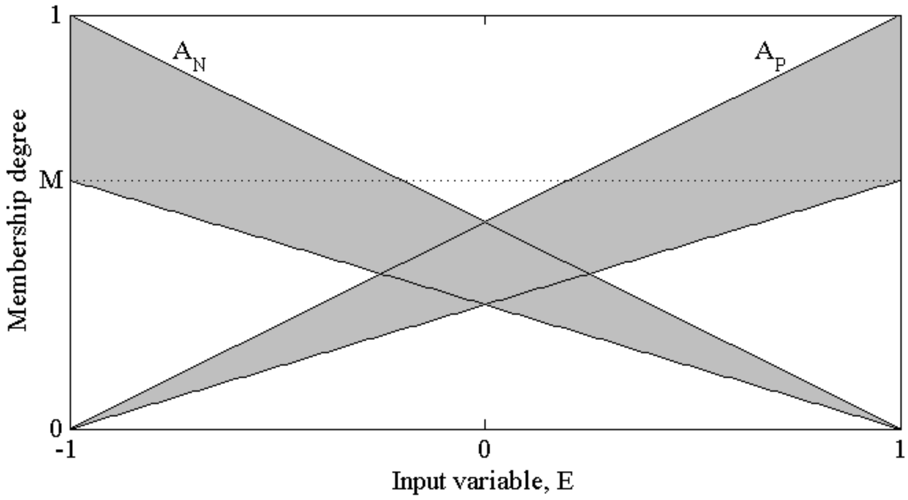

Figure 4.1 : Antecedent MFs of the 4-rule IT2-FPID controller for the input E.

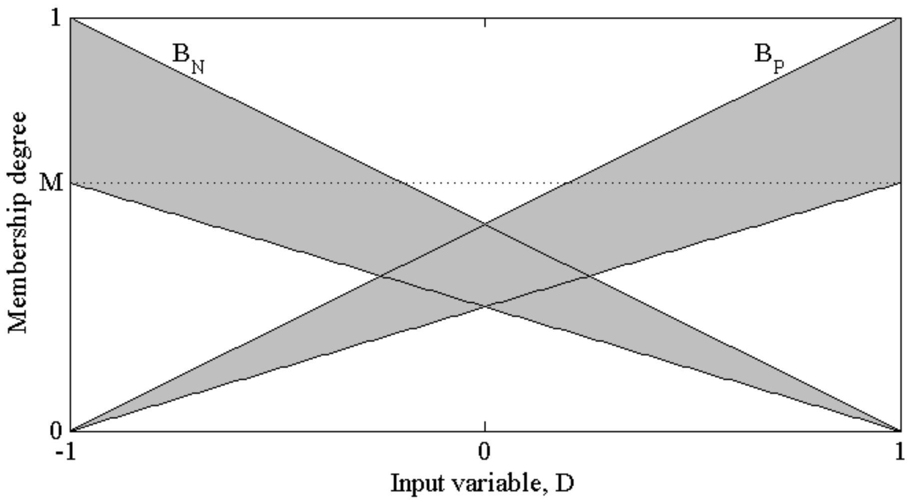

Figure 4.2 : Antecedent MFs of the 4-rule IT2-FPID controller for the input D.

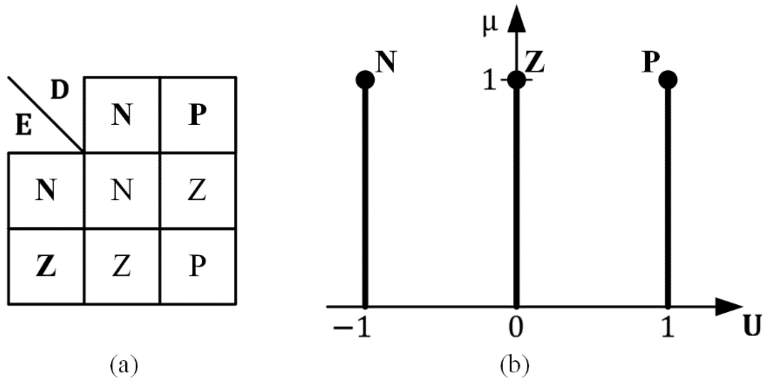

Figure 4.3 : The rule base and consequent sets of 4-rule IT2-FPID controller.

Then, only one SC occurs with respect to the apexes of the antecedent membership functions (two for the error input and two for the derivative of the error input). In other words, four rules construct only a SC as shown in Figure 17.a. For the employed SC of IT2-FPID controller, BFs and corresponding optimal SPs can be determined as mentioned previous section. The BFs for corresponding SC of the simplest IT2-FPID controller is calculated from Equation 3.26 and Equation 3.27 as

$$BF_1(D,M) = \frac{1 + D - M^2 + DM^2}{-1 - D - M^2 + DM^2} \tag{4.1}$$

$$BF_2(D,M) = \frac{1 - D - M^2 - DM^2}{1 - D + M^2 + DM^2} \tag{4.2}$$

Then, the optimal switching points (L^* and R^*) are determined by using Equation 3.24 and Equation 3.25 as follows:

$$L^* = \left\{\begin{matrix} 1 & E \le BF_2(D,M) \\ 3 & E > BF_2(D,M) \end{matrix}\right\} \tag{4.3}$$

$$R^* = \left\{\begin{matrix} 1 & E \le BF_1(D,M) \\ 3 & E > BF_1(D,M) \end{matrix}\right\} \tag{4.4}$$

Then by combining inequalities given in Equation 4.3 and Equation 4.4, all candidates of optimal SPs is determined. Then the output of the IT2-FLS is expressed in terms of three control laws as follows:

$$U = \left\{\begin{matrix} U_{11} & E \le BF_1(D,M) \le BF_2(D,M) \\ U_{13} & BF_1(D,M) \le E \le BF_2(D,M) \\ U_{33} & BF_1(D,M) \le BF_2(D,M) \le E \end{matrix}\right\} \tag{4.5}$$

Here the subscripts point out the optimal SPs (L^* and R^*) and the control laws are explicitly calcuted as

$$U_{11} = \frac{G_2(E + D) + G_1(1 + ED^2 + E^2D - E^2D^2)}{G_3 + 2G_1(E + D) + \ G_1(E^2 + D^2 - 2ED^2 - 2E^2D + E^2D^2)} \tag{4.6}$$

$$U_{13} = \frac{G_4(D + E) + G_4(ED^2 + E^2D)}{G_5 + G_6(ED) + G_1(-E^2 - D^2 + E^2D^2)} \tag{4.7}$$

$$U_{33} = \frac{G_2(E + D) + G_1(-1 + E^2D + D^2E + E^2D^2)}{G_3 - 2G_1(E + D) + G_1(E^2 + D^2 + 2ED^2 + 2E^2D + E^2D^2)} \tag{4.8}$$

where

$$G_1 = 1 - 2M^2 + M^4 \tag{4.9}$$

$$G_2 = -1 - 6M^2 - M^4 \tag{4.10}$$

$$G_3 = -3 - 10M^2 - 3M^4 \tag{4.11}$$

$$G_4 = 6M^2 + 2M^4 \tag{4.12}$$

$$G_5 = 1 + 6M^2 + 9M^4 \tag{4.13}$$

$$G_6 = 8M^2 - 8M^4 \tag{4.14}$$

5. SELF-TUNING STRUCTURES OF IT2-FPID CONTROLLERS

In this section, two self-tuning mechanisms of the employed IT2-FPID controller structure are proposed. The first self-tuning structure adjusts the common controller gain of the simplest IT2-FPID controller via a heuristic function (Sakalli et al., 2014a). Here, the employed simplest IT2-FPID controller is constructed with only four rules and the heights of the LMFs is assumed equal as mentioned previous section so it is assumed that the heights of the LMFs is only design parameter that changes the behavior of the IT2-FPID controller. Moreover, the output formulation of the simplest IT2-FPID controller is simplified for the steady state with respect to the analytical derivation of the 4-rule IT2-FPID controller. After, the formulation of the gain of the employed IT2-FLS is obtained, the equivalent structures of conventional PID controller, the simplest IT2-FPID controller is evaluated. Here, the IT2-FPID controller is represented in terms of a conventional PID controller with a nonlinear controller gain. Then the gain curve of the IT2-FPID controller is derived. Finally, a heuristic function adjusts online the controller gain by altering the size of the FOU with respect to the obtained simplest IT2-FPID controller formulation for the steady state. The second self-tuning structure determines the values of fuzzy rule weights of the IT2-FLS via an optimization procedure. This self-tuning structure is also the generalized form of those optimization based rule weighting of T1-FPID controllers (Yeşil et al., 2013). Here for the optimization based structure, the assessment of the actual control signal is assumed as an optimization problem. In fact, the rule weights represent the importance or influence of the corresponding rules since they are the only adjustable parameters in internal structure. Because the internal structure is generally fixed in many studies since the designer or the expert beforehand determines the elements of the FPID controller such as scaling factors, linguistic terms, antecedent and consequent membership functions and rule base. In this context, a cost function is generated in order to minimize the error of the closed loop system and the control effort of the IT2-FPID controller. Then, the rule weights are optimized with respect to the objective function in terms of tracking error and control signal in proposed self-tuning structure.

5.1 A Heuristic Self-Tuning Structure of IT2-FPID Controller

In this subsection, the explicit expression of the simplest IT2-FPID controller around the steady state is obtained with respect to the analytical derivation of the 4-rule IT2-FPID controller. From the point of the control theory view, the origin of the S-MAP for the IT2-FLS of the simplest IT2-FPID controller characterizes the steady-state behavior of the closed-loop system. Since the tracking error (e) and derivative of the error ($\dot{e}$) approach to zero when the inputs of the IT2-FLS (E and D) approach to zero in time with respect to Equation 2.3 and Equation 2.4. Then, the motivating result of this statement will lead one further controller analysis performing on the region that covers the origin or the steady state point of the closed-loop system. Thus, the control law that encapsulates the origin of the S-MAP is more essential for this study because it represents the region around the origin (the green region in following S-MAP). An illustrative example of the S-MAP for the employed IT2-FLS of the simplest IT2-FPID controller is illustrated in Figure 5.1.

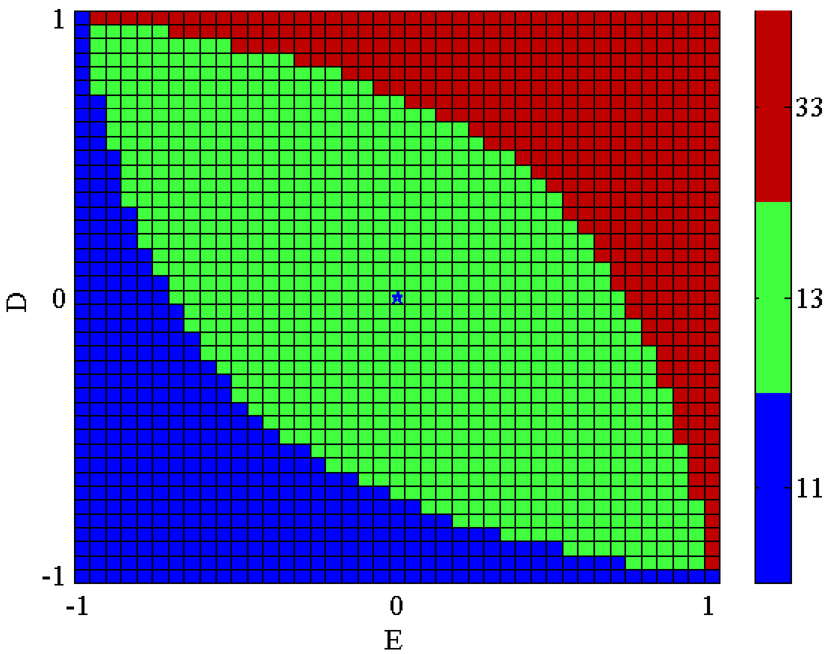

Figure 5.1 : Steady state point on the S-MAP.

Here the red star point represents the origin and the green region on the S-MAP obviously covers the origin of the S-MAP and the steady state behavior of the IT2-FPID controller. Then, the control law of the green region on the S-MAP, namely, U_{13} can be written as mentioned in previous section as

$$U_{13} = \frac{G_4(D+E) + G_4(ED^2 + E^2D)}{G_5 + G_6(ED) + G_1(-E^2 - D^2 + E^2D^2)} \quad \textbf{(5.1)}$$

where

$$G_1 = 1 - 2M^2 + M^4 \quad \textbf{(5.2)}$$

$$G_4 = 6M^2 + 2M^4 \quad \textbf{(5.3)}$$

$$G_5 = 1 + 6M^2 + 9M^4 \quad \textbf{(5.4)}$$

$$G_6 = 8M^2 - 8M^4 \quad \textbf{(5.5)}$$

Obviously, U_{13} constructs a nonlinear control law, which depends on a nonlinear function of the height of the LMFs (M), the error input (E) and the derivative of the error input (D). Here notice that, U_{13} is just the output of the employed IT2-FLS and the actual control signal is generated with respect to the control laws. Then, the boundary functions can be calculated by using Equation 3.26 and Equation 3.27. Therefore the handled control law, which is defined around the origin, is valid on condition that satisfy following inequality:

$$\frac{1 + D - M^2 + DM^2}{-1 - D - M^2 + DM^2} < E \leq \frac{1 - D - M^2 - DM^2}{1 - D + M^2 + DM^2} \quad \textbf{(5.6)}$$

The nonlinear terms in Equation 5.1 (E^2, D^2 and ED) can be eliminated by taking as zero since these values exponentially converge to zero at the origin. After eliminating the nonlinear terms, the control law around the origin, which is denoted as ($U_{(0,0)}$) can be expressed simpler as

$$U_{(0,0)} = \lim_{\begin{Bmatrix} E^2 \to 0 \\ D^2 \to 0 \\ ED \to 0 \end{Bmatrix}} (U_{13}) = \frac{G_4(D+E)}{G_5} \quad \textbf{(5.7)}$$

Finally, the output of the employed IT2-FLS can be expressed as follows:

$$U_{(0,0)} = V(M)(E + D) \quad \textbf{(5.8)}$$

where $V(M)$ is the nonlinear gain of the employed IT2-FLS of the simplest IT2-FPID controller and defined as

$$V(M) = \frac{G_4}{G_5} = \frac{6M^2 + 2M^4}{1 + 6M^2 + 9M^4} \quad \textbf{(5.9)}$$

Then by substituting Equation 2.5 and Equation 5.9, the closed-form formulation of the simplest IT2-FPID controller for the steady state can be obtained as

$$u = K_a V(M)(E + D) + K_b V(M) \int (E + D)\, dt \quad \textbf{(5.10)}$$

By substituting Equation 2.3 and Equation 2.4, the closed-form formulation of the simplest IT2-FPID controller for the steady state can be obtained as

$$u = K_a V(M)(K_e e + K_d \dot{e}) + K_b V(M) \int (K_e e + K_d \dot{e})\, dt \quad \textbf{(5.11)}$$

After rearranging the common terms in Equation 5.11, the closed-form formulation of the simplest IT2-FPID controller for the steady state can be obtained as the control law around the origin as follows:

$$u = V(M)(K_a K_e + K_b K_d)e + V(M) K_b K_e \int e\, dt + V(M) K_a K_d \dot{e} \quad \textbf{(5.12)}$$

Furthermore, the ratio of input SFs is denoted as α, the ratio of output SFs is symbolized as β and the additional term which is a function of relations of SFs is represented as γ for the sake of the simplicity. Therefore, these additional rational terms are defined as

$$K_d = \alpha K_e \quad \textbf{(5.13)}$$

$$K_b = \beta K_a \quad \textbf{(5.14)}$$

$$\gamma = 1 + \alpha\beta \quad \textbf{(5.15)}$$

After substituting Equation 5.13 to Equation 5.15 into Equation 5.12, the simpler expression of the closed-form formulation of the simplest IT2-FPID controller for the steady state is obtained as follows:

$$u = V(M) K_a K_e \gamma \left(e + \frac{\beta}{\gamma} \int edt + \frac{\alpha}{\gamma} \dot{e} \right) \quad \textbf{(5.16)}$$

Clearly, the closed-form formulation of the simplest IT2-FPID controller for the steady state is equivalent to the conventional PID controller structure given in Equation 5.17. However the important difference between the simplest IT2-FPID controller for the steady state and the conventional PID controller is that the gain of the simplest IT2-FPID controller is variable while the gain of the conventional PID controller is static. The conventional PID controller formulation is given below

$$u = K_c\left(e + \frac{1}{T_i}\int edt + T_d\frac{de}{dt}\right) \tag{5.17}$$

Here, K_c has two definitions, in other words, the static controller gain for the conventional PID controller and the variable controller gain for the simplest IT2-FPID controller. T_i and T_d represent the integral time constant and derivative time constant of the PID controller respectively. Then by matching Equation 5.16 and Equation 5.17term by term, the variable controller gain (K_c), integral and derivative time constants (T_i and T_d) of the simplest IT2-FPID controller for the steady state is obtained as

$$K_c = V(M)K_aK_e\gamma \tag{5.18}$$

$$T_i = \frac{\gamma}{\beta} \tag{5.19}$$

$$T_d = \frac{\alpha}{\gamma} \tag{5.20}$$

Consequently, the closed-form formulation of the simplest IT2-FPID controller around the steady state is obtained in terms of the nonlinear function ($V(M)$) and the SFs. Here, the nonlinear function changes directly the gain of the simplest IT2-FPID controller. In this context, the information might be used for constructing a self-tuning structure. Hence, the change of $V(M)$ respect to M is analyzed in detail and the gain curve is illustrated in Figure 5.2. From the prior knowledge of the IT2-FLS structure, the IT2-FLS reduces to a T1-FLS when M is chosen as 1 and the controller gain of the simplest T1-FPID controller can be calculated as 0.5 as shown in (Qiao and Muzimoto, 1996). Therefore, it can be expected that the controller gain of the IT2-FPID controller becomes 0.5 in case of $M = 1$. Moreover, an interesting observation here is that a T1-FLC is also obtained when $M = 0.448$ in addition to

$M = 1$ as shown in Figure 5.2. As shown in figure below, if the nonlinear function $V(M)$ is high, the closed–loop system has aggressive behavior, similarly, the closed-loop system has sluggish behavior if $V(M)$has relatively a low value. Consequently, it can be concluded that a smoother control action than T1-FPID controller can be achieved when M is chosen less than 0.44 while a aggressive control action than T1-FPID controller can be achieved when M is chosen between 0.448 and 1.

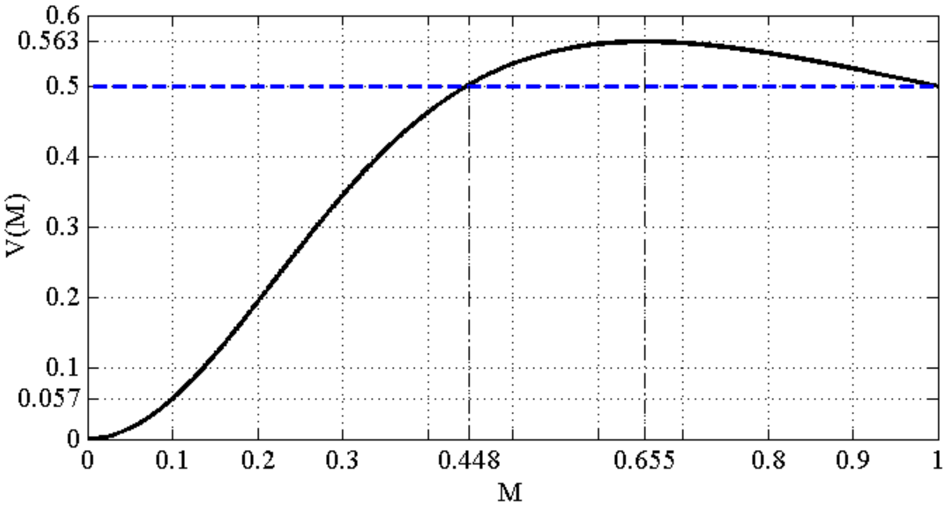

Figure 5.2 : Gain curve of the simplest IT2-FPID controller.

As it is known from the control theory, there is a tradeoff between the set point tracking and the disturbance rejection performances (Aström and Hagglund, 2005). If a closed loop system has an aggressive behavior, then the disturbances is rejected quickly but high overshoots and oscillations may occur. On the other hand, if a closed loop system has a sluggish behavior, then the overshoots and oscillations are reduced while the disturbances are rejected in longer time. Using these remarks and mentioned assumptions, the design parameter M can be assumed as the online tuning parameter which directly changes the gain of the simplest IT2-FPID controller. In this context, the obtained closed-form formulation of IT2-FPID controller for the steady state is handled in order to improve both set point tracking and disturbance rejection performances by tuning M in an online manner. In order to improve the closed-loop control performance the following meta-rules are constructed: when the system output is around the set point, the gain should be larger in order to reject disturbances as fast as possible and when the system is far away from the set point, the gain should be smaller in order to reduce overshoots. Consequently, it can be claimed that after a set point change, the controller gain should increase by time, therefore overshoots and oscillations will be reduced with negligible comprise of the settling time and the disturbances will also be rejected quickly. Then, the following simple heuristic function, which has only error as its input, is proposed for tuning M in an online manner:

$$M(E) = (1 - |E|)h_2 + h_1 \quad \textbf{(5.21)}$$

where h_1 and h_2 are constants which determine the minimum and maximum values of the $V(M)$. In most cases, h_1 determines the feasible lower limit of $V(M)$, and $h_1 + h_2$ determines the upper limit of the $V(M)$. Here notice that h_1 and h_2 can be determined by designer in the design phase of the controller with respect to the system or performance requirements. For example, h_1 and h_2 assure the minimum and maximum values of $V(M)$ for the interval determined by $M \in [0, 0.655]$ since $V(M)$ is monotonic for that interval as shown in Figure 5.2. The block diagram of the proposed self-tuning structure is illustrated in Figure 5.3.

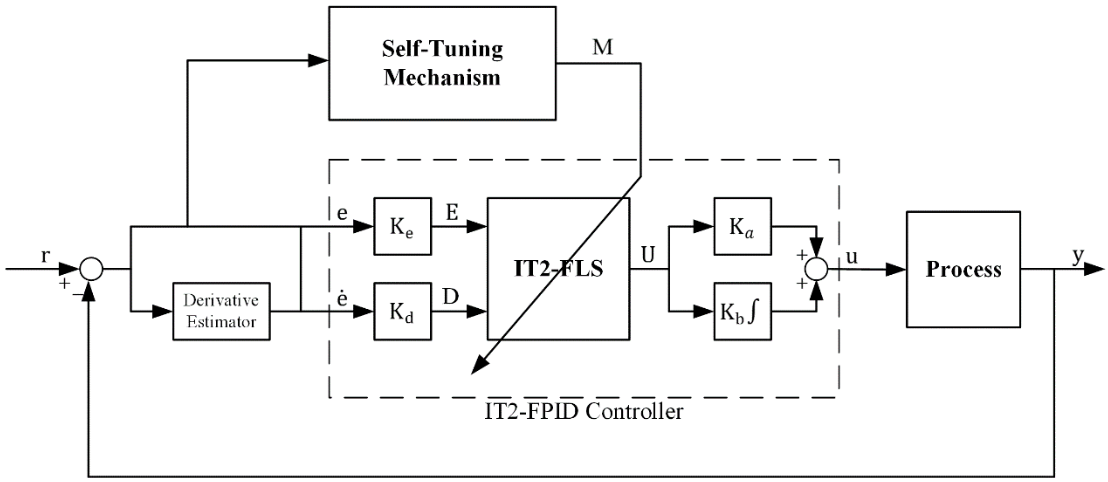

Figure 5.3 : Proposed self-tuning structure for simplest IT2-FPID controllers.

For the design of the employed self-tuning structure, an IT2-FLS might be designed initially in order to construct base of the self-tuning structure then the self-tuning structure might tunes the IT2-FPID controller via changing its controller gain in an online manner. Furthermore a bounded gain interval of the employed simplest IT2-FPID controller might be considered corresponding to the interval in $M \in [0,0.448]$ when it is desired smoother controller action . Here also, the lower value of M might be set as 0.1, since any value less than 0.1 results a very low controller gain, which extremely slows the closed loop response in practice. Moreover, another bounded gain interval of the employed simplest IT2-FPID controller might be considered corresponding to the interval in $M \in [0.448,1]$ when it is desired more aggressive controller action. What is more, when it is desired more complex and extended controller action the whole interval of the employed simplest IT2-FPID controller might be considered corresponding to an interval in $M \in [0,1]$. However in this thesis, only smoother control action is considered for the initial step. Also notice that, the employed simplest IT2-FPID controller structure has only a SC with a heuristic function. When considering more complex controller structure, number of the SCs increases and in this case the various heuristic self-tuning functions instead of one might be used in order to adjust the controller gains of each SCs of the IT2-FPID controller separately regarding to the performance requirements.

5.2 Rule Weighting of IT2-FPID Controllers

In this subsection, a self-tuning structure of IT2-FPID controller via rule weighting is proposed. Again, rule weights point out the importance or influence of corresponding fuzzy rule for a given input at a specified time (Karasakal et al., 2011). The rule weights (w) are assumed as tuning parameters and they might be adjusted via a heuristic function, an adaptive algorithm, or an optimization procedure in online manner. In this thesis, an optimization based self-tuning structure that adjusts the rule weights of the employed 9-rule IT2-FPID controller is examined as an extension of the procedure that is proposed for 9-rule ordinary T1-FPID controllers in (Yeşil et al., 2013). First, it is worth to mention that for the most part of the studies rule weights are set to one, in other words, they do not affect the output of the FLS. Then, although the definitions of the IT2-FPID controller demonstrate that nine rules generate the control signal, when the input membership functions are employed as symmetrical triangular uniformly distributed membership functions, at most four fuzzy rules will be activated for any input signal. This remark expresses the same phenomena with the decomposition property of the employed controller structure. In other words, for each activated SC, there are four rules and rule weights totally with different rule index. By looking the optimization point of view, only four parameters should be optimized regardless to the input or rule index. In this context, these rules are called as active rules (w_{act}); they also indicate rules of the activated SC.

The main idea of the optimization based online rule weighting mechanism is to evaluate the optimal rule weights that force the system to converge the reference signal as soon as possible with an applicable control action. In this context, the cost function (J), which is desired to be minimized, is constructed with respect to the general optimal control formulation as

$$J = Q \times e^2 + R \times u^2 \tag{5.22}$$

where u is the actual control signal of the employed IT2-DPID controller, e is the tracking error defined in Equation 2.1, Q and R are positive real numbers which determine priority, speed and aggressiveness of the controller. Here notice that the controller is implemented in each sampling time, thus the formulation should be updated in discrete time. It can be said that the tracking error becomes zero for the instant in which the system output attains the reference. Then, if the system output attains to the reference from the current system output at k^{th} instant after n sampling time, the tracking error at $(k+n)^{th}$ instant becomes zero. Accordingly, if it is desired that the system attains the reference n^{th} sampling later, the error after n steps ahead should be zero and the control signal and the objective value of the cost function should be calculated by considering the case in order to perform the optimization accurately. Without losing generality, in this thesis, the estimated error at $(k+1)^{th}$ instant is used in cost function, since it is desired to the system output equals to the reference as soon as possible or one step ahead. Here, linear models, transfer functions, non-linear models, fuzzy models, regression vectors, estimation strategies least square algorithms or assumptions might be used to estimate the potential errors in future, and also notice that the self-tuning method is still valid regardless to these operations. Then, the employed cost function which is used in optimization procedure is defined as

$$J = Q \times e(k+1)^2 + R \times u(k)^2 \tag{5.23}$$

The key point of the employed self-tuning structure is to determine the appropriate control signal, which minimizes the cost function given in Equation 5.22. The control signal is the output of IT2-FPID controller. It is generated by antecedent membership functions, consequent singleton sets, rule weights, and scaling factors as mentioned previous sections. In this self-tuning structure, antecedent membership functions, consequent singleton sets and scaling factors are assumed as constants, which are initially determined (by an expert or designer) while rule weights are assumed as optimization parameters. Then the output of the IT2-FPID controller is a function of active rule weights that is used in an activated SC ($u = f(w_{act})$). Moreover, the error is depends on reference and system output, here system output is dynamic and it is determined regarding to the system model and the control signal. Besides the system model consists of structural parameters or constants (P), which means that they cannot be tuned. Then the error in fact can be represented a dynamic function of the active rule weights ($e = f(w_{act}, P)$). Therefore, the employed cost function can also be written as a function of the active rule weights as

$$J(w_{act}) = Q \times e(w_{act})^2 + R \times u(w_{act})^2 \quad \textbf{(5.24)}$$

Obviously, the employed control cost function consists of four parameters to be optimized. Here notice that, the rule weights in an activated SC are desired to minimize and there are totally four rules and their weights in an activated SC. In this context, the main goal of the optimization procedure is to determine optimal rule weights with respect to the cost function. Therefore, an global optimization algorithm (Genetic Algorithm (GA) (Goldberg, 1989), Ant Colony Optimization Algorithm (ACO) (Dorigo and Stützle, 2003), Big Bang – Big Crunch Algorithm (BBBC) (Erol and Eksin, 2006) can evaluate the optimal rule weights of the employed IT2-FPID controller, which will minimize the tracking error with minimum control signal for each sampling time regarding to the employed cost function. The closed-loop system block diagram with the proposed online rule weighting mechanism for IT2-FPID controller is given in Figure 5.4.

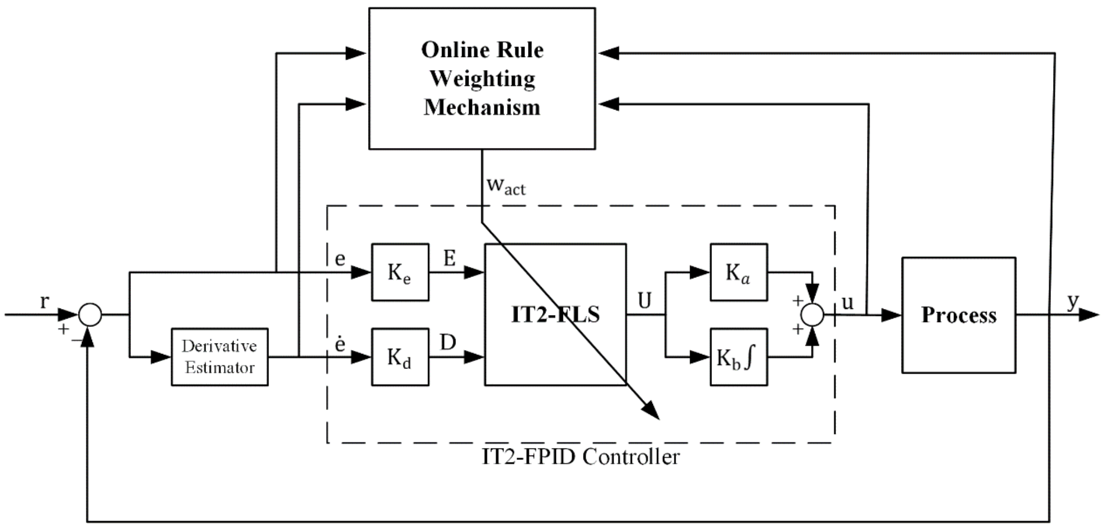

Figure 5.4 : Proposed online rule weighting mechanism for IT2-FPID controllers.

Consequently, the background of the design procedure of online rule weighting mechanism for IT2-FPID controllers is explained. In brief, the actual control signal is determined via changing the rule weights in an activated SC by performing an optimization procedure in order to minimize the cost function. The pseudocode of the proposed online rule weighting self-tuning structure of the IT2-FPID controller is summarized in the Table 5.1 for the closed loop control applications.

Table 5.1 : Pseudocode of proposed online rule weighting method.

Step 1	Measure the instantaneous error and the control signal. Remember previous errors and control signals.
Step 2	Determine the activated SC with respect to the measured error and its derivative (inputs of the employed IT2-FLS).
Step 3	Initialize/load the parameters and determine the active rule weights regarding to the activated SC.
Step 4	Run an optimization algorithm in order to calculate the optimal rule weights and update the rule weights with their new values.
Step 5	Calculate the actual control signal with respect to the optimized rule weights and implement to the system. Then go to Step 1.

6. EXPRERIMENTAL RESULTS

In this section, first, a real-time control study is presented is in order to compare IT2-FPID controller with conventional PID controller, T1-FPID controller and two Self-Tuning Type-1 Fuzzy PID (STT1-FPID) controllers as in (Sakalli et al., 2014b). For the real-time comparison studies, IT2-FPID, T1-FPID, Function Tuner based Type-1 Fuzzy PID (FTT1-FPID) (Woo et al., 2000) and Relative Rate Observer based Type-1 Fuzzy PID (RROT1-FPID) (Güzelkaya et al., 2003) controllers is handled in detail. Here also, it is investigated that the potential effects of extra degrees of freedom that lies on the FOU for IT2-FPID controller and self-tuning mechanisms for STT1-FPID controllers on the system performance. The real–time experimental studies have been performed on a nonlinear, open-loop unstable and time-varying magnetic levitation system namely, QUANSER MAGLEV plant. Magnetic levitation systems have been widely used in various study due to its challenging benchmark control system (Shiakolas et al., 2004; Yetendje et al., 2010). Secondly, a simulation study on a First Order plus Dead Time (FOPDT) process is presented in order to show the effectiveness of the proposed heuristic self-tuning structure of the simplest IT2-FPID controller as in (Sakalli et al., 2014a). The simulation studies is performed for four different cases (a nominal system model and three perturbed system models) in order to investigate the ability of the employed controllers in case of uncertainty. For this purpose, the uncertainty about the system model via alteration of parameters is considered for perturbed system models. Thirdly, the control performances of the proposed optimization based online rule-weighting mechanism for IT2-FPID controllers is analyzed on a two-cascaded tank process via simulations. Here handled two cascaded tank process is widely used second order nonlinear system. The proposed optimization based online rule weighting method for IT2-FPID controller is compared with an online rule weighting method (error based) for IT2-FPID controllers (Kumbasar et al., 2013b) and ordinary IT2-FPID controller in order to show the effectiveness of the proposed self-tuning structure.

6.1 A Real-Time Comparison Study on the MAGLEV Experimental Setup

In this subsection, the brief information about the real-time QUANSER Magnetic Levitation Plant (MAGLEV) experimental setup and the cascade control structure of the MAGLEV is presented. Then the control systems design strategies of employed controllers is explained. Finally, the real-time experimental results are presented.

6.1.1 MAGLEV experimental setup

The MAGLEV consists of an input which is the coil voltage (V_c) and two outputs which are the coil current (I_c) and ball position (x_b). The basic working principle of the MAGLEV can be summarized as; the coil voltage generates the coil current on the electromagnets coils with respect to the coil resistance and inductance. Here the coil current is the first output of MAGLEV and the coil voltage is the input of the MAGLEV. Then this current generates an electromagnetic force on the ball via coils placing in the electromagnet. The electromagnetic force and the gravity force provide the motion of the ball. Here, the ball position is the second output of the MAGLEV. Therefore, the model of the MAGLEV can be constructed with two parts, the electrical and mechanical model. The electrical part of the MAGLEV model can be obtained by Kirchhoff laws in terms of coil voltage and coil current .The mechanical part of the MAGLEV model can obtained by the motion equations of the ball in terms of forces and the ball position. Then, the differential equations related to the MAGLEV system are given as

$$\frac{\partial}{\partial t} I_c = \frac{(V_c - (R_c + R_s) I_c)}{L_c} \tag{6.1}$$

$$\frac{\partial^2}{\partial t^2} x_b = -\frac{K_m I_c^2}{2 M_b x_b^2} + g \tag{6.2}$$

where R_c is coil resistance, R_S is current sense resistance, L_c is coil inductance, K_m is electromagnet force constant, M_b is ball mass, g is gravitational constant. The parameters are given as $R_c = 10\Omega$, $R_s = 1\Omega$, $L_c = 412.5mH$, $g = 9.81 m/s^2$, $K_m = 6.53 \times 10^{-5} \frac{Nm^2}{A^2}$, $M_b = 0.068kg$, $r_b = 12.7\ mm$, $T_b = 14\ mm$ in (Sakalli et al., 2014b). The real-time experimental setup and the block diagram of the MAGLEV are illustrated in Figure 6.1 and Figure 6.2 respectively.

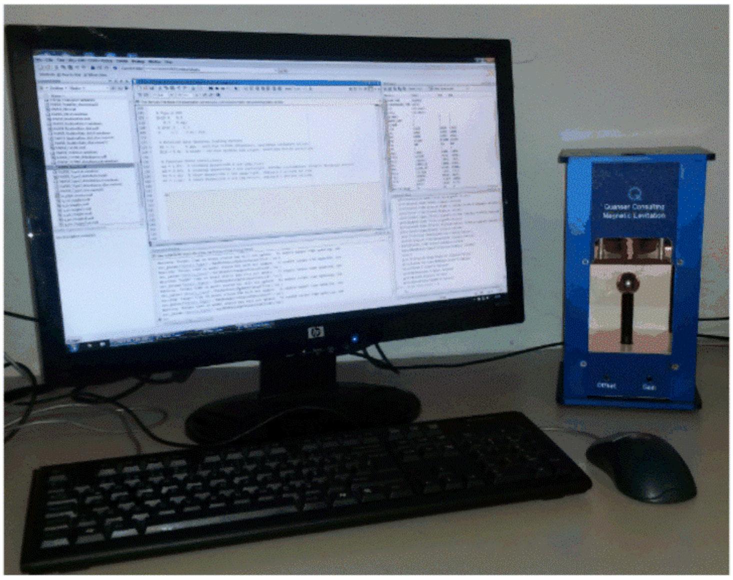

Figure 6.1 : The MAGLEV experimental setup.

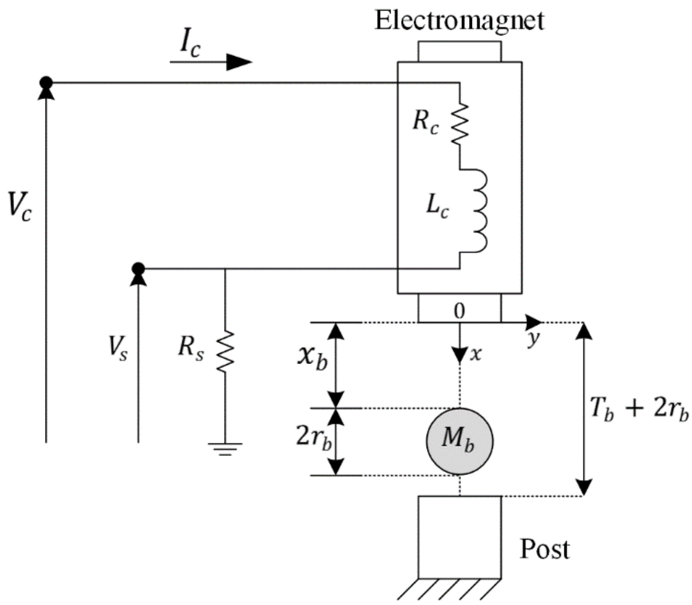

Figure 6.2 : Block diagram of the MAGLEV.

For the control strategy of the MAGLEV, the cascade control structure is preferred in order to achieve better control performance because of the multi output nature of the MAGLEV. In general, the cascade control structure is constructed with two controllers, an inner loop controller and an outer loop controller. By using cascade control structure, the disturbance rejection and set-point tracking performances are also improved due to two-layered controller structure. In this context, the coil current is controlled in inner loop while the ball position is controlled in outer loop for the control of the MAGLEV. The cascade control structure of the MAGLEV is illustrated in Figure 6.3.

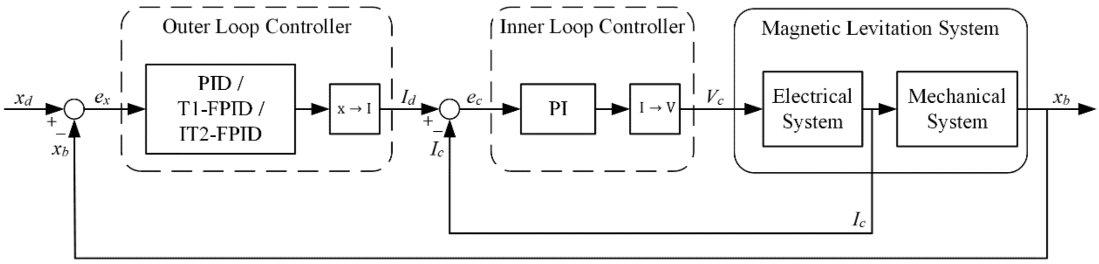

Figure 6.3 : Cascade control structure of the MAGLEV.

Here, x_d represents the desired ball position, x_b represents the measured ball position, e_x represents the error of the ball position for the closed loop system,I_d represents the desired coil current, I_c represents the measured coil current, e_c represents the error in the coil current for the closed loop system, V_c represents the coil voltage that is the control signal of the closed loop system. Then, the errors are defined as

$$e_x = x_d - x_b \tag{6.3}$$

$$e_c = I_d - I_c \tag{6.4}$$

The PI controller that is used in inner loop is designed via pole placement method and the controller parameters are calculated as $K_{pc} = 182.875$, $K_{ic} = 24801$. The PI controller is defined as

$$V_c = K_{pc}e_c + K_{ic}\int e_c\, dt \tag{6.5}$$

6.1.2 Control system design strategies

In this subsection, the design strategies of the employed controllers (PID, T1-FPID, FTT1-FPID, RROT1-FPID and IT2-FPID controllers) is presented in detail. The design parameters of the employed controllers are determined separately via an optimization procedure. Here, the optimization procedure is performed with respect to the nonlinear model of the MAGLEV and it is used for the design of the outer controller of the MAGLEV. The BB-BC algorithm is utilized in the optimization procedure due to its fast converge speed and low computational time. The population size and iteration number of the algorithm is chosen as 20 and 100 respectively. In addition, the employed controller is optimized with respect to the Integral Absolute Error (IAE) performance measure. The IAE is defined as

$$IAE = \int_{t=0}^{\infty} |e_x| dt \tag{6.6}$$

Moreover, the employed controllers are optimized with respect to a varying reference trajectory with the values of 11mm 9mm and 11mm (training reference trajectory) respectively. It is also assumed that the MAGLEV is at steady state point at $x_b^0 = 12mm$, $I_c^0 = 1.72A$ and $V_c^0 = 18.87V$ initially. Then the employed controllers are verified for a new varying reference trajectory with the values of 12mm 10mm and 9 mm (testing reference trajectory) respectively.

In the design strategy of the optimized PID controller, proportional, integral and derivative gains should be determined. The general formulation of the conventional PID controller is given in Equation 5.17. Then, the employed conventional PID controller is defined as

$$I_d = K_{px} e_x + K_{ix} \int e_x dt + K_{dx} \frac{de_x}{dt} \tag{6.7}$$

where K_{px}, K_{ix}, K_{dx} are the PID controller parameters used in outer loop. Here, totally three parameters should be determined for the PID controller. Then the optimization parameters are calculated as $K_{px} = 227.03$, $K_{ix} = 492.39$, $K_{dx} = 4.2$.

In the design strategy of the optimized T1-FPID controller, scaling factors should be determined. Here, 9-rule T1-FPID controller structure is used and the structural parameters of the employed T1-FPID controller is initially fixed. Moreover, K_e is determined with respect to the reference value change in order to keep universe of discourse for all FPID controllers. In this context, totally three parameters should be determined for T1-FPID controller. Then the optimization parameters are calculated as $K_d = 11.2$, $K_a = 0.67$, $K_b = 2.21$.

In design strategy of the FTT1-FPID controller, the parameters of the self-tuning mechanism should be determined. Here, the self-tuning mechanism adjusts the SFs in an online manner as follows:

$$K_b = f(e) K_b^0 \tag{6.8}$$

$$K_d = g(e) K_d^0 \tag{6.9}$$

where K_b^0 and K_d^0 are the initial values of the SFs. Here, $f(e)$ and $g(e)$ represent nonlinear mappings as follows:

$$f(e) = a_1|e| + a_2 \tag{6.10}$$

$$g(e) = b_1|1 - e| + b_2 \tag{6.11}$$

where a_1, a_2, b_1 and b_2 are the tuning parameters of FTT1-FPID controller to be determined. Moreover, the optimized T1-FPID controller parameters is also used for FTT1-FPID controller for the base T1-FPID controller. So, totally four parameters should be determined for FTT1-FPID controller. Then the optimization parameters are calculated as $a_1 = 1.67$, $a_2 = 0.53$, $b_1 = 0.01$ and $b_2 = 1.07$. The structure of FTT1-FPID controller is given in Figure 6.4.

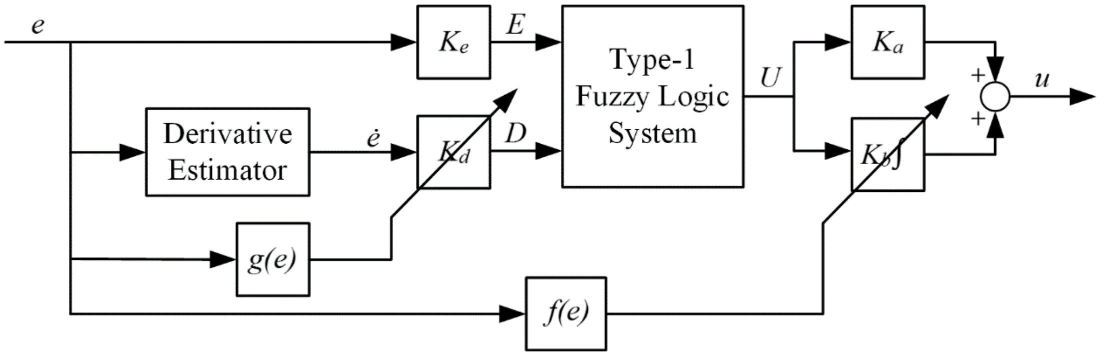

Figure 6.4 : FTT1-FPID controller structure.

In design strategy of the RROT1-FPID controller, the parameters of the self-tuning mechanism should be determined. Here, the self-tuning mechanism adjusts the SFs in an online manner as follows:

$$K_b = \frac{K_b^0}{K_f \gamma} \tag{6.12}$$

$$K_d = K_d^0 K_f K_{fd}\, \gamma \tag{6.13}$$

where K_b^0 and K_d^0 are the initial values of the SFs. Here, γ is the update coefficient and is generated from the fuzzy parameter regulator. The fuzzy parameter regulator is a Mamdani type fuzzy system consists of a 3x4 rule base given in (Güzelkaya et al., 2003), K_f is the output SF of the fuzzy parameter regulator and K_{fd} is an additional SF that affects only the derivative SF of the RROT1-FPID controller. Moreover, the optimized T1-FPID controller parameters is also used for RROT1-

FPID controller therefore they are initially fixed. Consequently, totally two parameters should be determined for RROT1-FPID controller. Then the optimization parameters are calculated as K_f=1.74 and K_{fd}=1.23. The structure of RROT1-FPID controller is given in Figure 6.5.

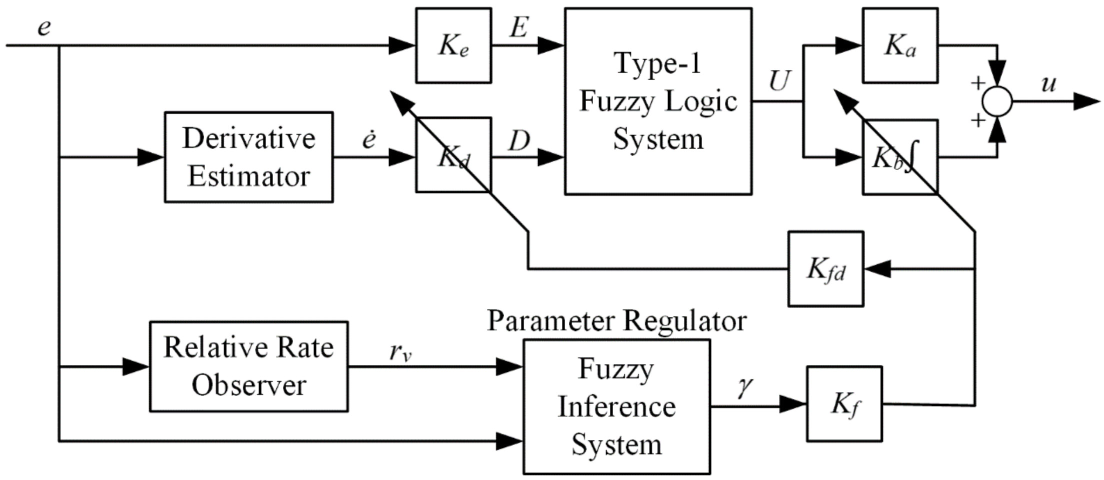

Figure 6.5 : RROT1-FPID controller structure.

In design strategy of the optimized IT2-FPID controller, the heights of the LMFs should be determined. The consequent singleton sets, rule base and scaling factors is selected as used in type-1 counterparts but the main difference between IT2-FPID and T1-FPID controllers is the FOU that lays on the antecedent membership functions of IT2-FPID controller. Moreover, the heights of Negative and Positive membership functions set to equal as $M_{11} = M_{13}$ and $M_{21} = M_{23}$ to obtain symmetrical control surface. Consequently, totally four parameters should be determined for IT2-FPID controller. Then the optimization parameters are calculated as $m_{11} = m_{13} = 0.81, m_{12} = 0.32, m_{21} = m_{23} = 0.70, m_{22} = 0.59$.

E \ **D**	**N**	**Z**	**P**
N	NB	N	Z
Z	N	Z	P
P	Z	P	PB

(a)

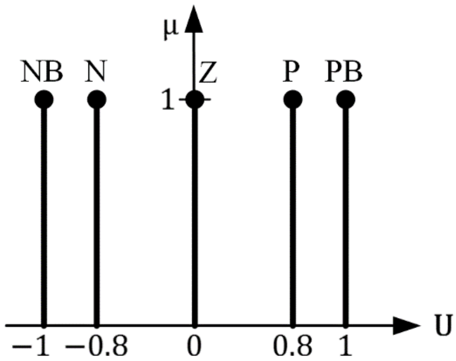

(b)

Figure 6.6 : Employed rule base and consequent sets.

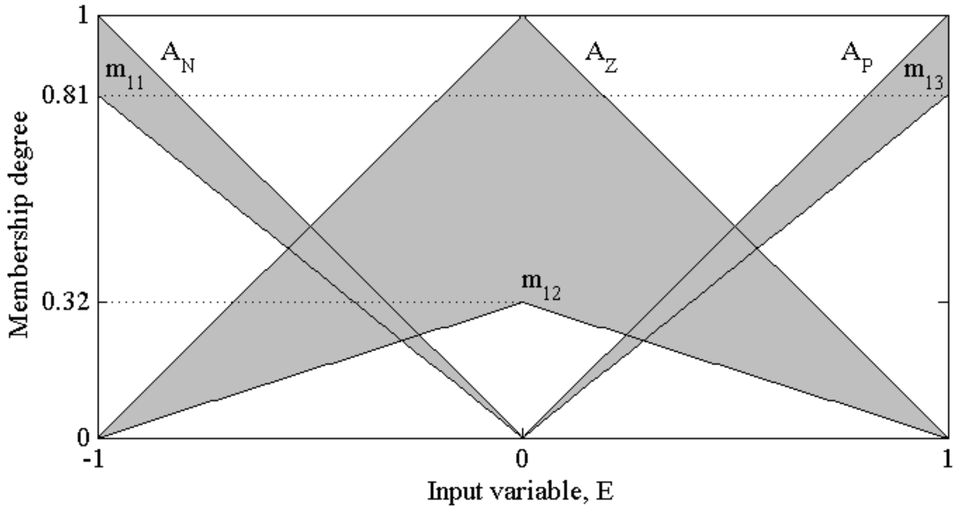

Figure 6.7 : Employed antecedent MFs for the error input.

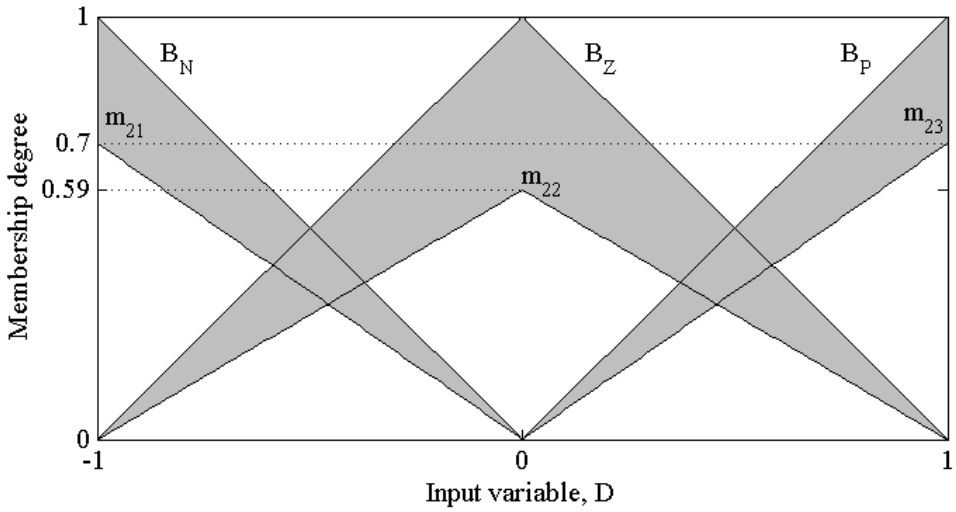

Figure 6.8 : Employed antecedent MFs for the derivative of the error input.

The membership functions and rule base of employed FPID controllers are illustrated in Figure 6.6 to Figure 6.8 in detail. Here note that, the antecedent membership functions of T1-FPID controllers are not mentioned because they use the UMFs in Figure 6.7 and Figure 6.8.

6.1.3 Real-time experimental results

In this subsection, the real-time experimental results of Optimized PID (OPID), Optimized T1-FPID (OT1-FPID), FTT1-FPID, RROT1-FPID and Optimized IT2-FPID (OIT2-FPID) controllers are presented on the MAGLEV system. Here note that, FTT1-FPID, RROT1-FPID controllers have OT1-FPID controller base. The comparison study will be divided into two parts for the training and testing reference trajectories. First, the control performances of the employed controllers for the training reference trajectory, at which they are designed, is examined. Then, the control performances of the employed controllers for the testing reference trajectory, at which they are not designed, is examined. The comparison cases (training and testing) are also divided into two parts in order to compare non-self-tuning and self-tuning structures separately in order to make a fair assessment. The real-time performances of the controllers are compared in terms of Settling Time (T_s), Overshoot (OS%) and IAE performance measures.

The first comparison study between OIT2-FPID and non-self-tuning structures is given in Figure 6.9.a while the comparison study between OIT2-FPID and self-tuning structures and Figure 6.9.b. Again, the first comparison study is performed for the training reference trajectory at which the controllers are optimized. The obtained performance measures are tabulated in Table 6.1.

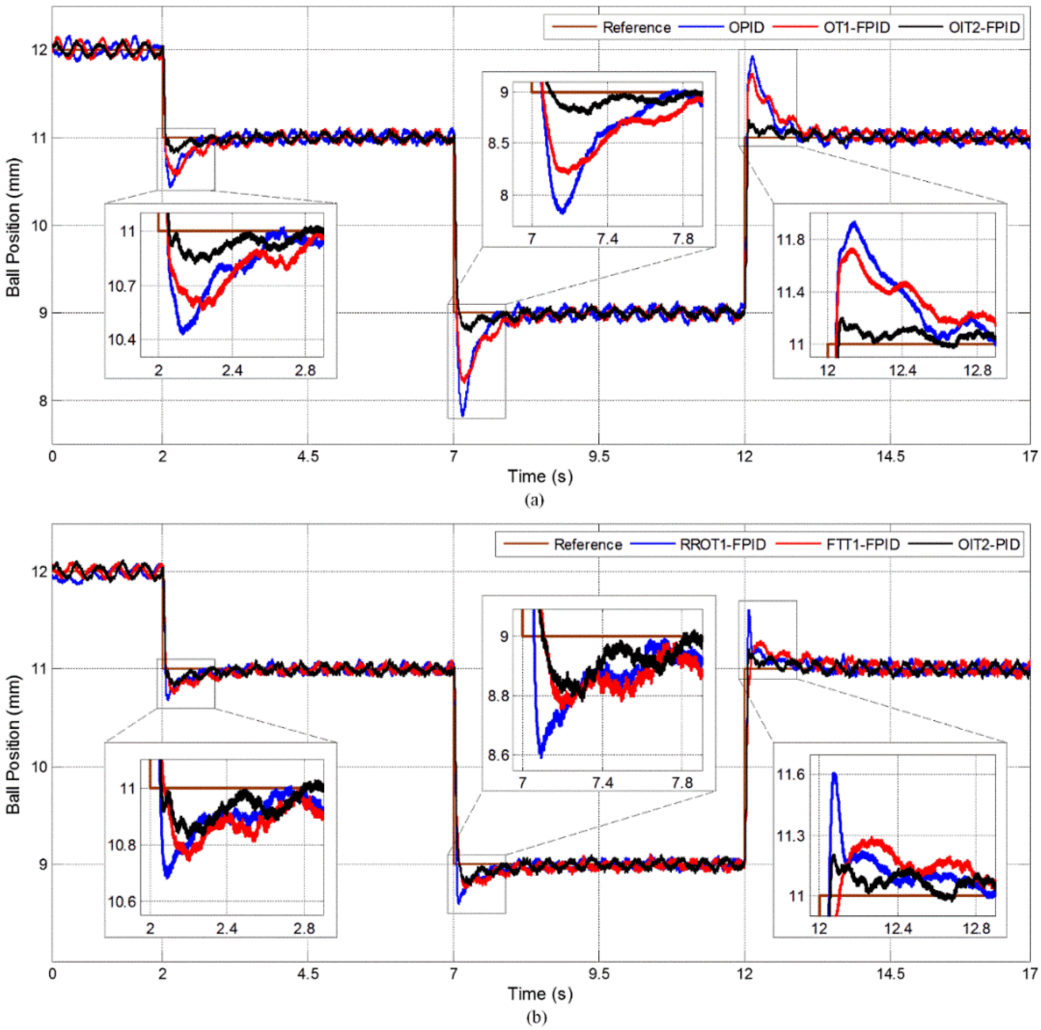

Figure 6.9 : Real-time experimental results for training reference trajectory.

Table 6.1 : Real-time experimental results for training reference trajectory

	12-11 mm		11-9 mm		9-11 mm		
	Ts	**OS%**	**Ts**	**OS%**	**Ts**	**OS%**	**IAE**
OPID	0.57 s	57%	0.98 s	59%	0.85 s	47%	1.532
OT1-FPID	0.79 s	44%	1.12 s	40%	1.23 s	36%	1.518
FTT1-FPID	0.63 s	25%	0.92 s	12%	0.79 s	14%	0.979
RROT1-FPID	0.45 s	32%	0.61 s	20%	0.66 s	30%	0.874
OIT2-FPID	0.36 s	18%	0.71 s	“11%	0.48 s	10%	0.779

In order to examine the transient state performances (Ts, OS%) of the control systems, we will examine the reference value variation from 11 mm to 9 mm in detail. In comparison with the OPID and OT1-FPID structures, the OIT2-FPID structure reduced settling time to 0.71 s and the overshoot to 11%. Moreover, if we examine the performances of the RROT1-FPID and FTT1-FPID, it can be concluded that the employed self-tuning mechanisms were able to enhance the T1-FPID control system performance. However, in comparison with RROT1-FPID, OIT2-FPID has reduced the overshoot by about 45% while it has increased the settling time relatively Whereas in the comparison with FTT1-FPID, the OIT2-FPID decreased the settling time about 23% while the overshoot value is almost the same. Moreover, the OIT2-FPID structure has better overall IAE performance measure in comparison to the other employed controllers. The first comparison study can be concluded as the OIT2-FPID structure was able to enhance the control system performance in comparison to both non-self-tuning (OPID and OT1-FPID) and self-tuning structures (FTT1-FPID and RROT1-FPID). Moreover, although the self-tuning structures provide the T1-FPID controller extra degrees of freedom, their performance results were not good as the OIT2-FPID ones in presence of noise since the their tuning mechanism is based on the value of the error. Thus, it can be concluded that the FOU of the OIT2-FPID give the opportunity to type-2 fuzzy structure to enhance the control performance and provides robustness against noise.

The second comparison study between OIT2-FPID and non-self-tuning structures is given in Figure 6.10.a while the comparison study between OIT2-FPID and self-tuning structures and Figure 6.10 and performance measures are given in Table 6.2.

Table 6.2 : Real-time experimental results for testing reference trajectory

	12-11 mm		11-9 mm		9-11 mm		
	Ts	**OS%**	**Ts**	**OS%**	**Ts**	**OS%**	**IAE**
OPID	*	*	0.92 s	48%	0.99 s	67%	1.798
OT1-FPID	*	*	1.12 s	43%	0.76 s	52%	1.530
FTT1-FPID	1.44 s	28%	1.29 s	17%	0.55 s	18%	0.842
RROT1-FPID	0.39 s	35%	0.89 s	25%	0.57 s	28%	0.932
OIT2-FPID	0.54 s	26%	0.77 s	11%	0.39 s	17%	0.875

* oscillating system response

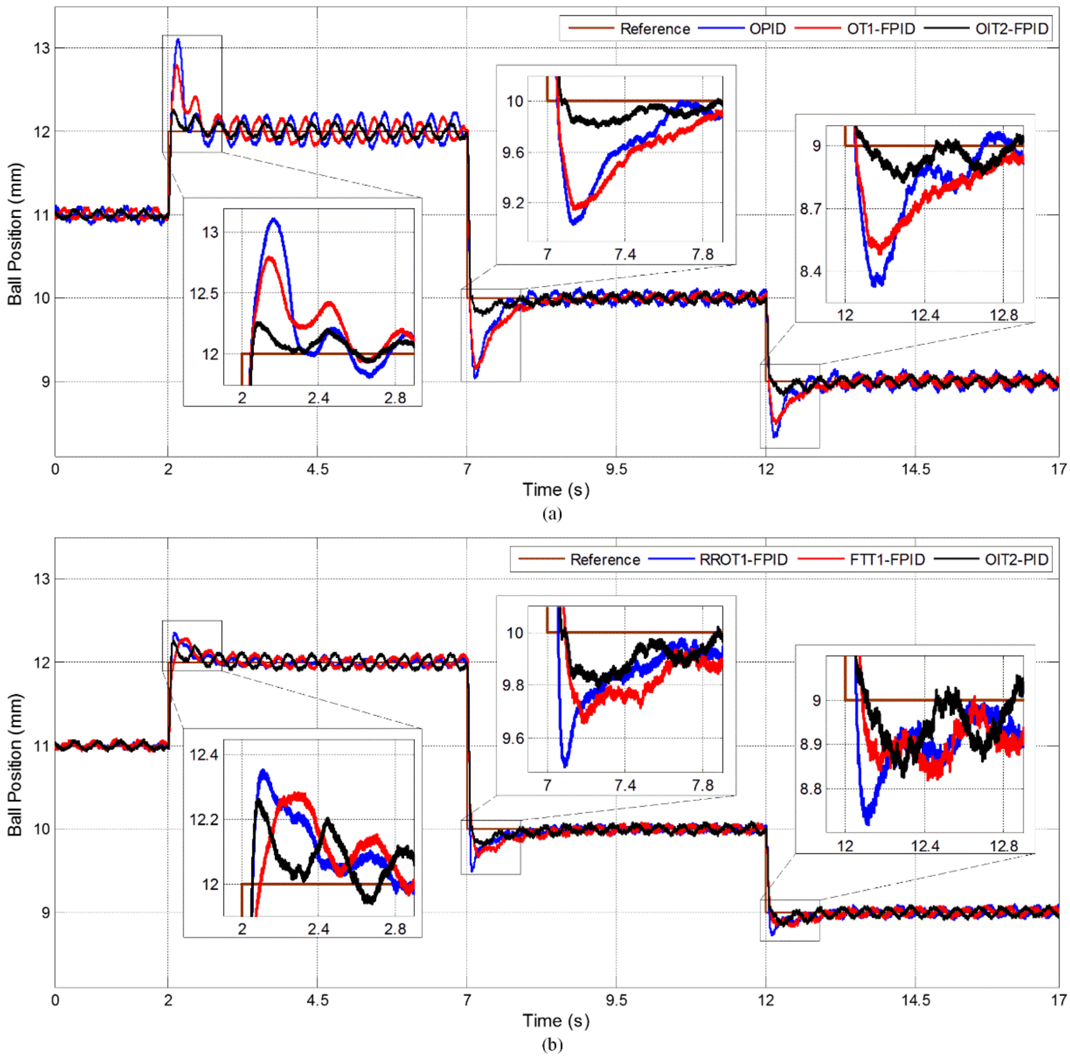

Figure 6.10 : Real-time experimental results for testing reference trajectory.

Again, the second comparison study is performed for the testing reference trajectory at which the controllers are not optimized to examine their robustness against unknown system dynamics. As it shown in the Table 6.2, OIT2-FPID structure has better control performance measures in comparison to the other controllers in general. For instance, for the reference value variation from 10mm to 9mm, OPID control system has worst performance measures. Here, both employed STT1-FPID structures enhanced the OT1-FPID structure but the FTT1-FPID structure has best IAE performance measure. In comparison with the OT1-FPID structure, the FTT1-FPID reduced settling time by about 27% while the OIT2-FPID structure reduced settling time by about 48% whereas both the FTT1-FPID and OIT2-FPID structures reduced the overshoot by about 67%. Moreover, for the reference variation form 11 mm to 12 mm, OPID and OT1-FPID controller structures have an oscillating system response, while the OIT2-FPID and FTT1-FPID and RROT1-FPID structures ended up with stable system responses where the OIT2-FPID has the fastest system response. It can be concluded that, the controller structures that include extra degrees of freedom (OIT2-FPID, FTT1-FPID, RROT1-FPID) have better transient responses and overall performance. Moreover, the extra degree of freedom of the IT2-FSs provides the OIT2-FPID structure to have more satisfactory control performances when compared to self-tuning structures. Consequently, the OIT2-FPID controller structure provided relatively better control performances than its counterparts in presence of noise and unknown dynamics compared to both non-self-tuning and self-tuning structures.

6.2 A Simulation Study of Proposed Heuristic Self-Tuning Structure

In this subsection, a FOPDT process with uncertainty is considered in order to show the effectiveness of the proposed heuristic self tuning structure for the simplest IT2-FPID controller. The proposed Self-Tuning Interval Type-2 Fuzzy PID (STIT2-FPID) controller is also compared IT2-FPID and T1-FPID controllers via simulations for the unit step and the disturbance rejection performances. In order to make a fair assessment overshoot (%OS), settling time (Ts) and Integral Absolute Error (IAE) performance measures are considered. Moreover, the robustness against parameter uncertainty of the proposed self-tuning structure is also investigated by considering perturbed system models. Then without losing generality, the FOPDT process model is defined as

$$G(s) = \frac{K}{\tau s + 1} e^{-\theta s} \tag{6.14}$$

where K is the process gain, τ is the time constant and θ is the dead time. Therefore, four different cases are considered in simulations; the nominal system $G_0(s)$, ($K = 1, \tau = 2, \theta = 0.6$) and perturbed systems; $G_1(s)$, ($K = 1.3, \tau = 1, \theta = 1.2$), $G_2(s)$, ($K = 0.7, \tau = 2.3, \theta = 0.9$) and $G_3(s)$, ($K = 1.5, \tau = 1.5, \theta = 0.3$). The consequent and antecedent membership functions and the rule base of T1-FLS and IT2-FLSs for 4-rule structures are selected as mentioned in Section 4. The SFs are fixed as $K_e = 1$, $K_d = 0.2$, $K_a = 2$, $K_b = 2$. Here, both the type-1 and interval type-2 controllers use same scaling factor set. The height of the LMF of the employed IT2-FPID controller is selected as 0.22 in order to show that the response of the simplest IT2-FPID controller will be relatively slower than T1-FPID. Moreover, upper and lower limits (h_1 and h_2) of the proposed heuristic self-tuning structure is set to 0.1 and 0.338. Thus, the feasible lower limit of $V(M)$ is limited to 0.1 while the upper limit of the $V(M)$ is set to 0.448 which means that smoother control action is obtained by STIT2-FPID controller. Then the proposed heuristic function that adjust the height of the LMFs for the employed FOPDT process is constructed as

$$M(E) = (1 - |E|)0.338 + 0.1 \tag{6.15}$$

For all simulation studies the step input is applied initially and an input disturbance is applied at 20th second with magnitude of 0.3. The closed loop system responses of the employed FPID controllers for the nominal system are illustrated in Figure 6.11 while corresponding control signals are given in Figure 6.12. Besides, the alteration of the tuning parameter (M) of the proposed self-tuning structure for simplest IT2-FPID controller is given in Figure 6.13. Then, overall performances measures of employed controllers are summarized in Table 6.3.

Table 6.3 : Performance measures of FPID controllers for the nominal system.

	OS%	Ts	AIE
T1-FPID	13.68	7.11	2.33
IT2-FPID	11.12	10.35	2.91
STIT2-FPID	10.61	7.58	2.40

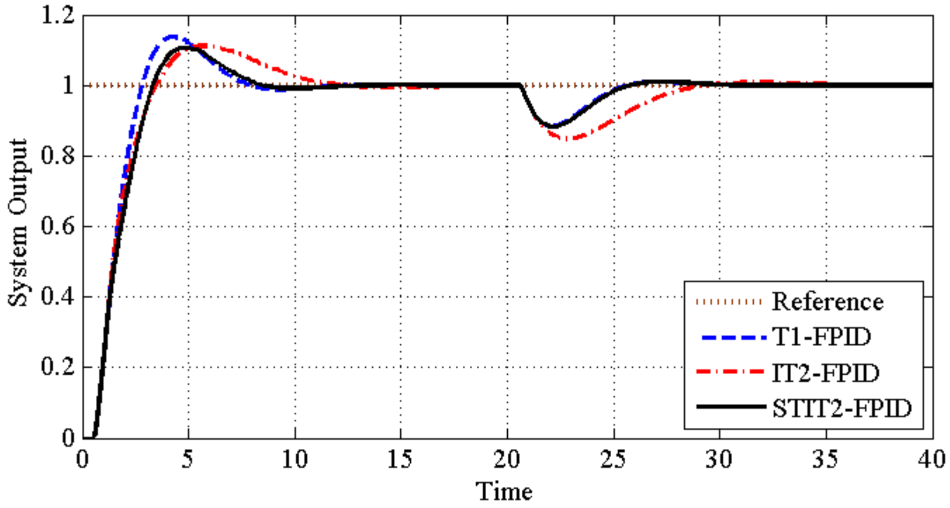

Figure 6.11 : Closed loop system responses for the nominal system.

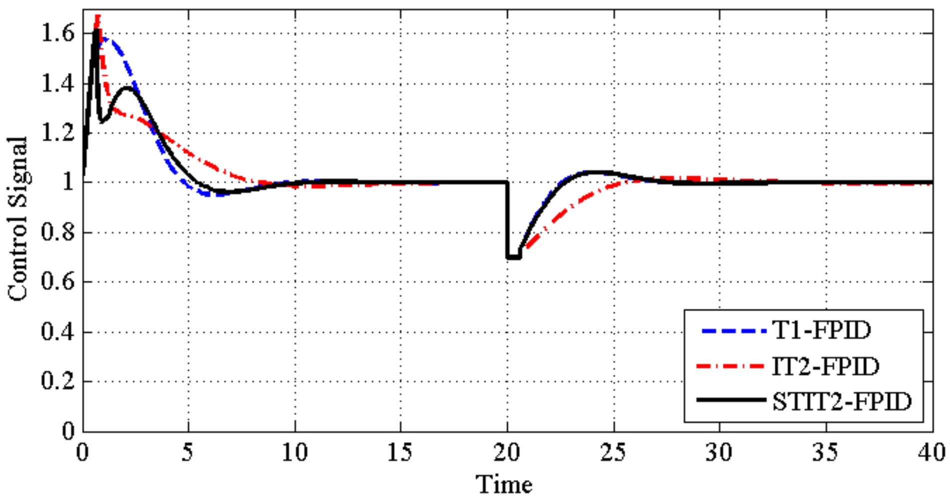

Figure 6.12 : Control signals for the nominal system.

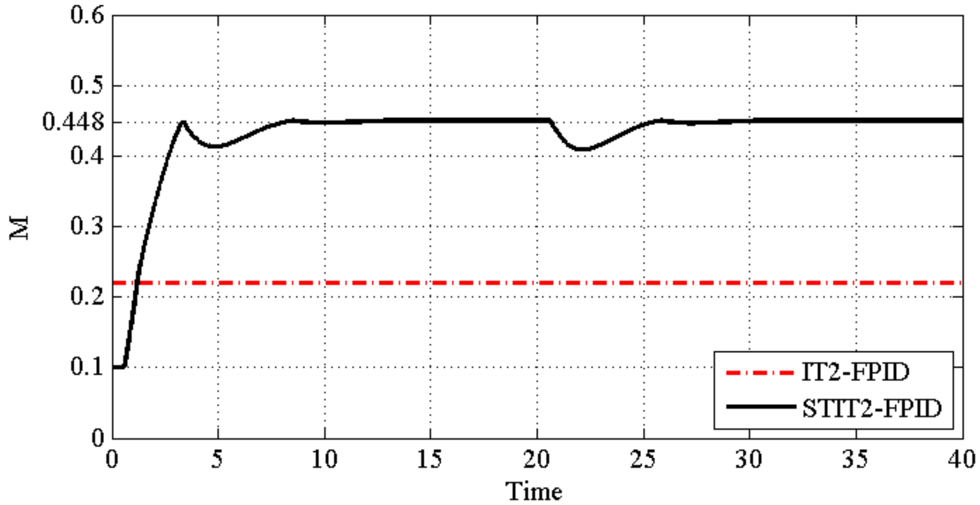

Figure 6.13 : Alteration of the contoller gain for the nominal system.

The STIT2-FPID controller improves the overall performances for the nominal system when compared to the IT2-FPID and T1-FPID counterparts. For example, as shown in Figure 6.11, for the nominal system response, the T1-FPID has the Ts with 7.11 s but the highest OS with 13.68% because of the aggressive nature of the T1-FLC, while the simplest IT2-FPID has less OS with 11.12% but the longest Ts with 10.35 s because of the smooth nature of the IT2-FPID (M=0.22). However, the STIT2-FPID structure has the best OS% and approximately same Ts with T1-FPID with 10.61% and 7.58 s respectively. Moreover, the control signal of the proposed STIT2-FPID control is more complex than its counterparts as shown in Figure 6.12 and the controller gain is adjusted with respect to heuristic update function effectively in an online manner as shown in Figure 6.13.

Secondly, the closed loop system responses for the employed perturbed systems and corresponding control signals are given in above figures. Here, high uncertainty about the model time parameters is considered at first, secondly moderate uncertainty about the model parameters is considered and then high uncertainty about the system gain is considered for the perturbed system simulations. The step input is applied initially and an input disturbance is applied at 20th second with magnitude of 0.3. The closed loop system responses and corresponding control signals for the perturbed system 1 ($G_1(s)$) are illustrated in Figure 6.14 and Figure 6.15 and the alteration of the M is given in Figure 6.16. The closed loop system responses for other perturbed systems ($G_2(s)$ and $G_3(s)$) is also given and the overall performances measures of employed controllers are summarized in Table 6.4, Table 6.5, and Table 6.6.

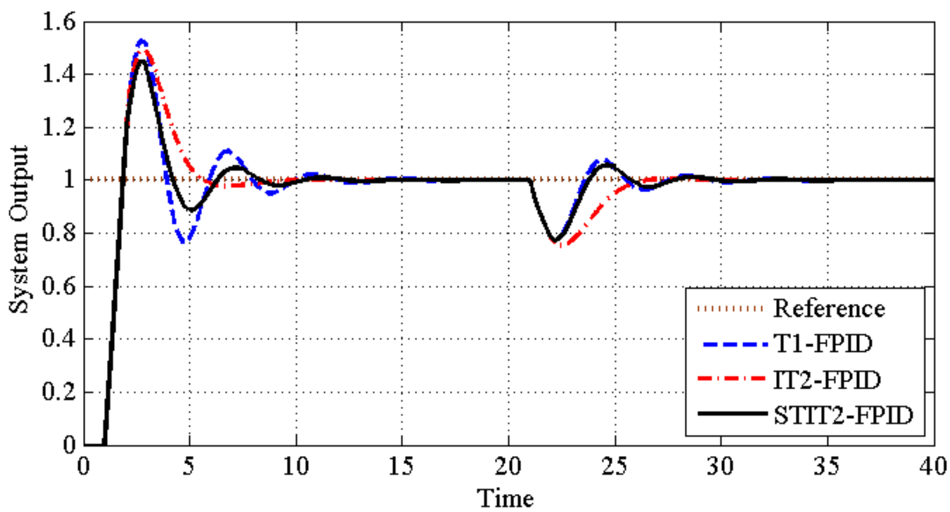

Figure 6.14 : Closed loop system responses for the perturbed system 1.

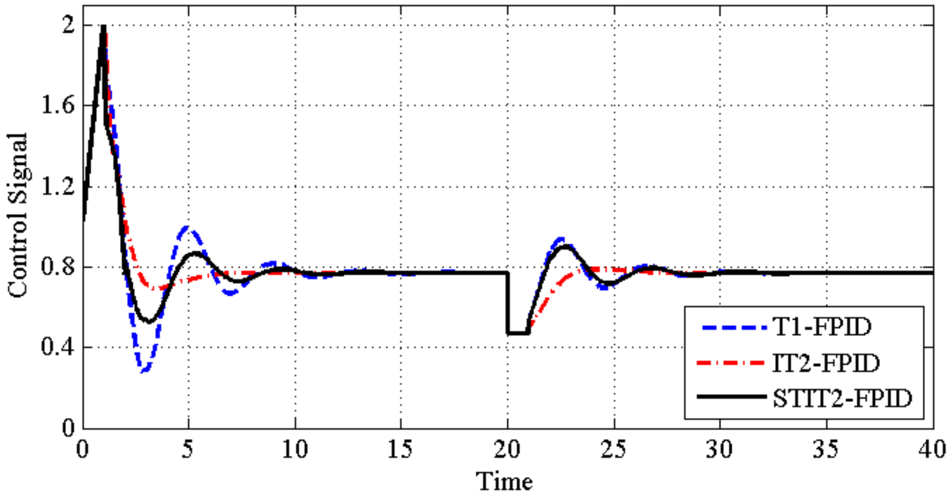

Figure 6.15 : Control signals for the perturbed system 1.

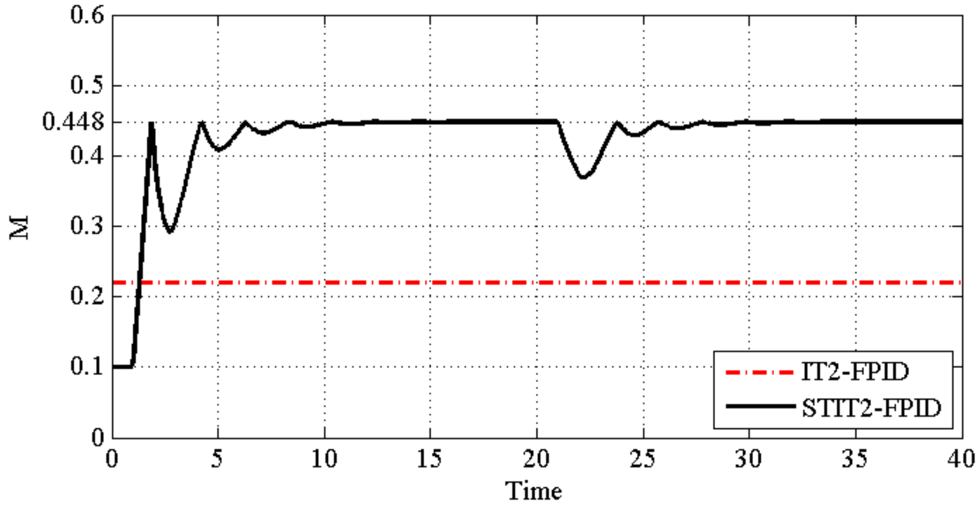

Figure 6.16 : Alteration of the controller gain for the perturbed system 1.

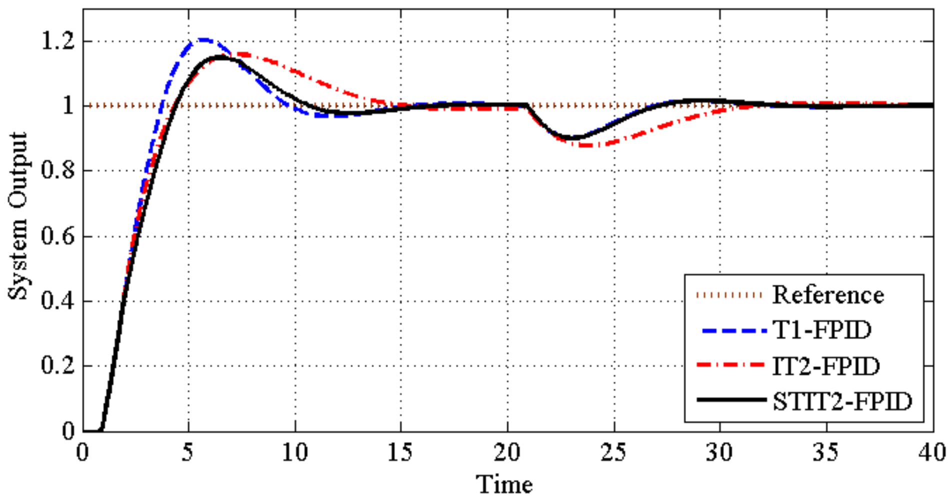

Figure 6.17 : Closed loop system responses for the perturbed system 2.

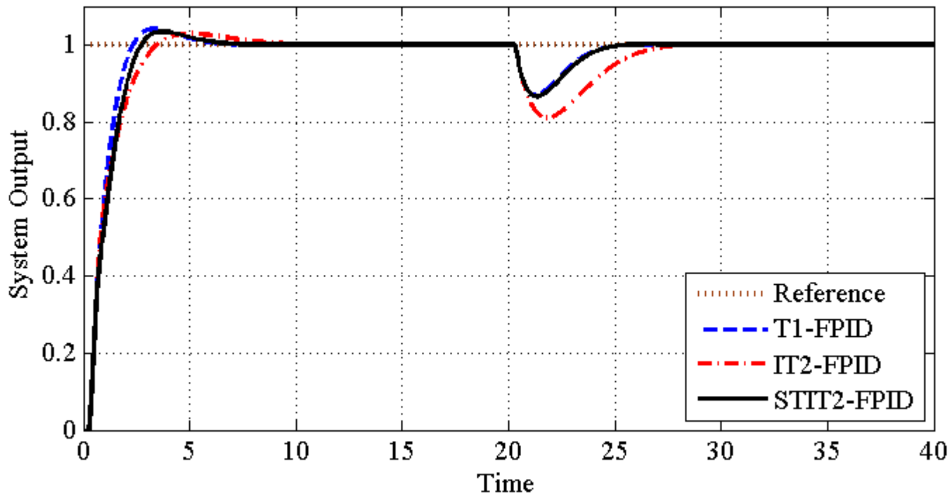

Figure 6.18 : Closed loop system responses for the perturbed system 3.

As shown Figure 6.14 to Figure 6.18, the proposed self-tuning structure provides consistent results in presence of uncertainties about the FOPDT model parameters. Moreover the proposed self-tuning structure simplest IT2-FPID controller has more complex control effort than its type-1 and interval type-2 bases as shown in Figure 6.15. The reason behind this remark is the adjustable gain of the proposed self-tuning structure. The controller gain is adjusted with respect to heuristic update function effectively in an online manner as shown in Figure 6.16. Furthermore, similar to nominal system responses, the proposed STIT2-FPID controller improves the overall performances for the perturbed systems when compared to the IT2-FPID and T1-FPID counterparts. However, the STIT2-FPID controller structure may slightly increase the possibility of oscillation comparing to its interval type-2 counterpart. For example, for the closed loop system response of the first perturbed system ($G_1(s)$), IT2-FPID has less oscillation around the set point, but STIT2-FPID controller still improves the overall performance since STIT2-FPID has nearly 10% better Ts and IAE values than IT2-FPID. Hence, the STIT2-FPID structure is still robust against disturbances and uncertainties because of its IT2-FPID base.

Table 6.4 : Performance measures of FPID controllers for the perturbed system 1.

	OS%	**Ts**	**AIE**
T1-FPID	52.76	11.15	3.20
IT2-FPID	49.19	7.13	3.12
STIT2-FPID	45.02	7.92	2.83

Table 6.5 : Performance measures of FPID controllers for the perturbed system 2.

	OS%	Ts	AIE
T1-FPID	20.29	13.49	3.50
IT2-FPID	15.83	13.48	4.04
STIT2-FPID	14.91	13.59	3.48

Table 6.6 : Performance measures of FPID controllers for the perturbed system 3.

	OS%	Ts	AIE
T1-FPID	4.04	4.85	1.37
IT2-FPID	2.89	6.56	1.90
STIT2-FPID	3.41	5.01	1.48

Consequently, it can be concluded that the proposed STIT2-FPID controller improves the overall performances in general comparing to its IT2-FPID and T1-FPID counterparts. The reason behind this is that the proposed STIT2-FPID act like the IT2-FPID when the system far away the reference which provides smooth control action for set point tracking and then it act like the T1-FPID when the system output about the set point which provides aggressive control action against disturbances. Hence, it can be interpreted that the proposed STIT2-FPID controller benefits the superiorities of the T1-FPID and IT2-FPID controllers.

6.3 A Simulation Study of Proposed Online Rule-Weighting Method

In this subsection, a two cascaded tank process is considered in order to show the effectiveness of the proposed online rule weighting method for the IT2-FPID controllers. The process is preferred due to its nonlinear and uncertain characteristics and different types of order. The employed two cascaded tank process is illustrated in Figure 6.19. Here, the above tank (Tank 2) is straight tank with a cross sectional area (A_2) and the below tank (Tank 1) is an inclined tank. The cross-sectional area of the below tank is related to the level of the tank. The angle of its sidewall is represented by β and the width of the below tank is represented L. The heights of the straight and inclined tanks are represented as h_1 and h_2 respectively. The inlet flow is represented by $F_{in}(t)$ while outlet flows are represented by $F_{out2}(t)$ and $F_{out1}(t)$. Here the input of the two cascaded tank process is assumed as inlet flow while the output of it is assumed as the height of the below tank (h_1). Then the differential equations related to the two cascaded tank process is given as

$$\frac{dh_1}{dt} = \frac{-\gamma_1\sqrt{2gh_1} + \gamma_2\sqrt{2gh_2}}{2(d + h_1 \tan\beta)L} \tag{6.16}$$

$$\frac{dh_1}{dt} = \frac{\gamma_2}{A_2}\sqrt{2gh_2} + \frac{1}{A_2}F_{in}(t) \tag{6.17}$$

The process parameters are taken as $A_2 = 85\ cm^2$, $L = 20$, $\beta = 5.1°$, $d = 3.32\ cm$, $\gamma_1 = 0.3539\ cm^2$, $\gamma_2 = 0.3027\ cm^2$, $g = 9.8\ ms^{-2}$ and the inlet flow range is given as $0 - 100\ cm^3/s$ (Wang and Aida, 2003). For all simulation studies, the initial levels of the tanks is assigned as $h_1 = 10\ cm$ and $h_2 = 2\ cm$ and the reference level of the below tank is determined as 6 cm. Moreover, the SFs are fixed as $K_e = 0.25$, $K_d = 0.5$, $K_a = 6$, $K_b = 0.01$, $M = 0.5$ for all employed 9-rule IT2-FPID controller structures regardless its self-tuning structure.

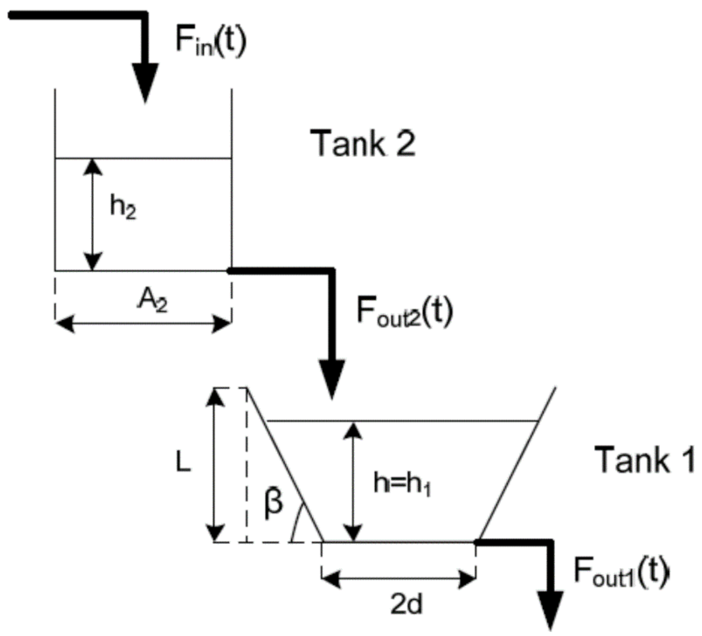

Figure 6.19 : Two cascaded tank process.

The proposed online rule weighting method IT2-FPID controllers is compared with an error based rule weighting method proposed by (Kumbasar et al., 2013) . In brief, The error based online rule weighting method for IT2-FPID controllers adjust the rule weights via two heuristic functions in terms of the error. The heuristic functions that are used for the rule weight adjustment is given as

$$f_1(E) = \alpha|E| \tag{6.18}$$

$$f_2(E) = 1 - |E| \tag{6.19}$$

where α is a constant in the interval [0,1]. Then, the update functions given above determines the rule weights of the IT2-FPID controllers in online manner with respect to the meta rules defined in (Karasakal et al., 2011). The meta rules are constructed with respect to the process output information, that is why the update functions given in Equation 6.18 and Equation 6.19 are the functions of the error input. Then, the mentioned meta rules is summarized on the rule table of the employed IT2-FPID controller as illustrated in Figure 6.20.

E \ D	N	Z		P
N	f_2	f_2	f_1	f_1
Z	f_2	f_2	f_2	f_2
P	f_1	f_1	f_2	f_2

Figure 6.20 : Meta rules of rule weight adjustment mechanism on the rule base.

The closed loop control performances and the control signals are illustrated in Figure 6.21 and Figure 6.22 respectively. For the optimization procedure, the constants of the cost function is chosen as $Q = 30$, and $R = 5$, while the population size and iteration number of the BB-BC algorithm is chosen as 30 and 50 respectively.

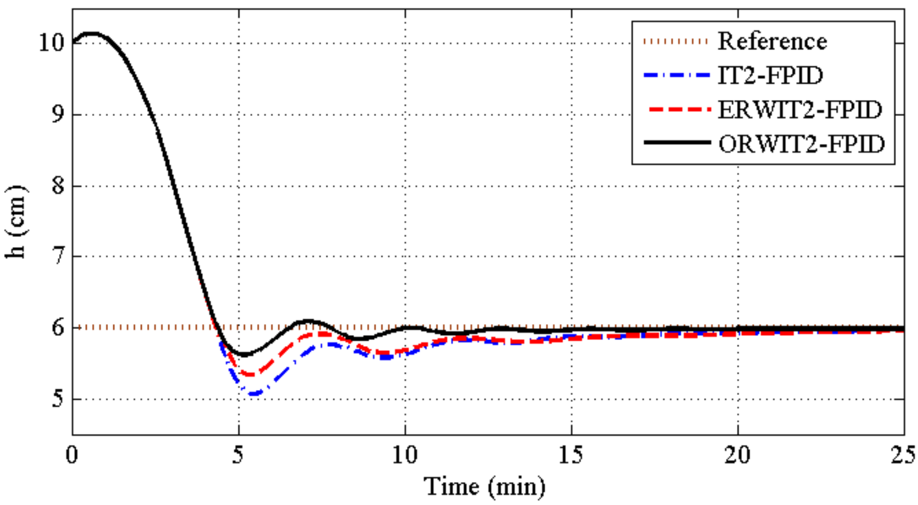

Figure 6.21 : Closed loop system responses of employed IT2-FPID controllers.

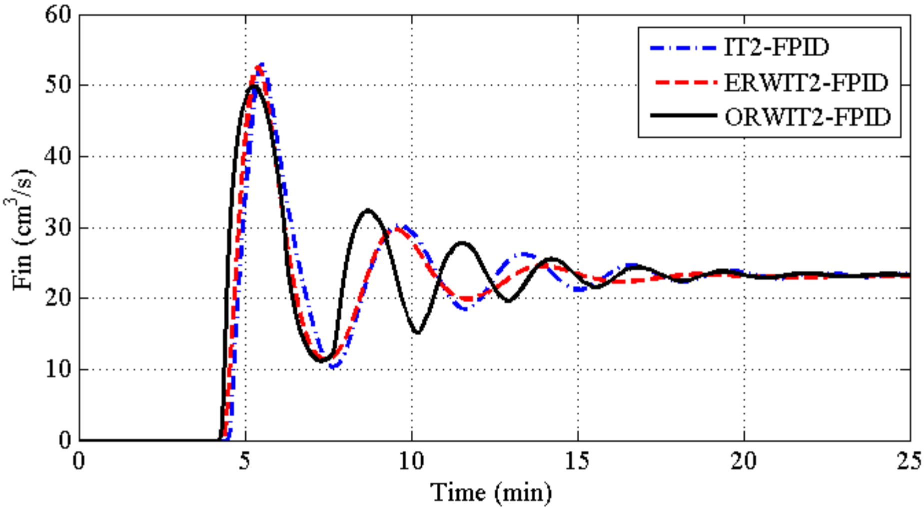

Figure 6.22 : Control signals of employed IT2-FPID controllers.

Table 6.7 : Performance measures of employed IT2-FPID controllers.

	Ts	OS%	IAE
IT2-FPID	17.5 min	23.37 %	40.637
ERWIT2-FPID	19.33 min	16.64 %	38.363
ORWIT2-FPID	9.25 min	9.57 %	32.514

As shown figures above, the proposed self-tuning structure improves the control performance in presence of model nonlinearities like the second order nonlinear model of the employed cascaded two tank process. The employed ERWIT2-FPID controller improves the performance of the its interval type-2 base, while the proposed ORWIT2-FPID controller improves the control performance the most due to its optimization based self-tuning structure. For example, as shown in Figure 6.21, the IT2-FPID has the performance measures as Ts with 17.5min and OS with 23.37% while ERW-IT2-FPID improves the performance as the OS with 16.64% by compromising from the Ts approximately 2 min. Moreover, the ORW-IT2-FPID improves the performance in every senses as the fastest Ts with 9.5min and the smallest OS with 9.57 %. Moreover, it can be concluded that the classical error based rule weighting structure make the control action always smoother than its IT2-FPID base whereas the proposed optimization based rule weighting method might make the control action both smoother and aggressive with respect to system performance requirements and the cost function in time when comparing to its IT2-FPID controller base. On the other hand, the one drawback of the online rule weighting method for IT2-FPID controllers is that the approach closely depends on the information of the model, here also notice that any information about the model including nonlinear models, fuzzy models, regression vectors or knowledge based models can be directly used in the optimization procedure in order to overcome the issue. Consequently, without losing generality, it can be also concluded that the closed loop system performances might be improved comparing to error based rule weight adjustment mechanisms and IT2-FPID controller base.

7. CONCLUSION

In this Master thesis, two alternative approaches to the Karnik-Mendel type reduction method is proposed, the mathematical derivations of the 4-rule IT2-FPID controller is analytically derived, two self-tuning structures of IT2-FPID controllers including heuristic function based and optimization based methods are proposed. For this purposes, the general and internal structures of the IT2-FPID controllers is first examined in detail, and the real-time experimental and simulation studies are performed in order to show the effectiveness of the proposed method and the controller structures.

Firstly, a novel graphical method called S-MAP is presented in order to visualize and understand better the variation of the switching points selection of the KM algorithm. The S-MAP provides useful information not only about the switching point selection but also the different control laws of the IT2-FPID controller. By using the S-MAP, the control laws becomes observable and more thoughtful in order to utilize for the further researchers. Moreover, a novel representation of the switching points of KM algorithm, namely BF-KM, is presented by first decomposing the IT2-FPID controller into subcontrollers and then derive boundary functions to determine the optimal switching points of each subcontroller. Therefore, the optimal switching points are determined through the obtained boundary functions, in this context, the proposed method eliminates the bottleneck of the iterative KM algorithm. In other words, the proposed BF-KM method determines the switching points directly without using an iterative algorithm. The goal of the method is also that the output formulation of the IT2-FPID controller can directly calculated with respect to the switching points that determined by the BF-KM. Here the proposed alternative approaches are in fact complementary studies because the BF-KM determines the switching points while the S-MAP clearly visualize them.

Secondly, the explicit mathematical expressions of 4-rule IT2-FPID controller and 9-rule IT2-FPID controller is obtained with the aids of the S-MAP and BF-KM. It is worth to mention that usage of the BF-KM make it possible to express an iterative algorithm that closely used in output formulation of the IT2-FPID controllers. The closed-from formulation of the simplest IT2-FPID controller is derived in terms of three different control laws. The mathematical expression of the simplest IT2-FPID controller also point out that the controller highly nonlinear control features to the engineers even it is the potential simplest structure of IT2-FPID controllers. Moreover, the obtained explicit mathematical expressions of the IT2-FPID controllers will be closely used in future with following topics, the stability analysis of the IT2-FPID controllers and the systematic controller design procedures of IT2-FPID controllers.

Thirdly, two novel online self-tuning structures for IT2-FPID controllers is presented based on a heuristic function and optimization. A simple heuristic function based self-tuning structure for the simplest IT2-FPID controller is proposed with respect to the controller gain of the employed controller around the steady state. The controller gain curve is obtained with respect to the alteration of the size of the FOU and the height of the lower membership functions. Then, in the light of the observations, a simple function is used in order to enhance control performance of the IT2-FPID controllers. The outcomes of the studies showed that the superiority of the proposed STIT2-FPID structure is related to hybrid nature of the self-tuning structure because it benefits the advantages of the T1-FPID and IT2-FPID controllers by changing the size of the FOU in an online manner. Then an optimization based self-tuning structure is presented, the self-tuning IT2-FPID controller adjusts its rule weights with respect to ta generic cost function in terms of tracking error and control signal in online manner. The performance of the proposed STIT2-FPID controller have achieved better control performances in presence of uncertainties and nonlinearities on the process model.

Furthermore, as part of this thesis, a comprehensive comparative real-time study is performed between T1-FPID, self-tuning T1-FPID, IT2-FPID controller structures on the real time MAGLEV experimental setup. The self-tuning mechanisms allow the T1-FPID structures to have more degrees of freedom like IT2-FPID controllers. In this context, it is also investigated if the power of the IT2-FPID lies in its ability to handle the high level of uncertainties rather than only having an extra degree of freedom.

It can be concluded that, the IT2-FPID control systems provide more satisfactory control performances due to its internal extra degree of freedom that lies on its antecedent membership functions, moreover, the IT2-FPID control systems seem to be more robust against noise and unknown system dynamics when compared to its type-1, self-tuning type-1 or traditional counterparts. Furthermore, various design strategies or self-tuning structures might be straight forwardly implemented into IT2-FPID controllers with the aim of the proposed alternative approaches to KM. It is also important to note that developed alternative approaches, derived mathematical expressions and proposed self-tuning structures are the initial steps in order to investigate the internal structures and potential abilities of the IT2-FPID controllers in details. In this context, it is not fair to draw a general conclusion for all type of IT2-FLSs, however, without losing generality it can be concluded that the employed IT2-FPID controller structure improves the control performances in general cases and it can be easily used in control applications. Future work of this thesis will focus on to developing more sophisticated tuning mechanism which might improve the control performance better, generalizing the BF-KM method and stability analysis of the IT2-FPID controllers.

REFERENCES

Ahn, K. K., and Truong, D. Q. (2009). Online tuning fuzzy PID controller using robust extended Kalman filter, *Journal of Process Control*, vol. 19, pp. 1011-1023.

Astrom, K. J., Hagglund, T. (2005). Advanced PID Control, ISA-The Instrumentation, Systems, and Automation Society.

Babuska, R., Oosterhoff, J., Oudshoorn, A., Bruijn, P. M. (2002). Fuzzy self-tuning PI control of pH in fermentation, *Engineering Applications of Artificial Intelligence*, vol. 15, pp. 3–15.

Begian, M. B., Melek, W., Mendel, J. (2008). Stability analysis of type-2 fuzzy systems, *in Proceedings IEEE International Conference on Fuzzy Systems*, pp. 947–953.

Begian, M. B., Melek, W., Mendel, J. (2010). On the stability of interval type-2 TSK fuzzy logic control systems, *IEEE Transactions on Systems, Man and Cybernetics Part B: Cybernetics*, vol. 40, pp. 798-818.

Bouallegue, S., Haggege, J., Ayadi, M., Benrejeb, M., (2011). PID-type fuzzy logic controller tuning based on particle swarm optimization, *Engineering Applications of Artificial Intelligence,* vol. 25, pp. 484-493.

Castillo, O., Huesca, G., Valdez, F. (2005). Evolutionary computing for optimizing type-2 fuzzy systems in intelligent control of non-linear dynamic plants, *In Proceeding of North American Fuzzy Information* Processing Society, pp. 247–251.

Castillo, O., and Melin, P. (2008). Type-2 Fuzzy Logic Theory and Applications, Berlin, Germany: Springer-Verlag.

Coupland, S., and John, R. (2007). Geometric type-1 and type-2 fuzzy logic Systems, *IEEE Transactions on Fuzzy Systems*, vol. 15, pp. 3-15.

Dodurka, M. F., Kumbasar, T., Sakalli, A., Yesil, E. (2014). Boundary function based Karnik-Mendel type-reduction method for interval type-2 fuzzy PID controllers, *IEEE International Conference on Fuzzy Systems* (accepted).

Dorigo, M., and Stützle, T. (2003). The ant colony optimization metaheuristic: algorithms, applications, and advances, *International Series in Operations Research & Management Science*, vol. 57, pp. 250-285.

Du, X., and Ying, H. (2010). Derivation and analysis of the analytical structures of the interval type-2 fuzzy-PI and PD controllers, *IEEE Transactions on Fuzzy Systems,* vol. 18, pp. 802-814.

Duan, X. G., Li, H. X., Deng, H. (2008). Effective tuning method for fuzzy PID with internal model control, *Industrial & Engineering Chemistry Research*, vol. 47, pp. 8317-8323.

Eksin, İ., Güzelkaya, M., Gürleyen, F. (2001). A new methodology for deriving the rule-base of a fuzzy logic controller with a new internal structure, *Engineering Applications of Artificial Intelligence,* vol. 14, pp.617-628.

Erol, O. K., and Eksin, I. (2006). A new optimization method: big bang big crunch, *Advances in Engineering Software*, vol. 37, pp. 106-111.

Galichet, S., and Foulloy, L. (1995). Fuzzy controllers: synthesis and equivalences, *IEEE Transactions on Fuzzy Systems*, vol.3, pp. 140–148.

Galluzzo, M., Cosenza, B., Matharu, A. (2008). Control of a nonlinear continuous bioreactor with bifurcation by a type-2 fuzzy logic controller, *Computers and Chemical Engineering*, vol. 32, pp. 2986-2993.

Goldberg, D. E. (1989). Genetic algorithms in search, optimization and machine learning, Addison-Wesley Longman Publishing USA.

Güzelkaya, M., Eksin, İ. and Yeşil, E. (2003). Self-tuning of PID-type fuzzy logic controller coefficients via relative rate observer, *Engineering Applications of Artificial Intelligence*, vol. 16, pp. 227-236.

Hagras, H. (2004). A hierarchical type-2 fuzzy logic control architecture for autonomous mobile robots, *IEEE Transactions on Fuzzy Systems*, vol.12, pp. 524-539.

Huang, T. T., Chung, H. Y., Lin, J. J., (1999). A fuzzy PID controller being like parameter varying PID, *IEEE International Fuzzy Systems Conference Proceeding*, vol. 1, pp. 269–275.

Karasakal, O., Güzelkaya M., Eksin İ., Yeşil, E. (2011). An error-based on-line rule weight adjustment method for fuzzy PID controllers, *Expert Systems with Applications*, vol. 38, pp. 10124-10132.

Karasakal, O., Güzelkaya M., Eksin İ., Yeşil, E., Kumbasar T. (2013). Online tuning of fuzzy PID controllers via rule weighting based on normalized acceleration, *Engineering Applications of Artificial Intelligence*, vol. 26, pp. 184-197.

Karnik, N. N., Mendel, J. M., Liang, Q. (1999). Type-2 fuzzy logic systems, *IEEE Transaction on Fuzzy Systems*, vol. 7, pp. 643–658.

Kumbasar, T., Yesil, E., Eksin, İ., Güzelkaya, M. (2008). Inverse fuzzy model control with online adaptation via big bang big crunch Optimization, *The 3rd International Symposium on Communications, Control and Signal Processing*.

Kumbasar, T., Eksin, İ., Güzelkaya, M., Yesil, E. (2011). Interval Type-2 Fuzzy Inverse Controller Design in Nonlinear IMC Structure, *Engineering Applications of Artificial Intelligence*, vol. 24, pp. 996 – 1005.

Kumbasar, T., Eksin, İ., Güzelkaya, M., Yesil, E. (2012). Type-2 fuzzy model based controller design for neutralization processes," ISA Transactions, vol. 51 (2), pp. 277–287.

Kumbasar, T., and Hagras, H. (2013a). A big bang-big crunch optimization based approach for interval type-2 fuzzy PID controller design, *IEEE International Conference on Fuzzy Systems*, pp. 1-8.

Kumbasar, T., Yeşil, E., Karasakal, O. (2013b). Self-tuning interval type-2 fuzzy PID controllers based on online rule weighting, *IEEE International Conference on Fuzzy Systems*, pp. 1-6.

Kumbasar, T. (2013c). A simple design method for interval type-2 fuzzy PID controllers, *Soft Computing*, 2013.

Kumbasar, T., Eksin, İ., Güzelkaya, M., Yesil, E. (2013d). Exact inversion of decomposable interval type-2 fuzzy logic systems, *International Journal of Approximate Reasoning*, vol. 2, pp. 253-272.

Lam H. K., and Seneviratne, L. D. (2008). Stability analysis of interval type-2 fuzzy-model-based control systems, *IEEE Transactions on Systems, Man and Cybernetics Part B: Cybernetics*, vol. 38, pp. 617-628.

Li, H. X., and Gatland, H. B., (1996). Conventional fuzzy control and its enhancement, *IEEE Transactions on Systems, Man, and Cybernetics*, vol. 26, pp. 791-796.

Li, H. X., Gatland H. B., Green, A.W. (1997). Fuzzy variable structure control, *IEEE Transactions on Systems, Man, and Cybernetics Part B*, vol. 27, pp. 306-312.

Liang, Q., and Mendel, J. (2000). Interval type-2 fuzzy logic systems: theory and design, *IEEE Transactions on Fuzzy Systems*, vol. 8, pp. 535–550.

Mamdani, E. H. (1974). Application of fuzzy logic algorithms for control of simple dynamic plant. *In Proceedings of the Institute of Electrical Engineering*, vol. 121, pp. 1585-1588.

Martinez, R., Castillo, O., Aguilar, L. T. (2009). Optimization of interval type-2 fuzzy logic controllers for a perturbed autonomous wheeled mobile robot using genetic algorithms, *Information Sciences*, vol. 179, pp. 2158-2174.

Mendel, J. (2000). Uncertain Rule-Based Fuzzy Logic: Introduction and New Directions, Prentice Hall, USA.

Mendel, J., John, R., Liu, F. (2006). Interval type-2 fuzzy logic systems made simple. *IEEE Transactions on Fuzzy Systems*, vol. 14, pp. 808-821.

Mendel, J. (2007). Type-2 fuzzy sets and systems: an overview, *IEEE Computational Intelligence Magazine*, vol. 2, pp. 20 –29.

Mizumoto, M. (1992). Realization of PID controls by fuzzy control methods, *Fuzzy Sets and Systems,* vol. 70, pp. 171–182.

Mudi, R. K., and Pal, N. R. (1999). A robust self-tuning scheme for PI- and PD-type fuzzy controllers, *IEEE Transactions of Fuzzy Systems*, vol. 7 pp. 2-16.

Nie, M., and Tan, W. W. (2008). Towards an efficient type-reduction method for interval type-2 fuzzy logic systems, *in Proceedings of IEEE International Conference on Fuzzy Systems*, pp. 1425–1432.

Nie, M., and Tan, W. W. (2010). Analytical structure and characteristic of symmetric Karnik-Mendel type-reduced interval type-2 fuzzy PI and PD controllers, *IEEE Transactions on Fuzzy Systems*, vol. 20, pp. 416-430

Qiao, W. Z., and Mizumoto, M. (1996). PID type fuzzy controller and parameters adaptive method, *Fuzzy Sets and Systems*, vol. 78, pp. 23-35.

Precup, R. E., and Preitl, S. (2004). Optimization criteria in development of fuzzy controllers with dynamics, *Engineering Applications of Artificial Intelligence*, vol. 17, pp. 661-674.

Sakalli, A., Kumbasar T., Dodurka M. F., Yesil, E. (2014a). The simplest interval type-2 fuzzy PID controller: structural analysis, *IEEE International Conference on Fuzzy Systems* (accepted).

Sakalli, A., Kumbasar T., Yesil E., Hagras, H. (2014b). Analysis of the performances of type-1, self-Tuning type-1 and interval type-2 fuzzy PID controllers on the magnetic levitation system, *IEEE International Conference on Fuzzy Systems* (accepted).

Shiakolas, P. S., and Piyabongkarn, D. (2010). Development of a Real-Time Digital Control System With a Hardware-in-the-Loop Magnetic Levitation Device for Reinforcement of Controls Education, *IEEE Transactions on Education*, vol. 46, pp. 79-86.

Sugeno, M., and Kang, G. T. (1988). Structure identification of fuzzy model, *Fuzzy Sets and Systems*, vol. 28, pp. 15-33.

Takagi, T., and Sugeno, M. (1985). Fuzzy identification of systems and its applications to modelling and control, *IEEE Transactions on Systems, Man, and Cybernetics,* vol. 15, pp. 116-132.

Wagner, C., and Hagras, H. (2010). Toward general type-2 fuzzy logic systems based on zSlices, *IEEE Transactions on Fuzzy Systems,* vol. 18, pp. 637-660.

Wang, D., and Aida, K. (2003). Research on fuzzy I-PD preview control for nonlinear system, *JSME International Journal Series, Special Issue on Advances in Motion and Vibration Control Technology*, vol. 46, pp. 1042-1050.

Woo, Z. W., Chung, H. Y., Lin, J. J. (2000). A PID type fuzzy controller with self-tuning scaling factors, *Fuzzy Sets and Systems*, vol. 115, pp. 321-326.

Wu, D., and Tan, W. W. (2005). Computationally efficient type-reduction strategies for a type-2 fuzzy logic controller, *in Proceedings of IEEE International Conference on Fuzzy Systems*, pp. 353–358.

Wu, D., and Tan, W. W. (2006a). Genetic learning and performance evaluation of internal type-2 fuzzy logic controllers. *Engineering Applications of Artificial Intelligence*, vol. 19, pp. 829-841.

Wu, D., and Tan, W. W. (2006b). A simplified type-2 fuzzy logic controller for real-time control, *ISA Transactions*, vol. 45, pp. 503–516.

Wu, D., and Mendel, J. (2007). Enhanced Karnik-Mendel algorithms for interval type-2 fuzzy sets and systems, *in Proceedings of Annual Meeting of* *the North American Fuzzy Information Processing Society*, pp. 184–189.

Wu, D., and Mendel, J. (2011). On the continuity of type-1 and interval type-2 fuzzy logic systems, *IEEE Transactions on Fuzzy Systems*, vol. 19, pp. 179-192.

Wu, D., and Tan, W. W. (2010). Interval type-2 fuzzy PI controllers: why they are more robust, *IEEE International Conference on Granular Computing*, pp. 802–807.

Wu, D. (2012). On the fundamental differences between type-1 and interval type-2 fuzzy logic controllers, *Transactions on Fuzzy Systems*, vol. 20, pp. 832–848.

Wu, H., and Mendel, J. (2002). Uncertainty bounds and their use in the design of interval type-2 fuzzy logic systems, *IEEE Transactions on Fuzzy Systems,* vol. 10, pp. 622–639.

Xu, J.X., Hang, C.C, Liu, C., (2000). Parallel structure and tuning of a fuzzy PID controller. *Automatica,* vol. 36, pp. 673–684.

Yeşil, E., Güzelkaya, M., Eksin, İ. (2003). Fuzzy PID controllers: an overview, *The Third Triennial ETAI International Conference on Applied Automatic Systems,* pp. 105-112.

Yeşil, E., Güzelkaya, M., Eksin, İ. (2004). Self-tuning fuzzy PID type load and frequency controller, *Energy Conversion and Management,* vol. 45, pp. 377-390.

Yesil E., Sakalli A., Ozturk C., Kumbasar T., (2013). Online fuzzy rule weighting method for fuzzy PID controllers via big bang - big crunch optimization, *IEEE International Conference on Fuzzy Systems*.

Yesil, E. (2014). Interval type-2 fuzzy PID load frequency controller using Big Bang-Big Crunch optimization, *Applied Soft Computing*, vol. 15, pp. 100-112, 2014.

Yetendje, A., Seron, M. M., Don, J. D., Martinez, J. J. (2010). Sensor fault-tolerant control of a magnetic levitation system, *International Journal of Robust and Nonlinear Control*, vol. 20 pp. 2108-2120.

Zadeh, L. A. (1965). Fuzzy sets, *Information and Control*, vol. 8, pp. 338-353.

Zadeh, L. A. (1975). The concept of a linguistic variable and it application to approximate reasoning-I, *Information Science*, vol. 19, pp. 829-841.

Zhao, Z.Y., Tomizuka, M., Isaka, S., (1993). Fuzzy gain scheduling of PID controllers. *IEEE Transactions on Systems Man and Cybernetics,* vol. 23, pp.1392–1398.

CURRICULUM VITAE

Name Surname: Ahmet Sakallı

Place and Date of Birth: Söke/Aydın, 04.09.1989

Address: Çeliktepe Mahallesi ŞehitKarakuşlar Caddesi No:19/8, Kağıthane / İstanbul

E-Mail: sakallia@itu.edu.tr

B.Sc.: Istanbul Technical University, Control Engineering

List of Publications:

- **Sakalli A.,** Kumbasar T., Dodurka M.F., Yesil E., 2014. The simplest Interval Type-2 Fuzzy PID Controller: Structural Analysis", *IEEE International Conference on Fuzzy Systems (FUZZ-IEEE 2014, WCCI 2014)*, Beijing, China. (accepted)
- **Sakalli A.,** Kumbasar T., Yesil E., Hagras H., 2014. Analysis of the Performances of Type-1, Self-Tuning Type-1 and Interval Type-2 Fuzzy PID Controllers on the Magnetic Levitation System, *IEEE International Conference on Fuzzy Systems (FUZZ-IEEE 2014, WCCI 2014),* Beijing, China. (accepted)
- Dodurka M.F., Kumbasar T., **Sakalli A.,** Yesil E., 2014. Boundary Function based Karnik-Mendel Type-Reduction Method for Interval Type-2 Fuzzy PID Controllers, *IEEE International Conference on Fuzzy Systems (FUZZ-IEEE 2014, WCCI 2014),* Beijing, China. (accepted)
- **Sakalli A.,** Yesil E., Musaoglu E., Ozturk C., Dodurka M.F., 2013. Heuristic Bubble Algorithm for a Linehaul Routing Problem: An Extension of a Vehicle Routing Problem with Pickup and Delivery, *14th IEEE International Symposium on Computational Intelligence and Informatics (CINTI 2013),* Budapest, Hungary.

▪ Yesil E., **Sakalli A.,** Ozturk C., Kumbasar T., 2013. Online Fuzzy Rule Weighting Method for Fuzzy PID Controllers via Big Bang-Big Crunch Optimization, *IEEE International Conference on Fuzzy Systems (FUZZ-IEEE 2013)*, Hyderabad, India.

▪ Yesil E., Ozturk C., Dodurka M.F., **Sakalli A.,** 2013. Fuzzy Cognitive Maps Learning Using Artificial Bee Colony Optimization, *IEEE International Conference on Fuzzy Systems (FUZZ-IEEE 2013),* Hyderabad, India.

▪ Dodurka M.F., Yesil E., Ozturk C., **Sakalli A.,** Guzay C., 2013. Concept by Concept Learning of Fuzzy Cognitive Maps, *The Artificial Intelligence Applications and Innovations Conference (AIAI 2013)*, Cyprus.

▪ Yesil E., Dodurka M.F., **Sakalli A.,** Ozturk C., Guzay C., 2013. Self-Tuning PI Controllers via Fuzzy Cognitive Maps, *The Artificial Intelligence Applications and Innovations Conference (AIAI 2013)*, Paphos, Cyprus.

▪ Yesil E., **Sakalli A.,** Guzay C., 2012. İkinci Mertebeden Ölü Zamanlı Sistemler İçin Bulanık Mantık Tabanlı PID Kontrolörü Tasarımı, *Otomatik Kontrol Ulusal Toplantısı (TOK 2012)*, Niğde, Türkiye.

PUBLICATIONS/PRESENTATIONS ON THE THESIS

▪ **Sakalli A.,** Kumbasar T., Dodurka M.F., Yesil E., 2014. The simplest Interval Type-2 Fuzzy PID Controller: Structural Analysis", *IEEE International Conference on Fuzzy Systems (FUZZ-IEEE 2014, WCCI 2014)*, Beijing, China. (accepted)

▪ **Sakalli A.,** Kumbasar T., Yesil E., Hagras H., 2014. Analysis of the Performances of Type-1, Self-Tuning Type-1 and Interval Type-2 Fuzzy PID Controllers on the Magnetic Levitation System, *IEEE International Conference on Fuzzy Systems (FUZZ-IEEE 2014, WCCI 2014),* Beijing, China. (accepted)

▪ Dodurka M.F., Kumbasar T., **Sakalli A.,** Yesil E., 2014. Boundary Function based Karnik-Mendel Type-Reduction Method for Interval Type-2 Fuzzy PID Controllers, *IEEE International Conference on Fuzzy Systems (FUZZ-IEEE 2014, WCCI 2014),* Beijing, China. (accepted)

▪ Yesil E., **Sakalli A.,** Ozturk C., Kumbasar T., 2013. Online Fuzzy Rule Weighting Method for Fuzzy PID Controllers via Big Bang-Big Crunch Optimization, *IEEE International Conference on Fuzzy Systems (FUZZ-IEEE 2013)*, Hyderabad, India.